

Electronic Supplementary Information

Axial and helical thermally activated delayed fluorescence bicarbazole emitters: Opposite modulation of circularly polarized luminescence through intramolecular charge-transfer dynamics

Pathira Sumsalee,^a Laura Abella,^b Thierry Roisnel,^a Sabrina Lebrequier,^c Grégory Pieters,^c Jochen Autschbach^{b,*}, Jeanne Crassous^a and Ludovic Favereau^{a,*}

^a Univ Rennes, CNRS, ISCR-UMR 6226, ScanMAT-UMS 2001, F-35000 Rennes, France.
E-mails: ludovic.favereau@univ-rennes1.fr.

^b Department of Chemistry, University at Buffalo, State University of New York, Buffalo,
NY 14260, USA. E-mail: jochena@buffalo.edu.

^c Université Paris-Saclay, CEA, INRAE, Département Médicaments et Technologies pour la
Santé (DMTS), SCBM, 91191 Gif-sur-Yvette, France.

Table of Contents

A. General methods	S2
B. Synthetic procedures	S3
C. Steady-state photophysical chiroptical characterizations	S9
D. X-Ray experimental data	S17
E. HPLC separation	S19
F. NMR spectra	S35
G. Theoretical calculations	S42
H. References	S58

A. General methods

^1H and ^{13}C NMR spectra were recorded at room temperature on an *AVANCE III 400 BRUKER* or an *AVANCE I 500 BRUKER* at Centre Régional de Mesures Physiques de l'Ouest (CRMPO), Université de Rennes 1. Chemical shifts δ are given in ppm and coupling constants J in Hz. Chemical shifts for ^1H NMR spectra are referenced relative to residual protium in the deuterated solvent ($\delta = 7.26$ ppm, CDCl_3). ^{13}C shifts are referenced to CDCl_3 peaks at $\delta = 77.16$ ppm.

High-resolution mass (HR-MS) determinations were performed at CRMPO on a Bruker MaXis 4G by ASAP (+ or -) or ESI and MALDI with CH_2Cl_2 as solvent techniques. Experimental and calculated masses are given with consideration of the mass of the electron.

UV-Visible (UV-vis, in $\text{M}^{-1} \text{cm}^{-1}$) absorption spectra were recorded on a UV-2401PC Shimadzu spectrophotometer.

Steady-state luminescence spectra were measured using an Edinburgh FS920 Steady State Fluorimeter combined with a FL920 Fluorescence Lifetime Spectrometer. The spectra were corrected for the wavelength dependence of the detector, and the quoted emission maxima refer to the values after correction. Life-times measurements were conducted with 375 nm diode laser excitation (EPL-series) plugged to a TCSPC pulsed source interface. Absolute fluorescence quantum yields ϕ were recorded with a Hamamatsu C9920-03 integrating sphere.

Electrochemical measurements were performed with a potentiostat PGSTAT 302N controlled by resident GPES (General Purpose Electrochemical System 4.9) software using a conventional single auxiliary electrode were platinum electrode potassium chloride calomel electrode (SCE). The supporting electrolyte was 0.1 N Bu_4NPF_6 (tetrabutylammonium hexafluorophosphate) in dichloromethane and solutions were purged with argon before the measurements. All potentials are quoted r experiments, the scan rate was either 100, 200 or 400 mV/s.

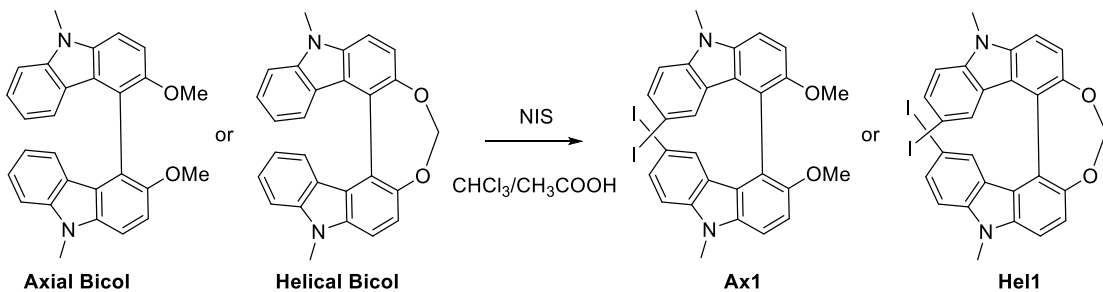
Electronic circular dichroism (ECD, in $\text{M}^{-1} \text{cm}^{-1}$) was measured on a Jasco J-815 Circular Dichroism Spectrometer (IFR140 facility - Biosit - Université de Rennes 1).

The circularly polarized luminescence (CPL) measurements were performed using a home-built CPL spectrofluoropolarimeter (constructed with the help of the JASCO Company). The samples were excited using a 90° geometry with a Xenon ozone-free lamp 150 W LS. The following parameters were used: emission slit width ≈ 2 mm, integration time = 4 sec, scan speed = 50 nm/min, accumulations = 10. The concentration of all the samples was ca. 10^{-6} M.

Thin-layer chromatography (TLC) was performed on aluminum sheets precoated with Merck 5735 Kieselgel 60F254. Column chromatography was carried out with Merck 5735 Kieselgel 60F (0.040-0.063 mm mesh). Chemicals were purchased from Sigma-Aldrich, Alfa Aesar or TCI Europe and used as received.

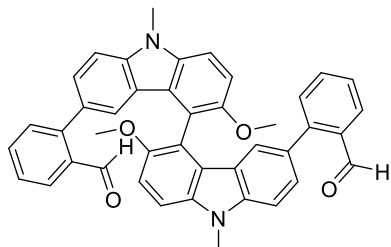
B. Synthetic procedures

BICOL was prepared following the previously reported procedure.¹ Bis-iodo Axial BICOL, **Ax1**, and Bis-iodo helical BICOL, **He1**, were obtained by iodination reaction using the following procedure: In round bottom flask, a mixture of axial or helical BICOL (100 mg, 1 eq.) in CHCl₃/CH₃COOH 6:3 ml was stirred at 0 °C under argon. N-iodosuccinimide (1.8 eq.) was slowly added and stirred at 0 °C. After 5 hours (the reaction was followed by thin layer chromatography), the resulting mixture was then purified through a flash column using CHCl₃ as the eluent. The desired compound was finally obtained as a white solid in 89%. The product was directly used in the next step without characterization.



He1-*o*-CHO, He1-*o*-CN, Ax-*o*-CHO, Ax-*p*-CN and He1-*p*-CN were synthesized by using Suzuki cross coupling reactions with corresponding arylboronic acids.

(±)-2,2'-(3,3'-dimethoxy-9,9'-dimethyl-9H,9'H-[4,4'-bicarbazole]-6,6'-diyl)dibenzaldehyde: (±)-**Ax-*o*-CHO**



In a dried Schlenk, 3,6-diiodo-axial BICOL (0.23 g, 0.34 mmol), 2-cyanophenyl boronic acid (0.21 g, 1.37 mmol), K₂CO₃ (0.31 g, 2.30 mmol) were dissolved in a mixture of DMF (12 mL) and water (4 mL) under argon. The mixture was degassed by argon bubbling for 15 minutes before Pd(PPh₃)₄ (0.079 g, 0.07 mmol) was added and the resulting solution refluxed for 8 hours. After cooling down to room temperature, the reaction was poured into 20 mL of water and the organic layer was extracted 3 times with methylene chloride (3*20 mL) and thus washed with brine (20 mL) and dried over MgSO₄. Solvents were removed under vacuum and the product was purified by chromatography (EtOAc/heptane, 25:75) to give white product 86%.

¹H NMR (400 MHz, chloroform-d (CDCl₃) δ 9.42 (s, 2H), 7.91 (dd, *J* = 7.8, 1.5 Hz, 2H), 7.52 – 7.46 (m, 2H), 7.46 – 7.39 (m, 4H), 7.39 – 7.36 (m, 2H), 7.34 (dd, *J* = 8.4, 1.8 Hz, 4H), 7.15 (dd, *J* = 7.8, 1.2 Hz, 2H), 6.52 (d, *J* = 1.8 Hz, 2H), 3.94 (s, 6H), 3.81 (s, 6H).

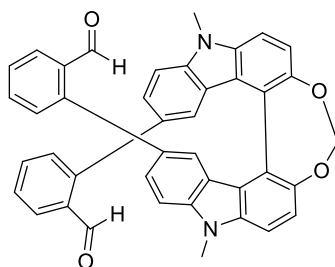
¹³C NMR (400 MHz, chloroform-d (CDCl₃) δ 192.3, 151.1, 146.9, 141.6, 137.2, 135.2 – 116.4, 116.7 – 95.5, 57.8, 29.5.

HR-MS Q-Exactive, ESI, 370 °C; ion [M+Na]⁺, C₄₂H₃₂N₂O₄Na m/z calculated 651.22543, m/z experimental 651.2250 ($\Delta=1$ ppm).

Experimental optical rotation values

(+)-**Ax-o-CHO**: $[\alpha]_D^{25} = +98 \pm 2\%$, $[\phi]_D^{25} = +613$ ($c = 1.3 \times 10^{-3}$, CHCl₃).
(-)-**Ax-o-CHO**: $[\alpha]_D^{25} = -96 \pm 2\%$, $[\phi]_D^{25} = -603$ ($c = 1.2 \times 10^{-3}$, CHCl₃).

(\pm)-2,2'-(8,17-dimethyl-8,17-dihydro-[1,3]dioxepino[4,5-c:7,6-c']dicarbazole-11,14-diyldibenzaldehyde: (\pm)-**Hel-o-CHO**



Following the same procedure than **Ax-o-CHO**, **Hel-o-CHO** was obtained as a yellow solid in 68% yield.

¹H NMR (400 MHz, chloroform-d (CDCl₃) δ 9.19 (s, 2H), 7.81 (dd, $J = 7.4, 1.9$ Hz, 2H), 7.62 – 7.55 (m, 2H), 7.55 – 7.48 (m, 4H), 7.39 – 7.30 (m, 8H), 7.03 (d, $J = 1.8$ Hz, 2H), 5.69 (s, 2H), 4.04 (s, 6H).

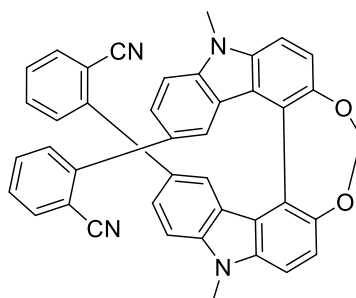
¹³C NMR (400 MHz, chloroform-d (CDCl₃) δ 191.9, 146.5, 141.6, 139.3, 133.1, 132.7, 131.5, 128.4, 127.6, 126.8, 124.9, 122.2, 120.7, 119.3, 109.4, 108.2, 103.8, 29.4.

HR-MS Q-Exactive, ESI, 370 °C; ion [M+Na]⁺, C₄₂H₃₂N₂O₅Na m/z calculated 667.22034, m/z experimental 667.2195 ($\Delta=0$ ppm).

Experimental optical rotation values

(+)-**Hel-o-CHO**: $[\alpha]_D^{25} = +129 \pm 2\%$, $[\phi]_D^{25} = +790$ ($c = 1.3 \times 10^{-3}$, CHCl₃).
(-)-**Hel-o-CHO**: $[\alpha]_D^{25} = -132 \pm 2\%$, $[\phi]_D^{25} = -808$ ($c = 1.2 \times 10^{-3}$, CHCl₃).

(\pm)-2,2'-(8,17-dimethyl-8,17-dihydro-[1,3]dioxepino[4,5-c:7,6-c']dicarbazole-11,14-diyldibenzonitrile: (\pm)-**Hel-o-CN**



Following the same procedure than **Ax-o-CHO**, **Hel-o-CN** was obtained as a yellow solid in 52% yield.

¹H NMR (400 MHz, chloroform-d (CDCl₃) δ 7.70 (dd, *J* = 8.5, 1.8 Hz, 2H), 7.62 – 7.58 (m, 2H), 7.58 – 7.51 (m, 6H), 7.24 – 7.18 (m, 4H), 7.09 (d, *J* = 1.8 Hz, 2H), 5.70 (s, 2H), 5.63 – 5.56 (m, 2H), 4.04 (s, 6H).

¹³C NMR (400 MHz, chloroform-d (CDCl₃) δ 146.8, 146.1, 141.8, 139.4, 133.1, 131.8, 130.2, 128.5, 126.5, 125.2, 122.7, 120.9, 119.1, 110.7, 109.4, 107.4, 103.9, 30.2.

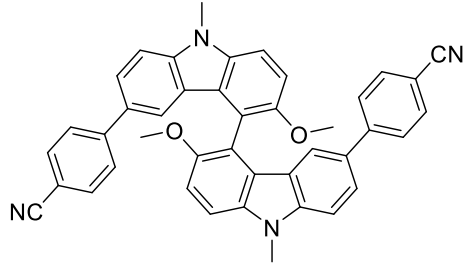
HR-MS Q-Exactive, ESI, 370 °C; ion [M+Na]⁺; C₄₁H₂₆N₄O₂Na m/z calculated 629.1948, m/z experimental 629.1954 ($\Delta=1$ ppm).

Experimental optical rotation values

(+)-**Hel-o-CN**: $[\alpha]_D^{25} = +232 \pm 2\%$, $[\phi]_D^{25} = +1405$ (*c* = 1.3×10^{-3} , CHCl₃).

(-)-**Hel-o-CN**: $[\alpha]_D^{25} = -228 \pm 2\%$, $[\phi]_D^{25} = -1381$ (*c* = 1.2×10^{-3} , CHCl₃).

(±)-4,4'-(3,3'-dimethoxy-9,9'-dimethyl-9H,9'H-[4,4'-bicarbazole]-6,6'-diyl)dibenzonitrile: (±)-**Ax-p-CN**



Following the same procedure than **Ax-o-CHO**, **Ax-p-CN** was obtained as a yellow solid in 86% yield.

¹H NMR (400 MHz, chloroform-d (CDCl₃) δ 7.58 (m, 8H), 7.48 (d, *J* = 8.8 Hz, 2H), 7.36 (d, *J* = 8.5 Hz, 2H), 7.25 – 7.18 (m, 4H), 6.85 (dd, *J* = 1.9, 0.6 Hz, 2H), 3.95 (s, 6H), 3.8 (s, 6H).

¹³C NMR (400 MHz, chloroform-d (CDCl₃) δ 151.56, 146.36, 142.15, 137.47, 132.25, 128.78, 126.80, 124.57, 123.40, 122.31, 120.67, 119.70 (d, *J* = 96.4 Hz), 112.83, 109.15, 108.54 (d, *J* = 9.9 Hz), 58.06.

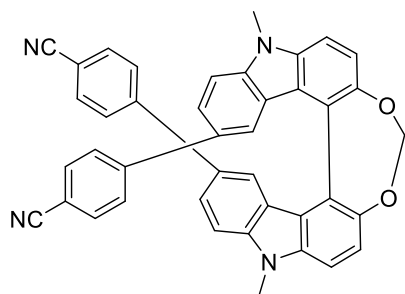
HR-MS Q-Exactive, ESI, 370 °C; ion [M+Na]⁺; C₄₂H₃₀N₄O₂Na m/z calculated 645.2261, m/z experimental 645.2254 ($\Delta=1$ ppm).

Experimental optical rotation values

(+)-**Ax-p-CN**: $[\alpha]_D^{25} = +136 \pm 2\%$, $[\phi]_D^{25} = +846$ (*c* = 1.3×10^{-3} , CHCl₃).

(-)-**Ax-p-CN**: $[\alpha]_D^{25} = -132 \pm 2\%$, $[\phi]_D^{25} = -822$ (*c* = 1.2×10^{-3} , CHCl₃).

(\pm)-4,4'-(8,17-dimethyl-8,17-dihydro-[1,3]dioxepino[4,5-c:7,6-c']dicarbazole-11,14-diyl)dibenzonitrile: (\pm)-**Hel-p-CN**



Following the same procedure than **Ax-o-CHO**, **Hel-p-CN** was obtained as a white solid in 74% yield.

¹H NMR (400 MHz, chloroform-d (CDCl₃) δ 7.63 (d, *J* = 8.7 Hz, 2H), 7.59 – 7.51 (m, 4H), 7.48 (dd, *J* = 8.5, 1.8 Hz, 2H), 7.42 – 7.34 (m, 6H), 7.20 (dd, *J* = 1.8, 0.6 Hz, 2H), 6.93 – 6.17 (m, 2H), 5.71 (s, 2H), 4.10 (s, 6H).

¹³C NMR (400 MHz, chloroform-d (CDCl₃) δ 146.7, 141.8, 139.4, 131.8, 129.5, 127.2, 125.3, 123.5, 122.7, 120.9, 119.6, 119.0, 109.4, 108.0, 103.9, 29.6.

HR-MS Q-Exactive, ESI, 370 °C; ion [M+Na]⁺, C₄₂H₃₀N₄O₂Na m/z calculated 629.1948, m/z experimental 629.1947 ($\Delta=0$ ppm).

Experimental optical rotation values

(+)-**Hel-p-CN**: $[\alpha]_D^{25} = +618 \pm 2\%$, $[\phi]_D^{25} = +3749$ (*c* = 1.3×10^{-3} , CHCl₃).

(-)-**Hel-p-CN**: $[\alpha]_D^{25} = -626 \pm 2\%$, $[\phi]_D^{25} = -3797$ (*c* = 1.2×10^{-3} , CHCl₃).

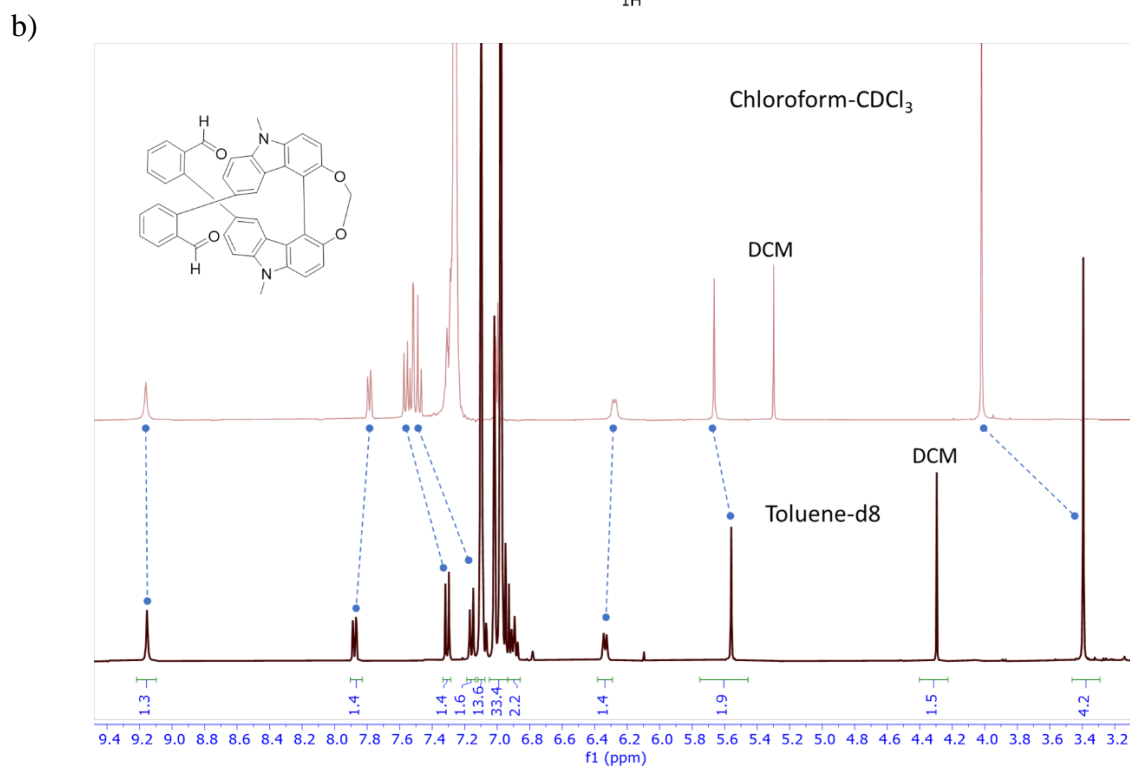
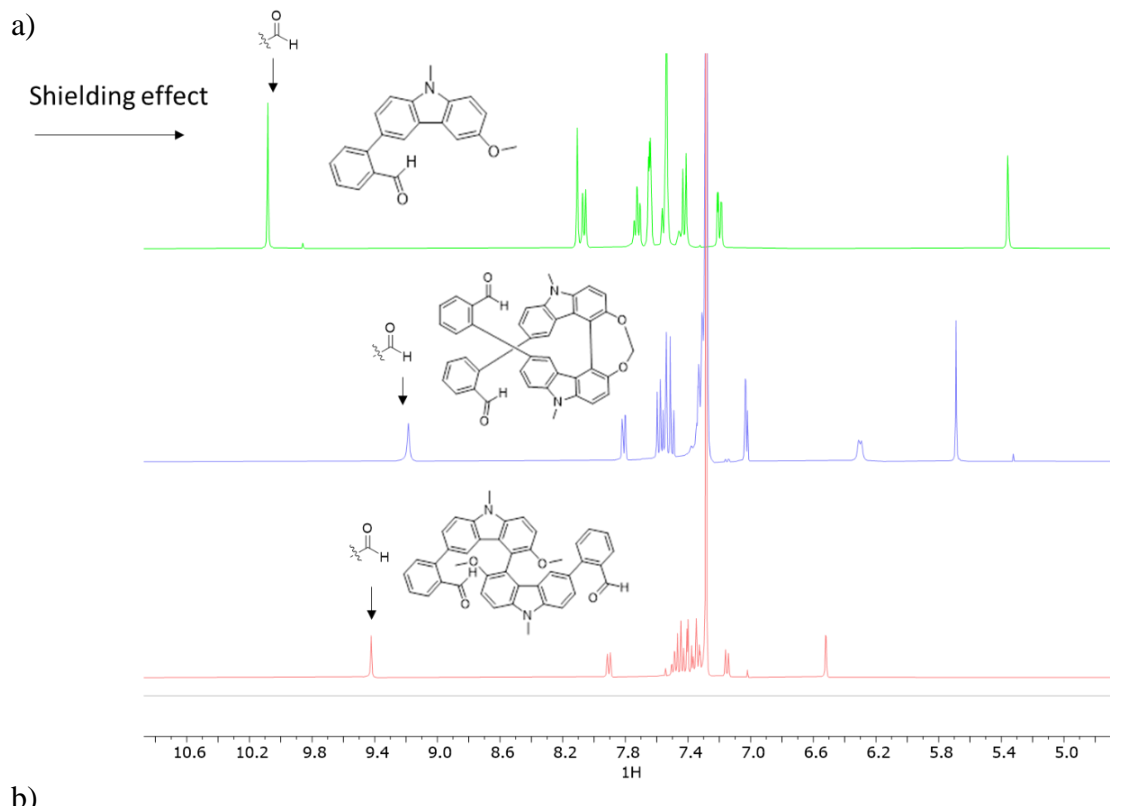
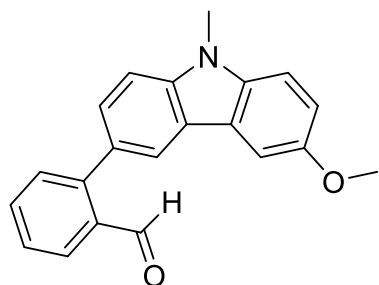


Figure S1. a): ^1H NMR portion of **Ax-*o*-CHO**, **Hel-*o*-CHO** and **CBz-*o*-CHO** spectra showing the shielding of the aldehydic proton signal owing to the current ring effect induced by the opposite carbazole unit (not present on the model compound **CBz-*o*-CHO**). b): ^1H NMR portion of **Hel-*o*-CHO** recorded in deuterated chloroform (red top spectrum) and toluene (brown bottom spectrum).

2-(6-methoxy-9-methyl-9H-carbazol-3-yl)benzaldehyde: **CBz-*o*-CHO**



In a dried Schlenck, 3-iodo-6-methoxy carbazole (0.35 g, 1.038 mmol), 2-formylphenyl boronic acid (0.47 g, 3.115 mmol), K_2CO_3 (0.60 g, 4.15 mmol) were dissolved in a mixture of DMF (15 mL) and water (5 mL) under argon. The mixture was degassed by argon bubbling for 15 minutes before $\text{Pd}(\text{dpf})\text{Cl}_2$ (0.1038 g, 0.07 mmol) was added and the resulting solution refluxed for 8 hours. After cooling down to room temperature, the reaction was poured into 20 mL of water and the organic layer was extracted 3 times with methylene chloride (3*20 mL) and thus washed with brine (20 mL) and dried over MgSO_4 . Solvents were removed under vacuum and the product was purified by chromatography (EtOAc/heptane, 25:75) to give white product 52%.

^1H NMR (400 MHz, methylene chloride-d (CD_2Cl_2) δ 10.08 (s, 1H), 8.11 (d, $J = 1.3$ Hz, 1H), 8.06 (dd, $J = 7.8, 1.4$ Hz, 1H), 7.73 (td, $J = 7.5, 1.5$ Hz, 1H), 7.67 – 7.63 (m, 2H), 7.54 (t, $J = 2.2$ Hz, 3H), 7.42 (d, $J = 8.9$ Hz, 1H), 7.20 (dd, $J = 8.9, 2.5$ Hz, 1H), 3.95 (s, 3H), 3.92 (s, 3H).

^{13}C NMR (400 MHz, methylene chloride-d (CD_2Cl_2) δ 192.6, 153.9, 146.9, 141.2, 136.6, 134.0, 133.3, 131.3, 127.8, 127.3, 127.0, 122.7, 122.5, 121.9, 115.4, 109.5, 108.5, 103.1, 55.9, 31.8, 29.2, 29.0, 22.6, 13.8.

C. Steady-state photophysical and chiroptical characterizations

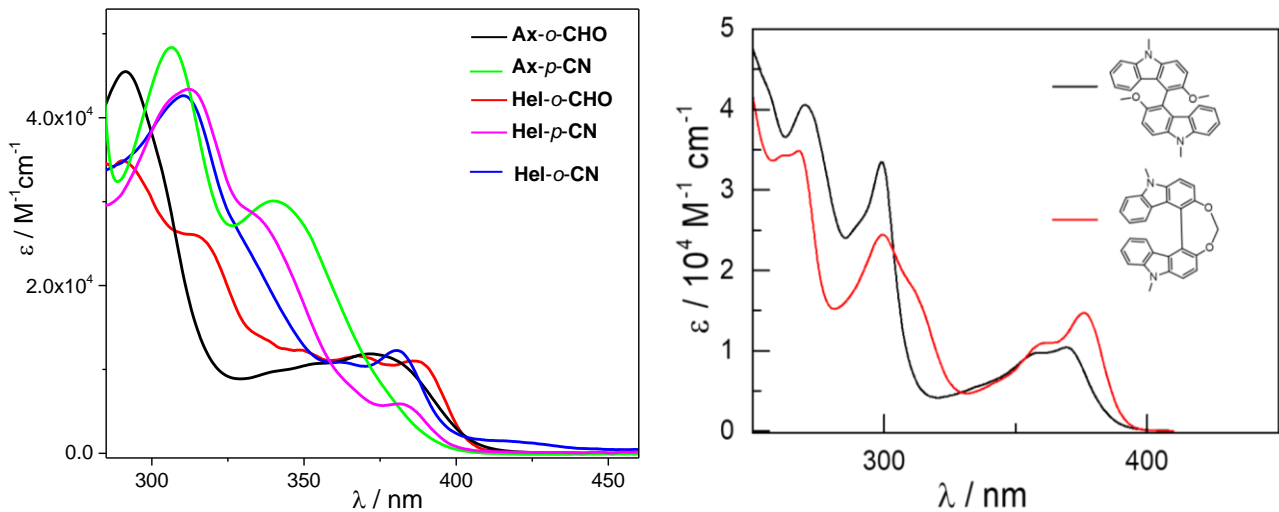


Figure S2. Left: UV-vis spectra of **Hel-o-CHO** (red), **Hel-o-CN** (blue), **Ax-o-CHO** (black), **Ax-p-CN** (green) and **Hel-p-CN** (purple) measured in toluene ($\sim 10^{-5}$ M) at 298 K, and right: their corresponding bicarbazole precursors measured in chloroform ($\sim 10^{-5}$ M) at 298 K.

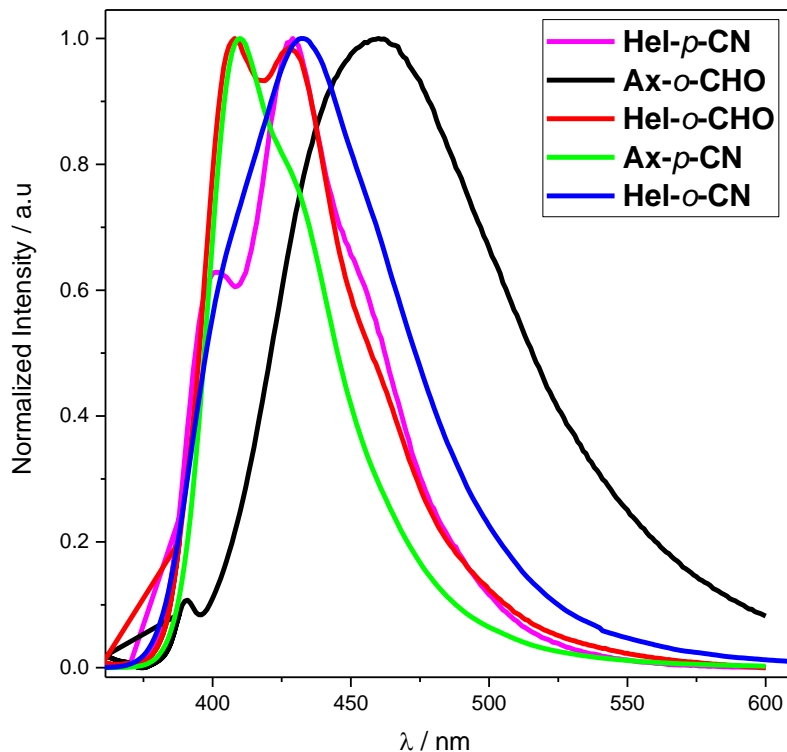


Figure S3. Normalized luminescence spectra of **Hel-o-CHO** (red), **Hel-o-CN** (blue), **Ax-o-CHO** (black), **Ax-p-CN** (green) and **Hel-p-CN** (purple) measured in toluene ($\sim 10^{-5}$ M) at 298 K.

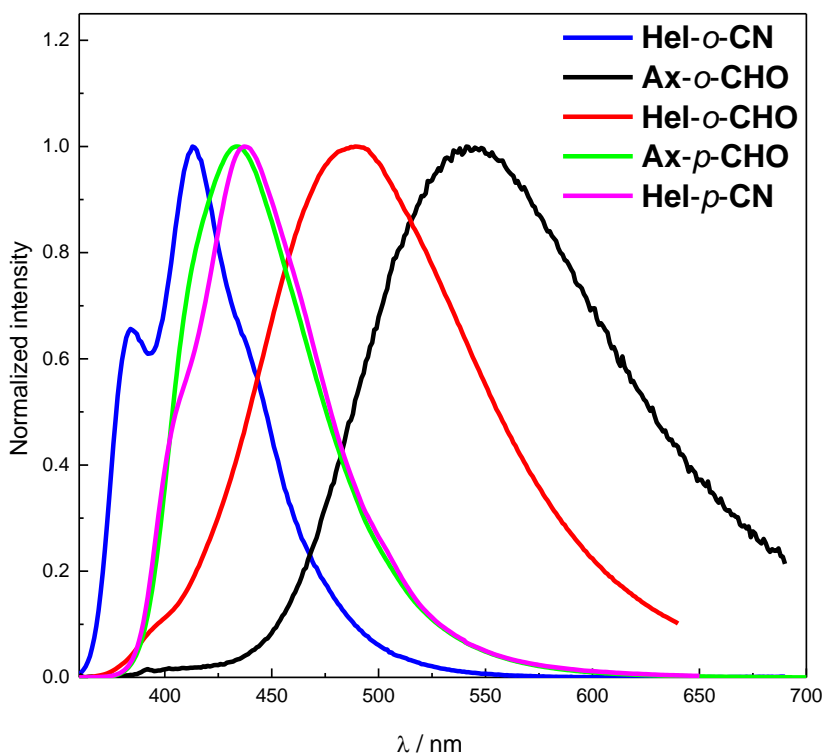


Figure S4. Normalized luminescence spectra of **Hel-*o*-CHO** (red), **Hel-*o*-CN** (blue), **Ax-*o*-CHO** (black), **Ax-*p*-CN** (green) and **Hel-*p*-CN** (purple) measured in chloroform ($\sim 10^{-5}$ M) at 298 K.

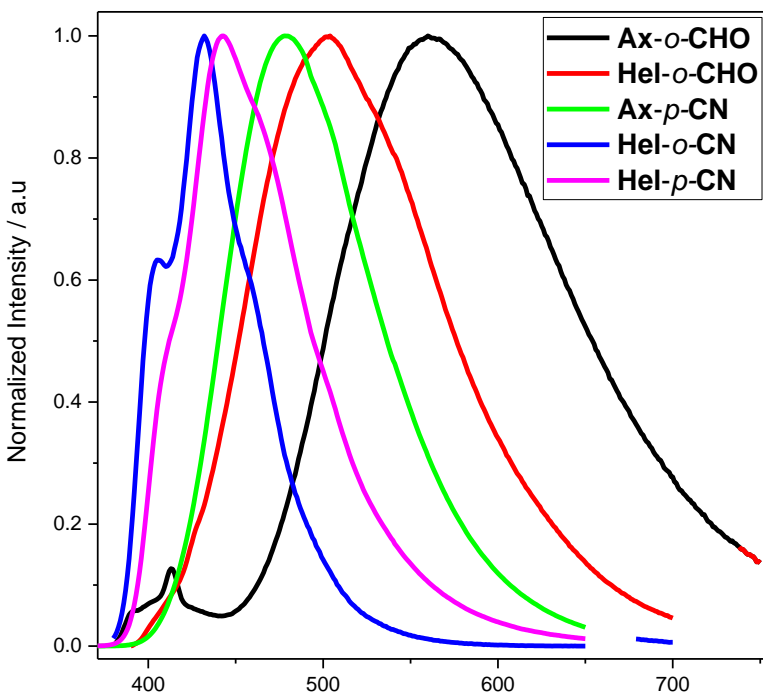


Figure S5. Normalized luminescence spectra of **Hel-*p*-CHO** (red), **Hel-*o*-CN** (blue), **Ax-*o*-CHO** (black), **Ax-*p*-CN** (green) and **Hel-*p*-CN** (purple) measured in dimethylformamide ($\sim 10^{-5}$ M) at 298 K.

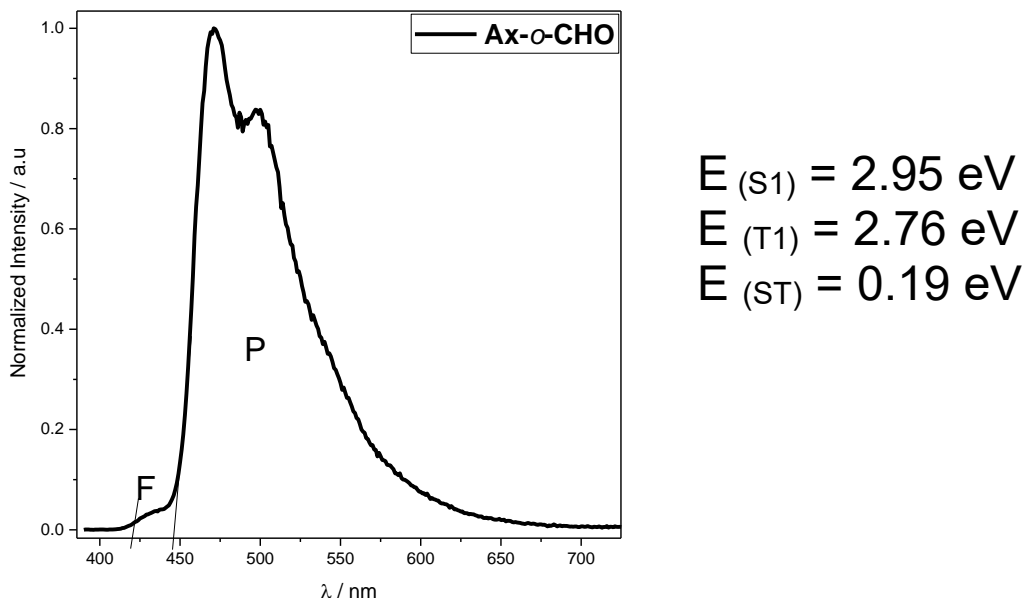
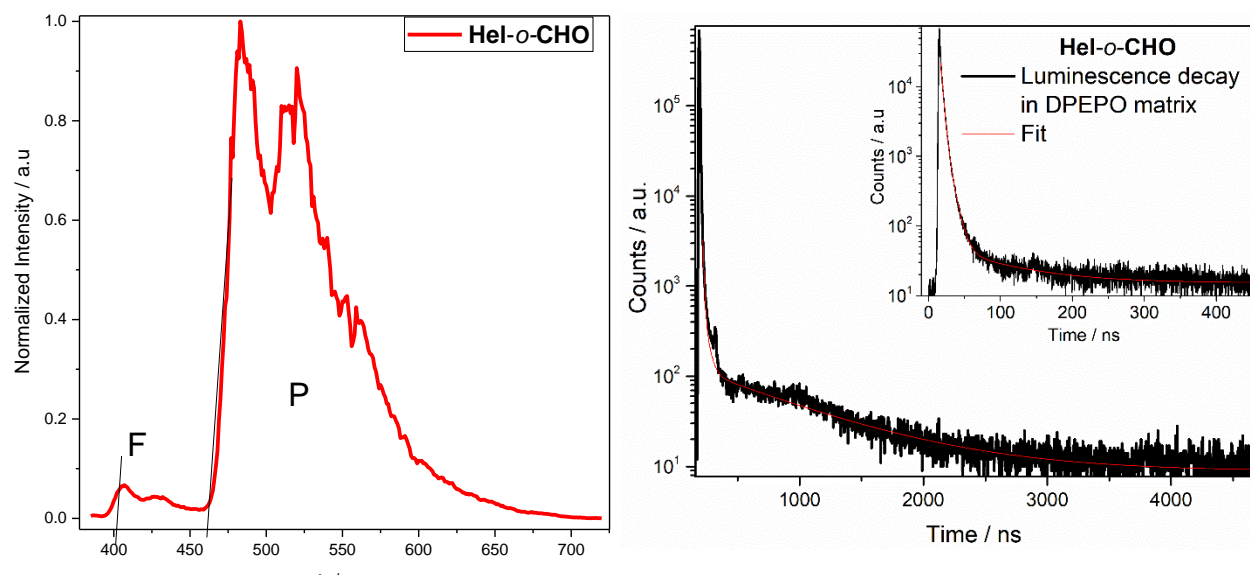
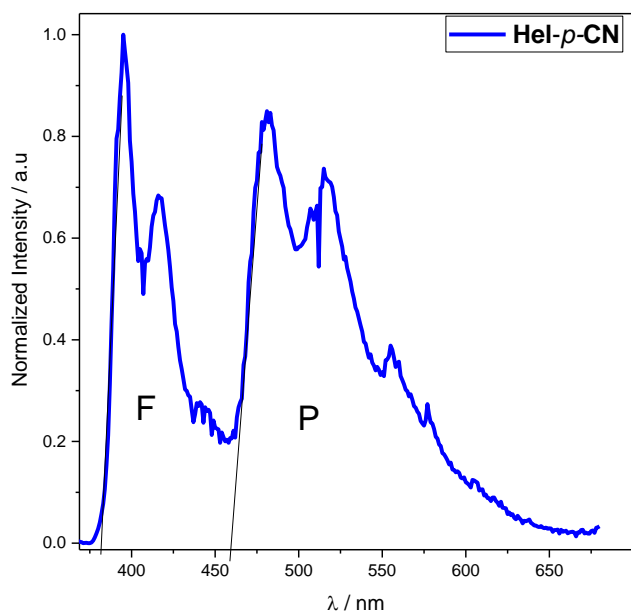


Figure S6. Normalized luminescence spectrum of **Ax-o-CHO** in 2-methyltetrahydrofuran at 77 K and excited at 375 nm (the onset of both fluorescence (F) and phosphorescence (P) emissions are taken to estimate the singlet and triplet energy levels).



$$E_{(S1)} = 3.06 \text{ eV} / E_{(T1)} = 2.67 \text{ eV} / E_{(ST)} = 0.39 \text{ eV}$$

Figure S7. Left: Normalized luminescence spectrum of **Hel-o-CHO** in 2-methyltetrahydrofuran at 77 K and excited at 375 nm (the onset of both fluorescence (F) and phosphorescence (P) emissions are taken to estimate the singlet and triplet energy levels). Right: Luminescence decays of (+)-**Hel-o-CHO** (black signal, corresponding fits in red) recording under vacuum in solid matrix [bis[2-(diphenylphosphino)phenyl] ether oxide, DPEPO] with an inset focusing on the short lifetime decays.

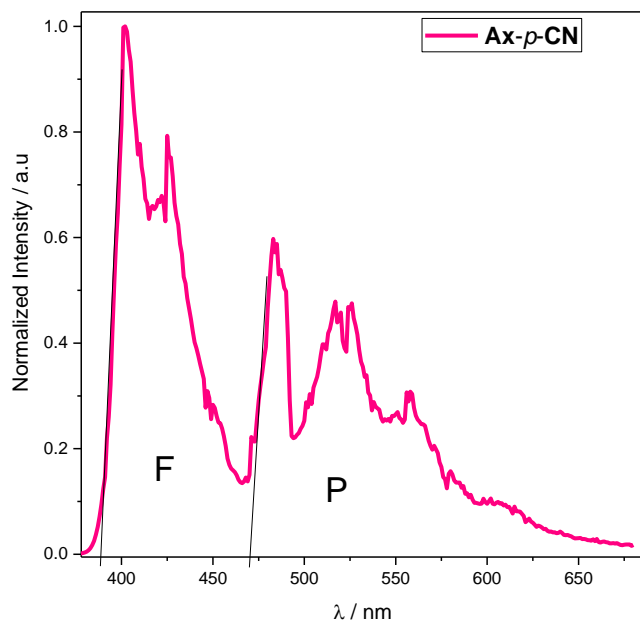


$$E_{(S1)} = 3.26 \text{ eV}$$

$$E_{(T1)} = 2.69 \text{ eV}$$

$$E_{(ST)} = 0.57 \text{ eV}$$

Figure S8. Normalized luminescence spectrum of **HeI-*p*-CN** in 2-methyltetrahydrofuran at 77 K and excited at 360 nm (the onset of both fluorescence (F) and phosphorescence (P) emissions are taken to estimate the singlet and triplet energy levels).



$$E_{(S1)} = 3.20 \text{ eV}$$

$$E_{(T1)} = 2.64 \text{ eV}$$

$$E_{(ST)} = 0.54 \text{ eV}$$

Figure S9. Normalized luminescence spectrum of **Ax-*p*-CN** in 2-methyltetrahydrofuran at 77 K and excited at 360 nm (the onset of both fluorescence (F) and phosphorescence (P) emissions are taken to estimate the singlet and triplet energy levels).

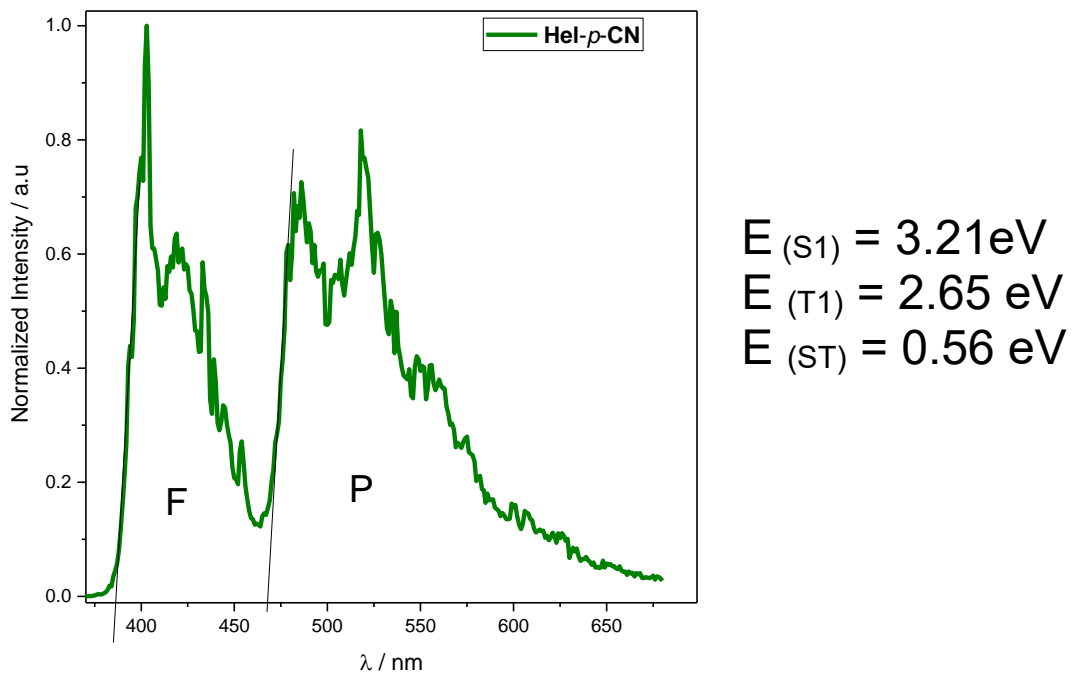


Figure S10. Normalized luminescence spectrum of **Hel-p-CN** in 2-methyltetrahydrofuran at 77 K and excited at 360 nm (the onset of both fluorescence (F) and phosphorescence (P) emissions are taken to estimate the singlet and triplet energy levels).

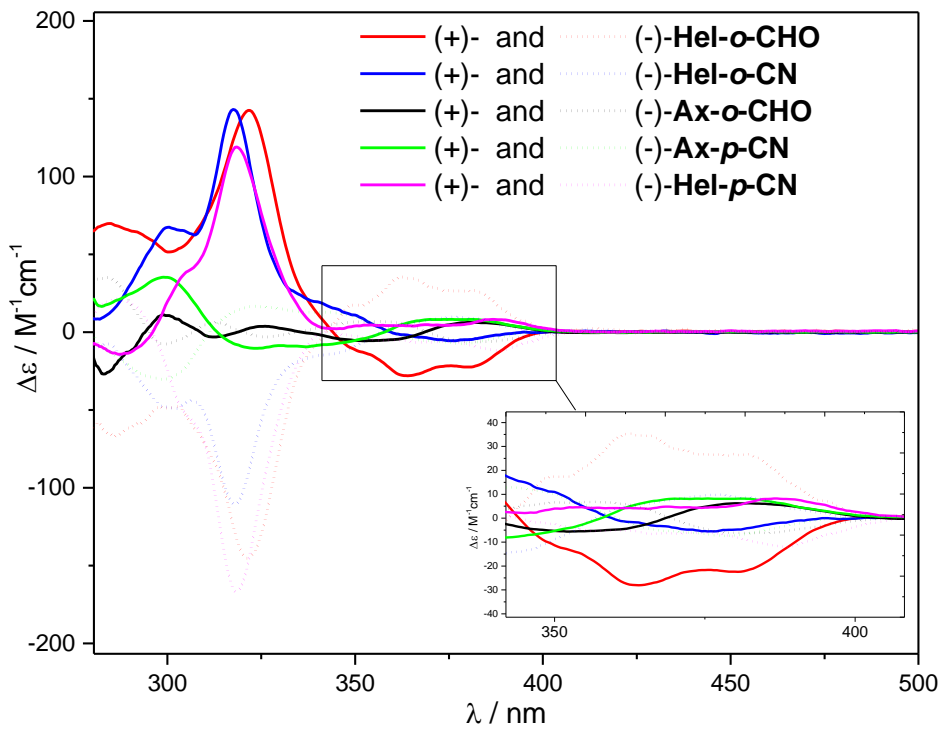


Figure S11. ECD spectra of **Hel-o-CHO** (red), **Hel-o-CN** (blue), **Ax-o-CHO** (black), **Ax-p-CN** (green) and **Hel-p-CN** (purple) measured in toluene ($\sim 10^{-5} \text{ M}$) at 298 K.

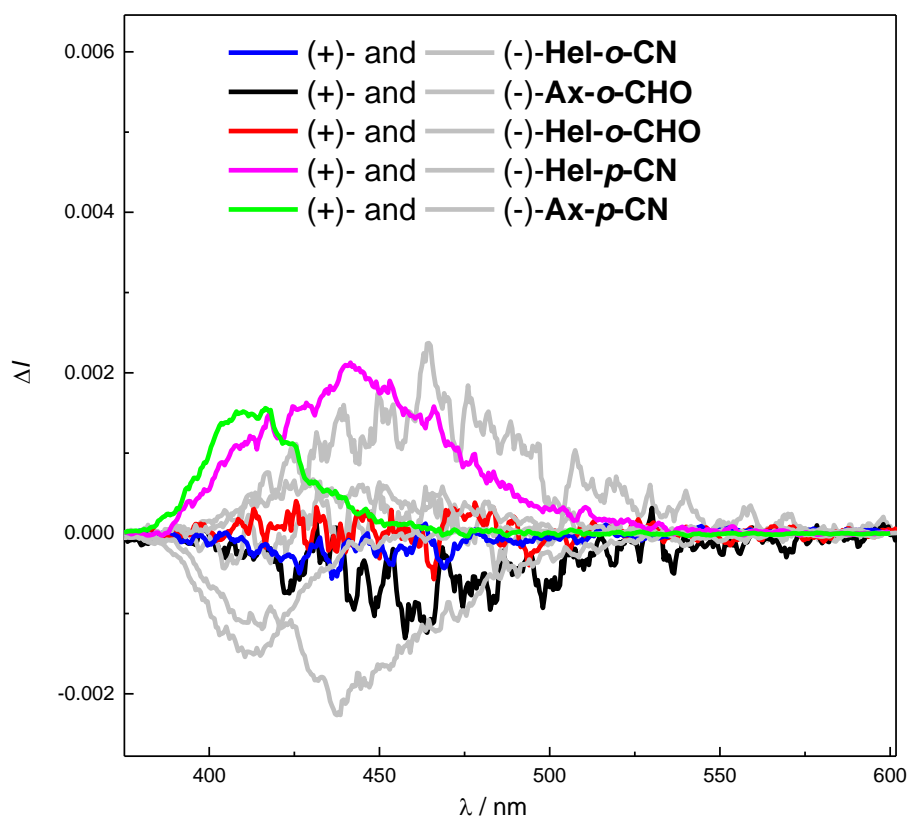


Figure S12. CPL spectra of **Hel-*o*-CHO** (red), **Hel-*o*-CN** (blue), **Ax-*o*-CHO** (black), **Ax-*p*-CN** (green) and **Hel-*p*-CN** (purple) measured in toluene ($\sim 10^{-5} \text{ M}$) at 298 K.

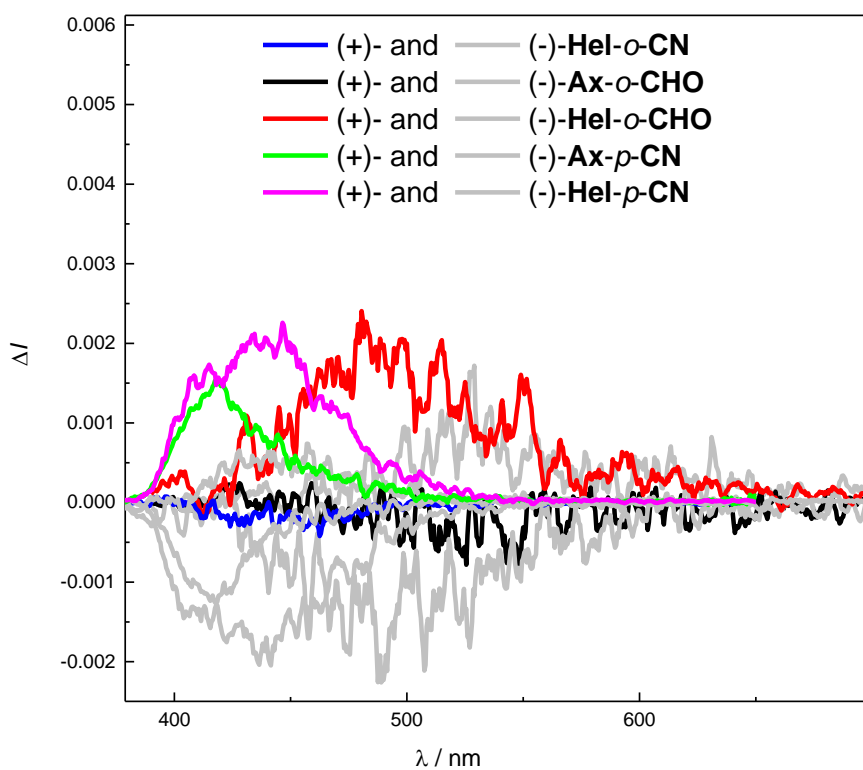


Figure S13. CPL spectra of **Hel-*o*-CHO** (red), **Hel-*o*-CN** (blue), **Ax-*o*-CHO** (black), **Ax-*p*-CN** (green) and **Hel-*p*-CN** (purple) measured in chloroform ($\sim 10^{-5} \text{ M}$) at 298 K.

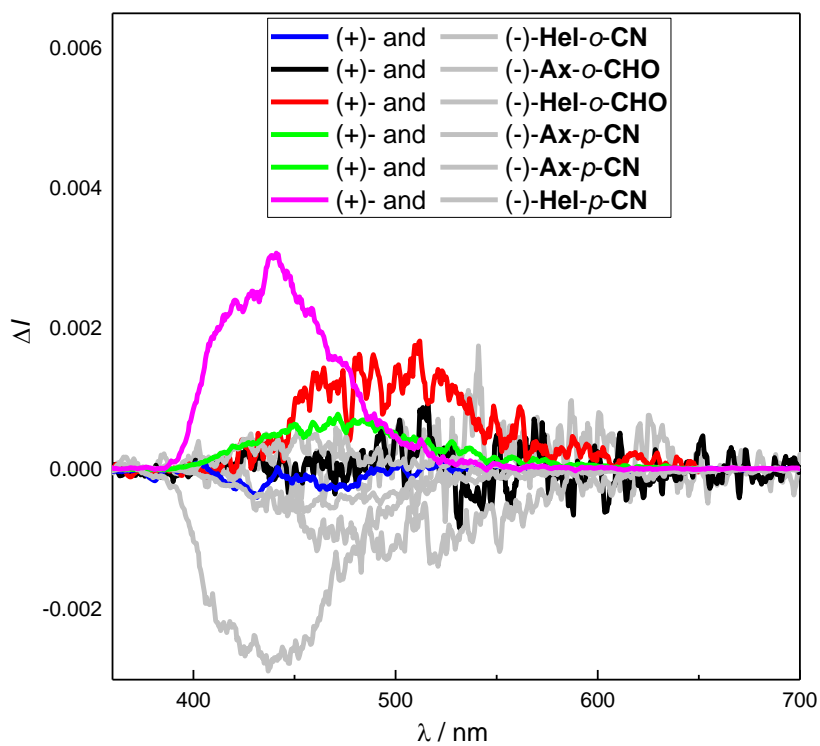


Figure S14. CPL spectra of **Hel-*o*-CHO** (red), **Hel-*o*-CN** (blue), **Ax-*o*-CHO** (black), **Ax-*p*-CN** (green) and **Hel-*p*-CN** (purple) measured in dimethylformamide ($\sim 10^{-5} \text{ M}$) at 298 K.

Table S1. Summary of the photophysical and chiroptical data for **Hel-*o*-CHO**, **Hel-*o*-CN**, **Ax-*o*-CHO**, **Ax-*p*-CN** and **Hel-*p*-CN**.

Compound	$\lambda_{\text{abs}} \text{ Tol}^{\text{a}}$	$ \text{g}_{\text{Abs}} ^{\text{a}}$	$\lambda_{\text{em}} \text{ Tol}$	$\lambda_{\text{em}} \text{ CHCl}_3$	$\lambda_{\text{em}} \text{ DMF}$	$\tau_{\text{Fluo}}^{\text{c}} [\text{ns}]$	$ \text{g}_{\text{lum}} (\times 10^{-3})$		
	(onset in nm)	($\times 10^{-3}$)	(nm) / $\phi_{\text{fluo}}^{\text{b}} (\%)$	(nm) / $\phi_{\text{fluo}}^{\text{b}} (\%)$	(nm) / $\phi_{\text{fluo}}^{\text{b}} (\%)$		Tol	CHCl ₃	DMF
Hel-<i>o</i>-CHO	410	0.0	439 / 2	477 / 7	490 / 6	2.6 / 10.8 (8 / 36 / 804) ^d	~ 0.0	2.0	1.6
Hel-<i>o</i>-CN	375	0.6	435 / 20	435 / 10	455 / 13	4.0	0.5	0.5	0.4
Hel-<i>p</i>-CN	401	2.0	438 / 17	438 / 15	444 / 20	2.7	2.5	2.5	3.0
Ax-<i>o</i>-CHO	415	1.0	460 / 3	531 / 4	543 / 2	3.1 (8.4 / 71 / 1040) ^d	1.0	0.7	0.5
Ax-<i>p</i>-CN	390	2.2	412 / 25	436 / 37	461 / 84	3.8	1.5	1.4	1.1

^a In toluene solution. ^b Absolute quantum yield (error $\pm 10\%$), measured using an integrating sphere (Tol for toluene, CHCl₃ for chloroform and DMF for dimethylformamide). ^c Fluorescence lifetime measured in dichloromethane solution (error $\pm 5\%$) and weight in parenthesis. ^d Lifetimes measured in DPEPO matrix.

Table S2. Electrochemical data for **Hel-*o*-CHO**, **Hel-*o*-CN**, **Ax-*o*-CHO**, **Ax-*p*-CN** and **Hel-*p*-CN**. The redox potentials are referenced *versus* saturated calomel electrode (SCE) and given in V with Fc/Fc⁺ as an internal reference and 0.1 M Bu₄NPF₆ in dichloromethane as the electrolyte.

Compound	Hel- <i>o</i> -CHO	Hel- <i>o</i> -CN	Hel- <i>p</i> -CN	Ax- <i>o</i> -CHO	Ax- <i>p</i> -CN
E¹_{ox}	1.17	1.21	1.21	0.95	0.98
E²_{ox}	1.39	1.39	1.19	1.19	1.19

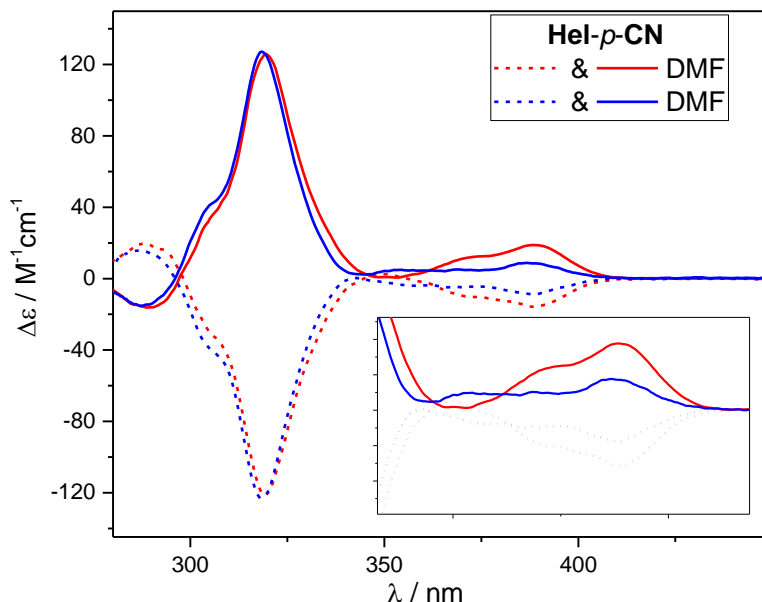


Figure S15. ECD spectra of (+)-Hel-*p*-CN (solid lines) and (-)-Hel-*p*-CN (dashed lines) in toluene (blue) and in dimethylformamide (red) ($\sim 10^{-5}$ M) at 298 K.

D. X-Ray experimental data

Empirical formula	C ₄₃ H ₃₃ C ₁₃ N ₂ O ₄
CCDC number	2085967
Extended formula	C ₄₂ H ₃₂ N ₂ O ₄ ;CHCl ₃
Formula weight	748.06 g/mol
Temperature	150(2) K
Radiation type	Mo-K _α
Wavelength	0.71073 Å
Crystal system, space group	triclinic, P 1
Unit cell dimensions	a = 8.9208 (12) Å b = 13.4572 (16) Å c = 15.7062 (19) Å α = 107.913 (4) ° β = 91.259 (5) ° γ = 95.152 (4) °
Volume	1784.4(4) Å ³
Z, Calculated density	2, 1.392 g·cm ⁻³
Absorption coefficient	0.305 mm ⁻¹
F(000)	776
Crystal size	0.550 x 0.350 x 0.210 mm
Crystal color	yellow
Crystal description	prism
Diffractometer	APEXII Kappa-CCD diffractometer
	θ range for data collection 2.403 to 27.538°
(sinθ=λ) _{max} (Å ⁻¹)	0.651
h _{min} , h _{max}	-11, 11
k _{min} , k _{max}	-12, 17
l _{min} , l _{max}	-20, 19
Reflections collected / unique	29926 / 8200 [^a R(int) = 0.0439]
Reflections [I > 2σ]	6634
Completeness to θ max	0.994
Absorption correction type	multi-scan
Max. and min. transmission	0.938, 0.890
Refinement method	Full-matrix least-squares on F ²
H-atom treatment	H-atom parameters constrained
Data / restraints / parameters	8200 / 0 / 473
^b Goodness-of-fit	0.992
Final R indices [I > 2σ]	^c R1 = 0.0402, ^d wR2 = 0.1117
R indices (all data)	^c R1 = 0.0529, ^d wR2 = 0.1231
Δρ _{max} , Δρ _{min}	0.459, -0.593 e·Å ⁻³

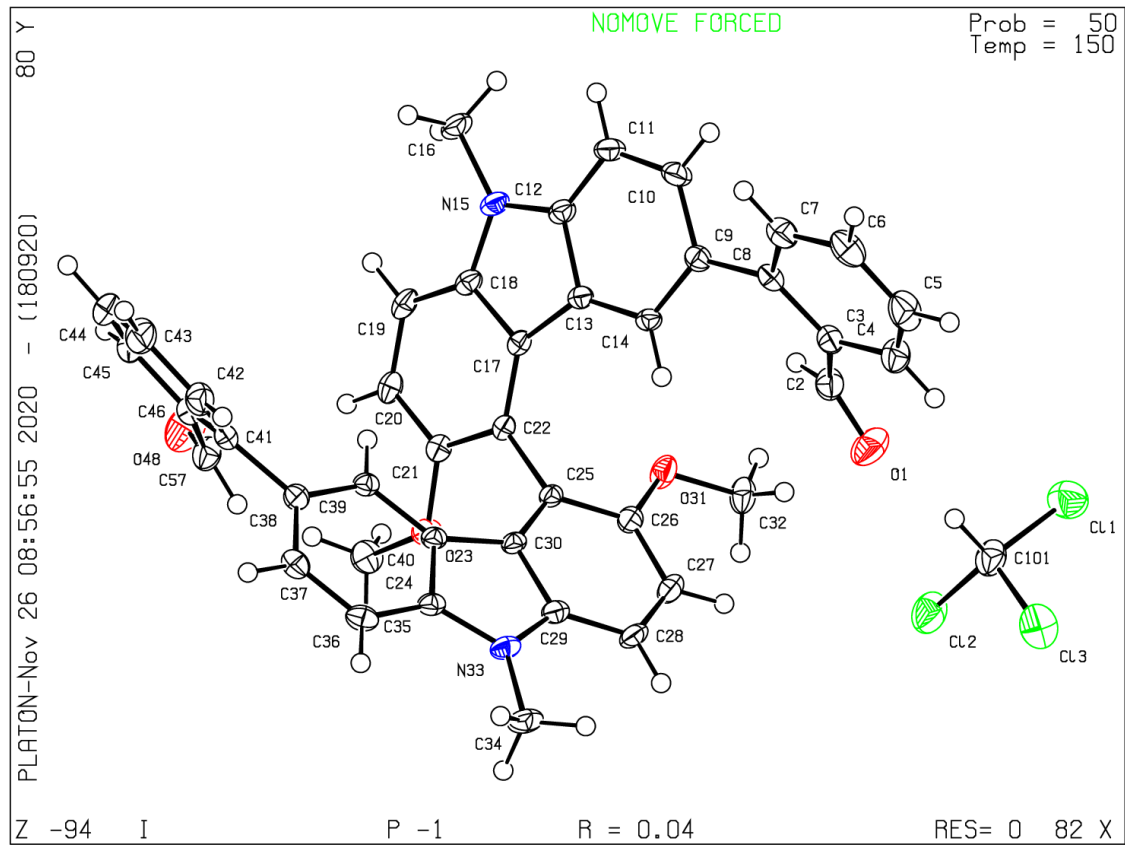


Figure S16. ORTEP diagrams of compound **Ax-o-CHO** with ellipsoids at 50% probability)at 150 K(.

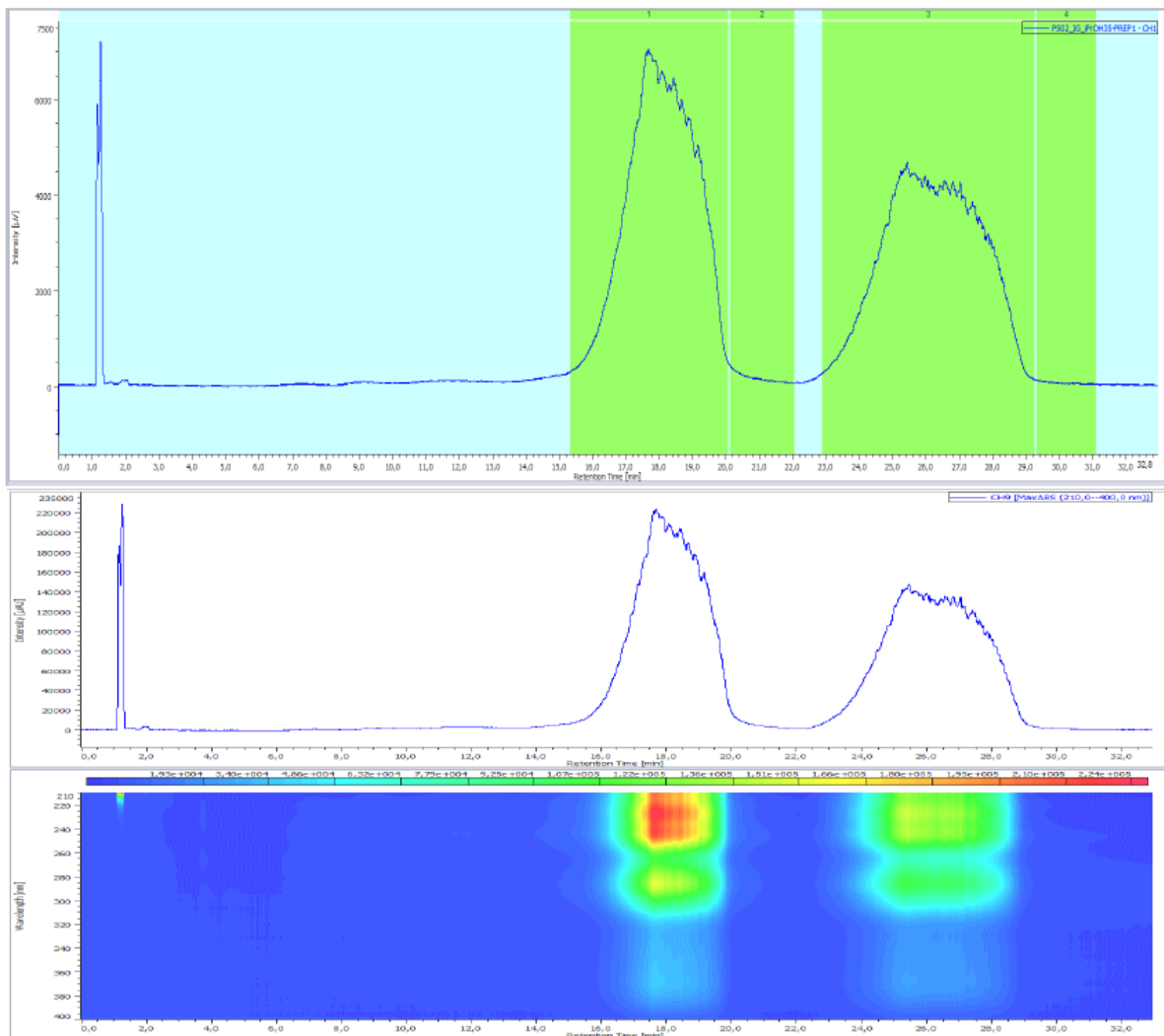
E. HPLC separation

Conditions Analytiques :	
Colonne :	CHIRALPAK IG 250 x 4,6 mm, 5µm
Débit :	4 mL/min
Détection :	200-400 nM MaxAbs
température pression BPR	40°C - 120bars
Solvant :	A : CO ₂
	B : i-PrOH
Gradient :	Isocratique %A : 65 %B : 35

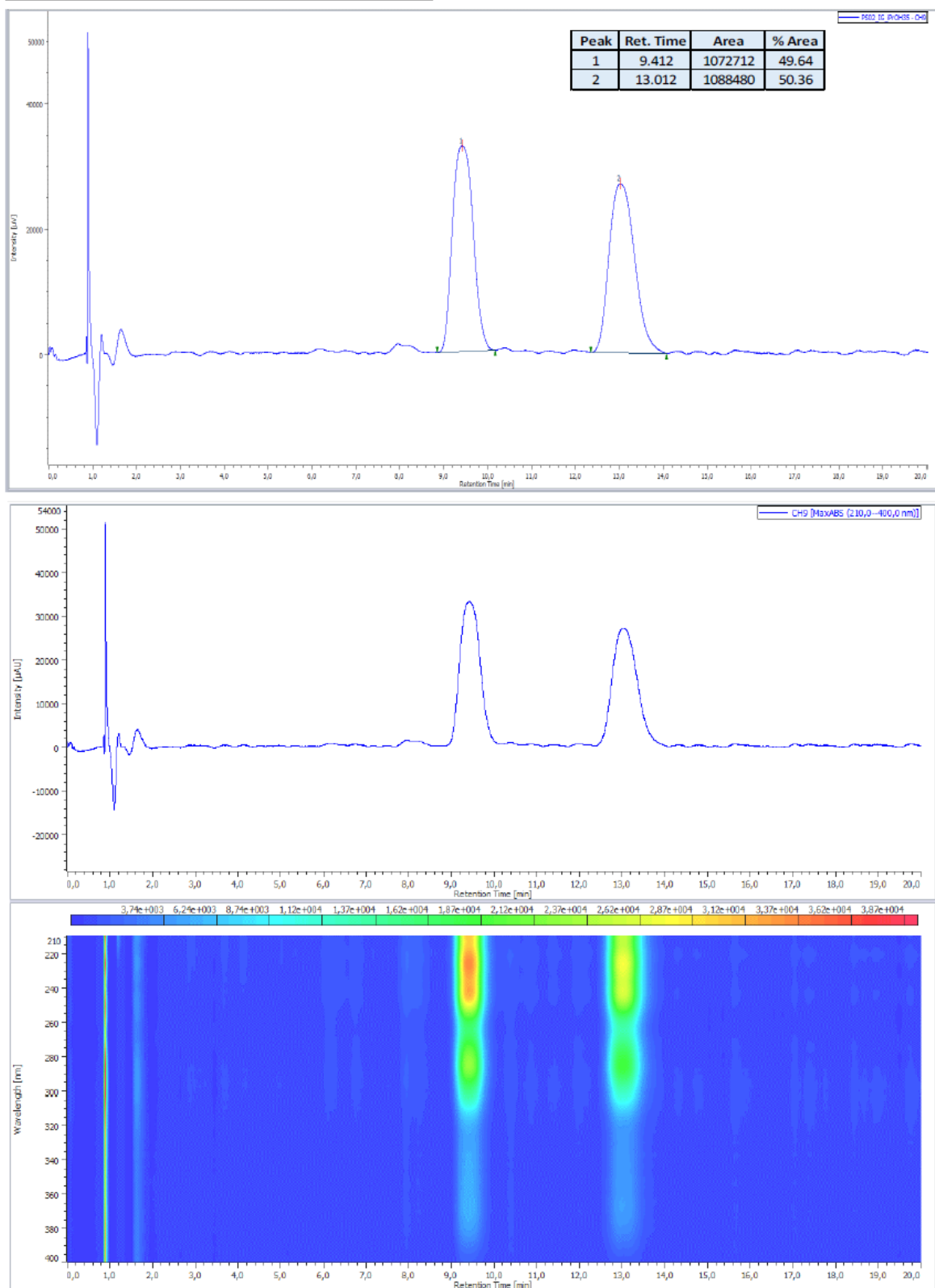
Date : 03/05/2021
Opérateur : LEBREQUIER Sabrina
Demandeur : PIETERS Grégory
Encadrant : PIETERS Grégory

Conditions Prep :	
Colonne :	CHIRALPAK IG 250 x 21 mm, 5µm
Débit :	80 mL/min
Détection :	200-400 nM MaxAbs
température pression BPR	40°C - 100 bars
Solvant :	A : CO ₂
	B : i-PrOH
Gradient :	Isocratique %A : 65 %B : 35

Profil de purification :

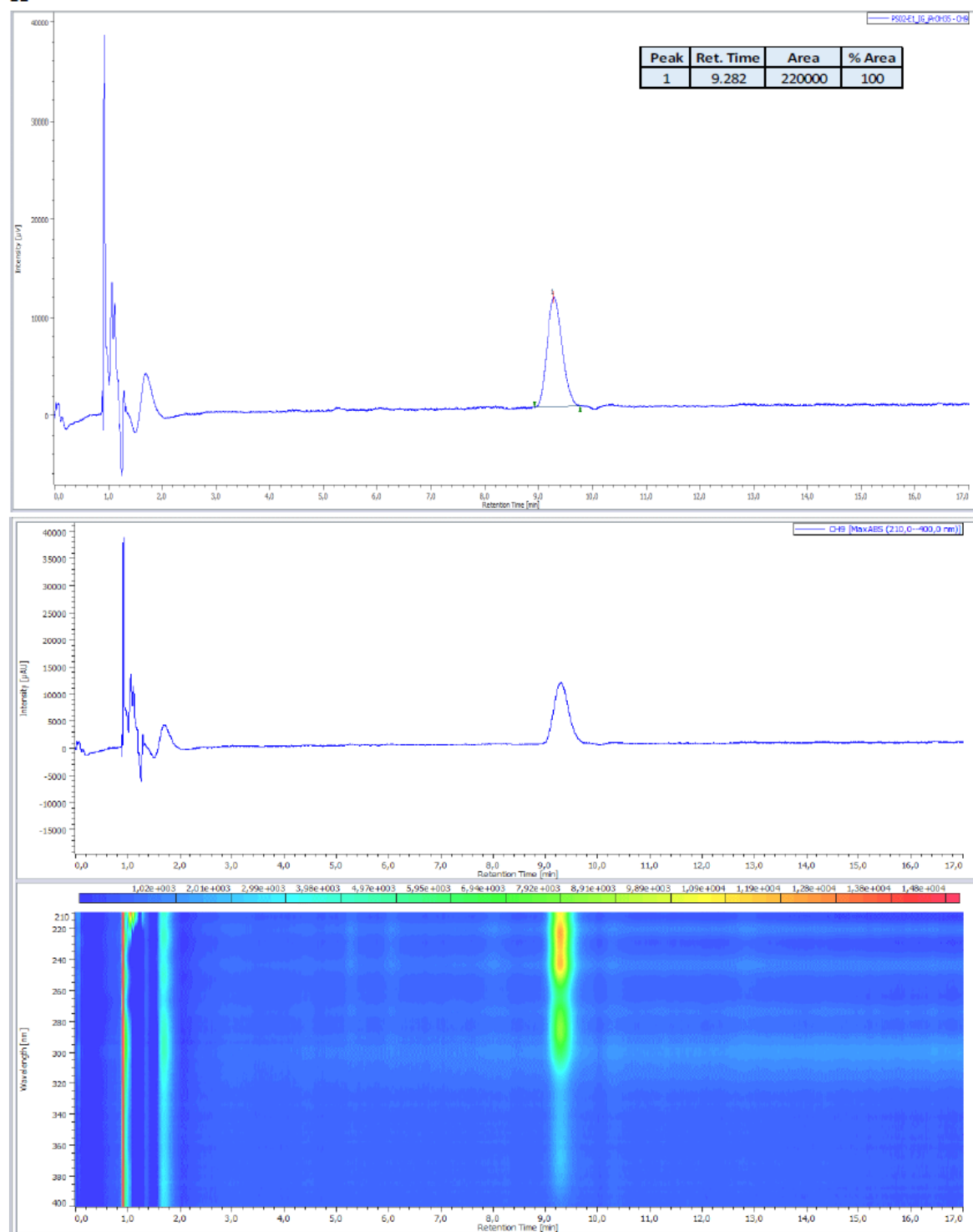


Conditions analytiques : Racémique avant purification :



Vérification des énantiomères

E1



E2

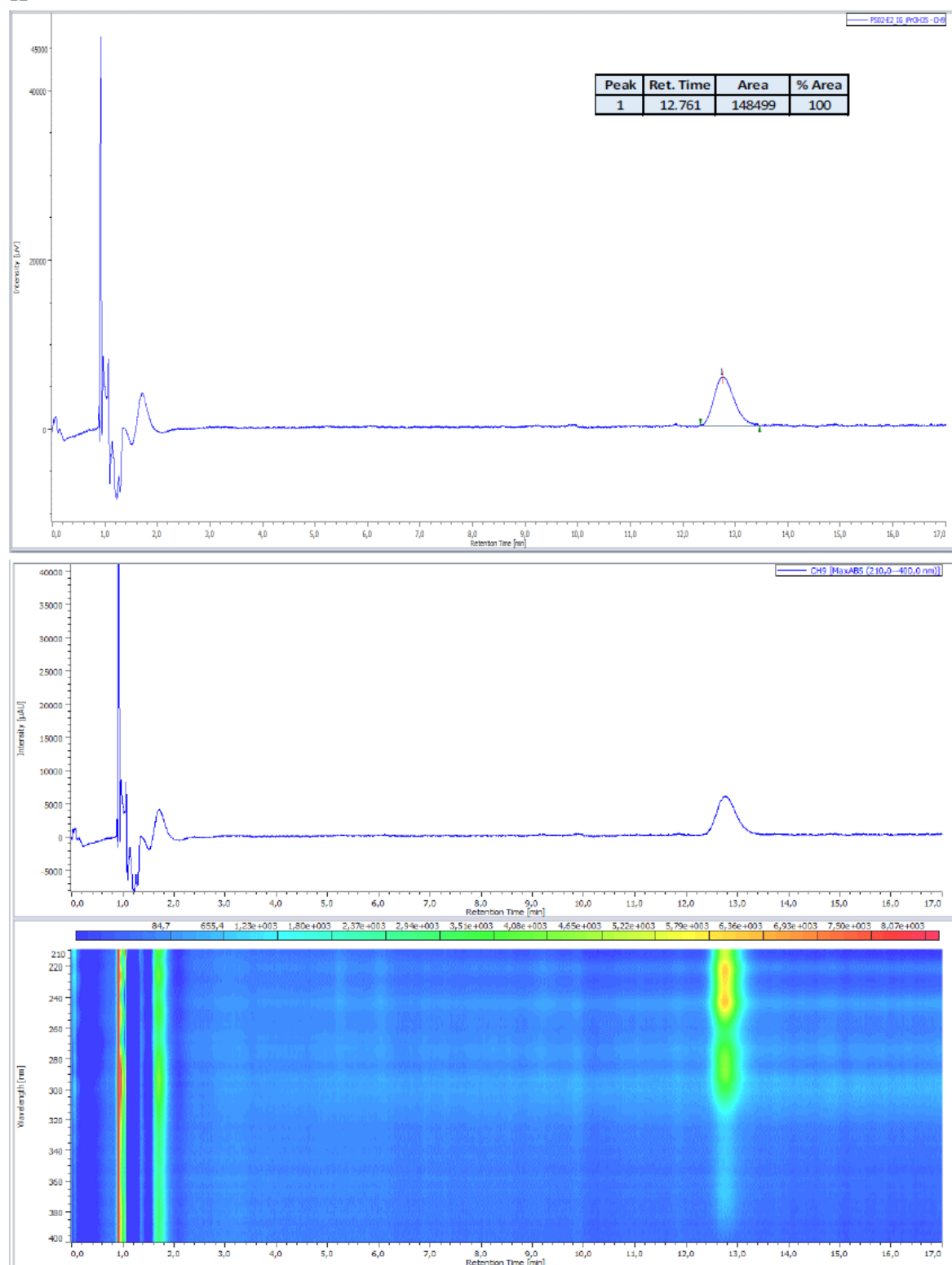


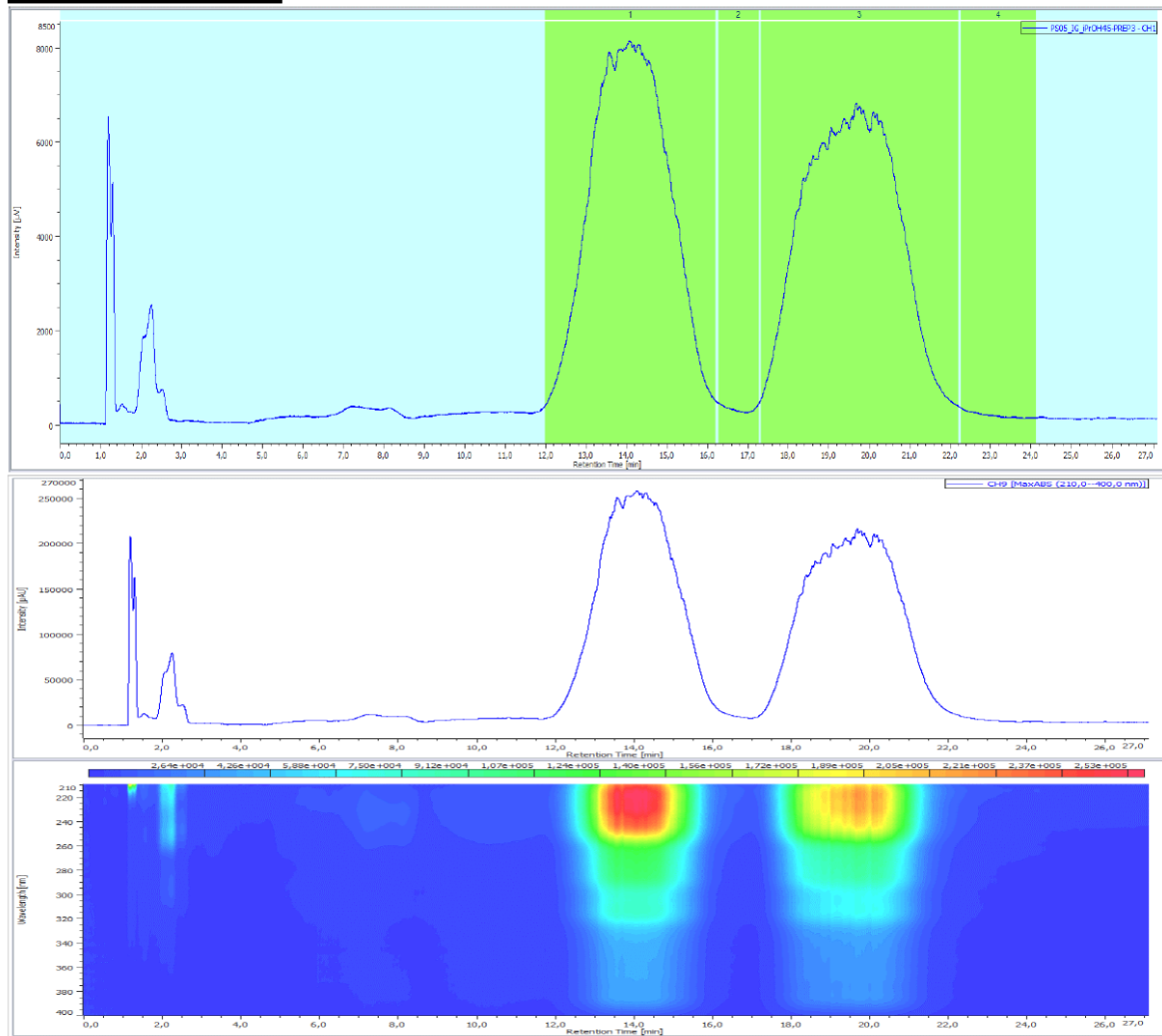
Figure S17. Chiral HPLC of Ax-*o*-CHO.

Conditions Analytiques :	
Colonne :	CHIRALPAK IG 250 x 4,6 mm, 5µm
Débit :	4 mL/min
Détection :	200-400 nM MaxAbs
température pression BPR	40°C - 120bars
Solvant :	A : CO ₂
	B : i-PrOH
Gradient :	Isocratique %A : 55 %B : 45

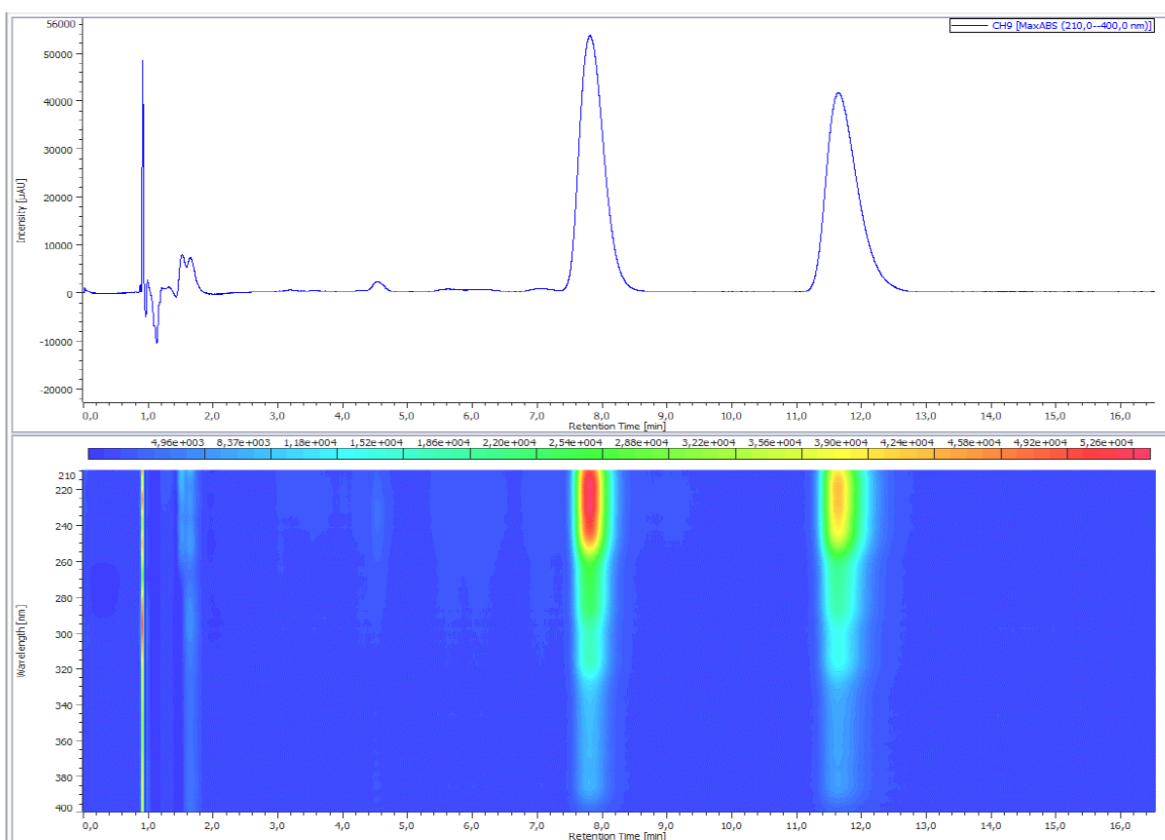
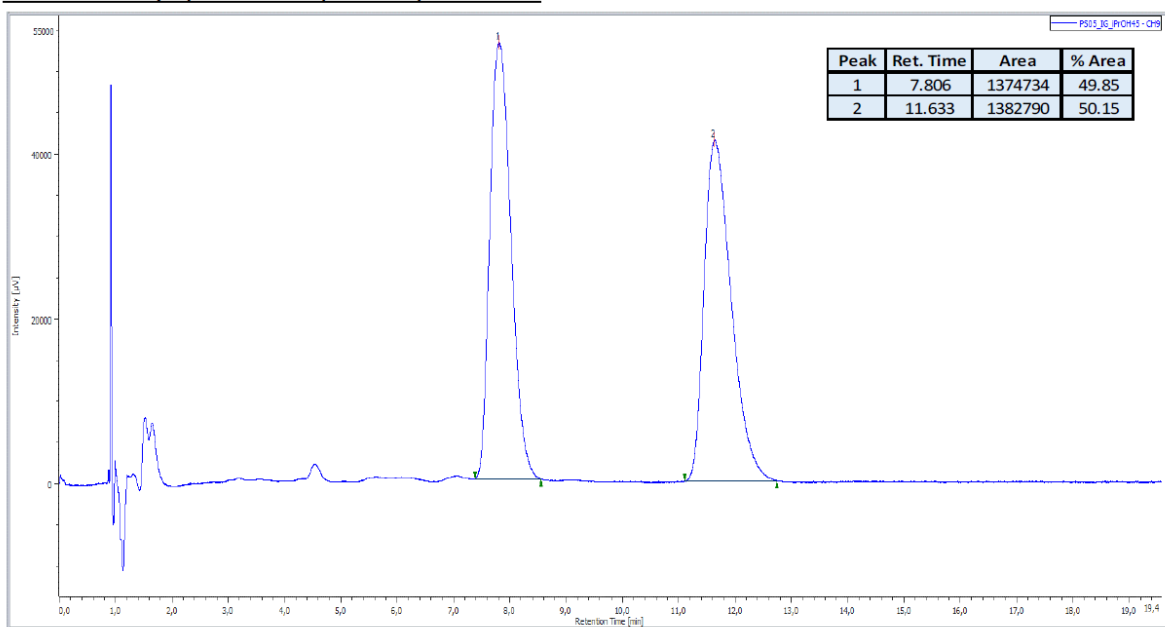
Date : 17/05/2021
Opérateur : LEBREQUIER Sabrina
Demandeur : PIETERS Grégory
Encadrant : PIETERS Grégory

Conditions Prep :	
Colonne :	CHIRALPAK IG 250 x 21 mm, 5µm
Débit :	80 mL/min
Détection :	200-400 nM MaxAbs
température pression BPR	40°C - 100 bars
Solvant :	A : CO ₂
	B : i-PrOH
Gradient :	Isocratique %A : 55 %B : 45

Profil de purification :

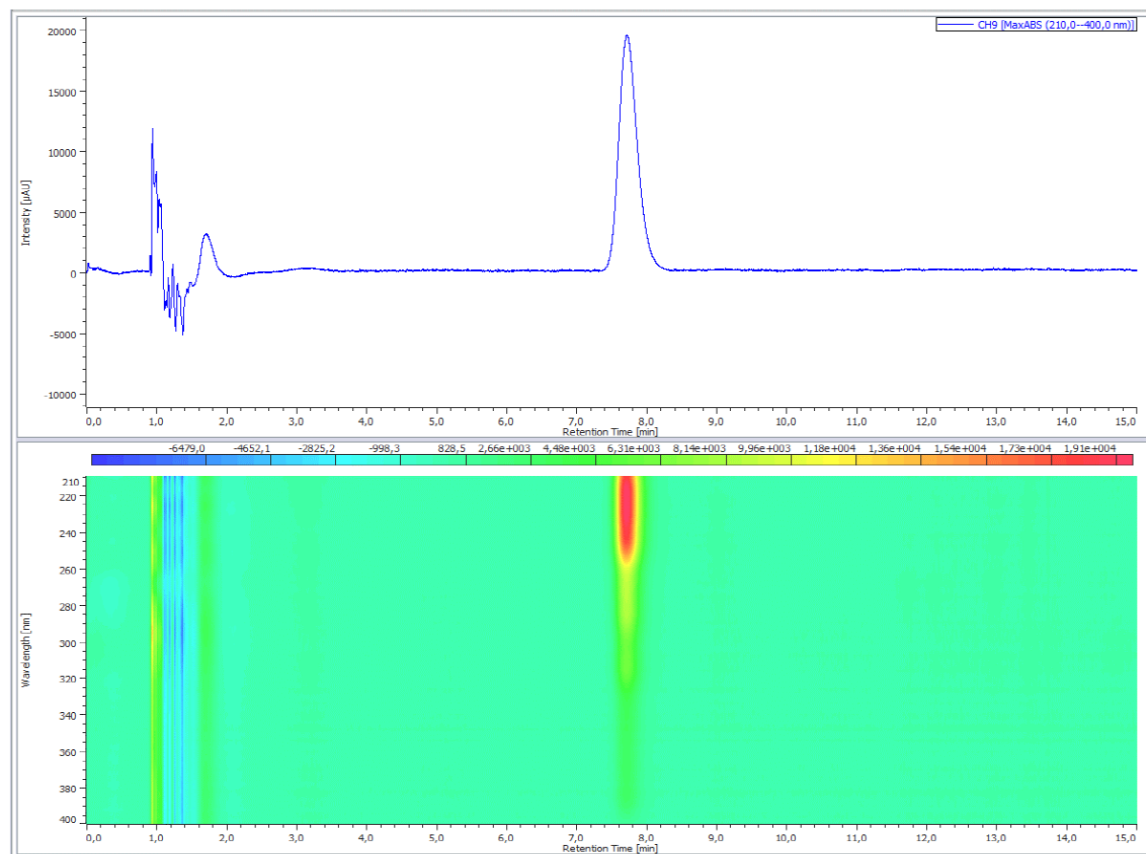
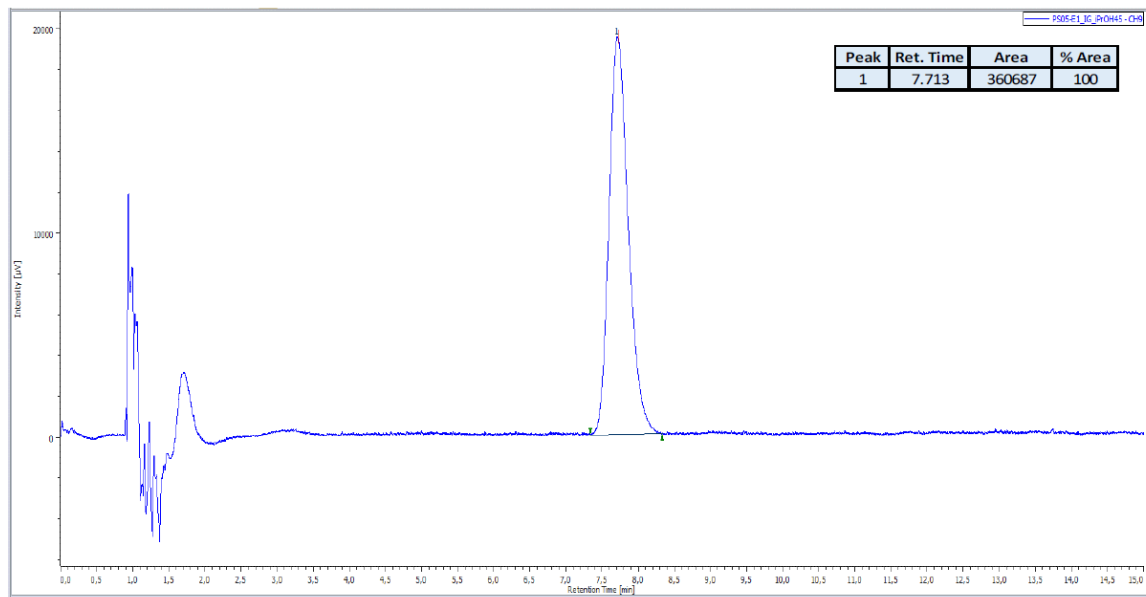


Conditions analytiques : Racémique avant purification :



Vérification des énantiomères

E1



E2

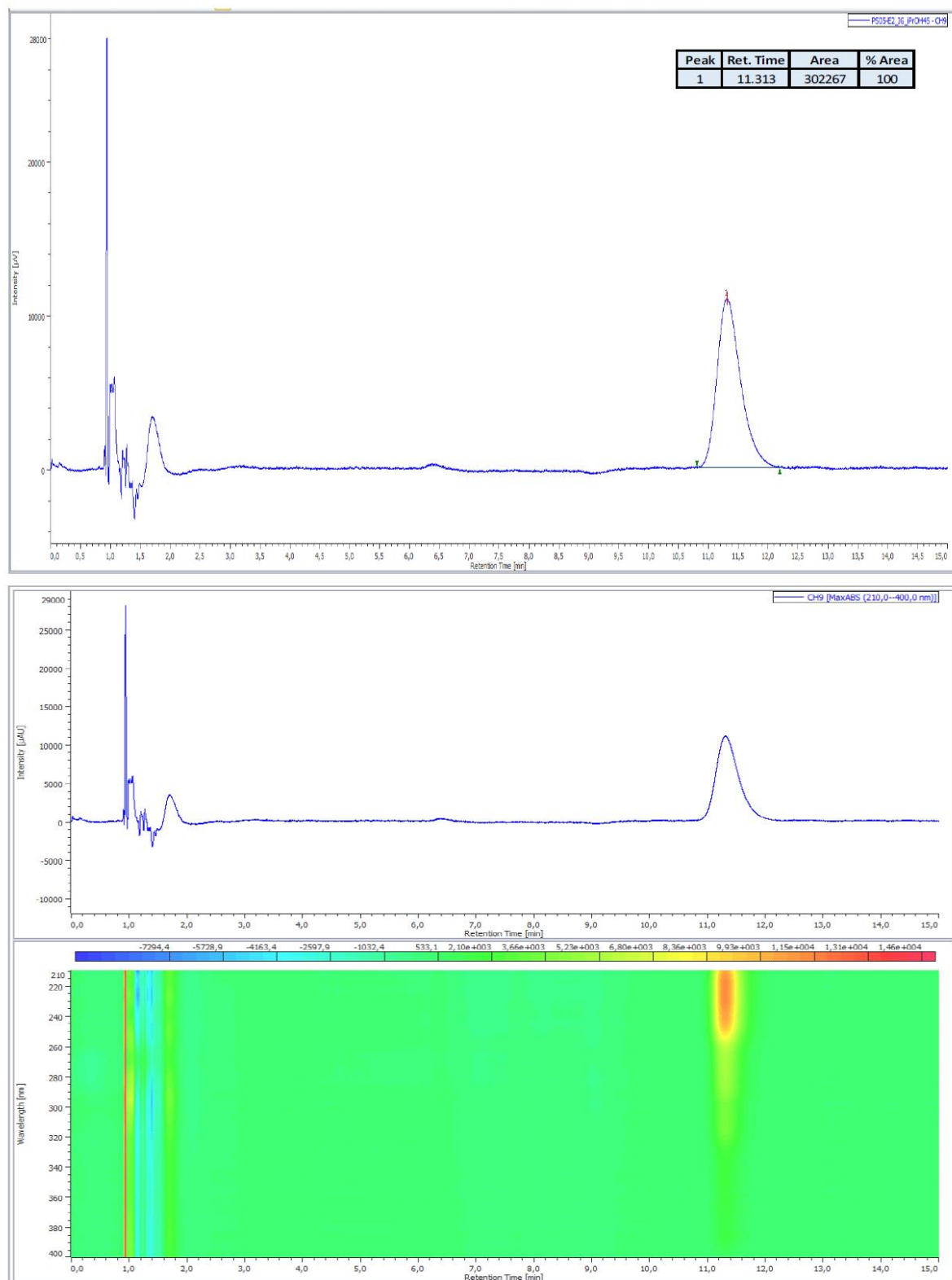


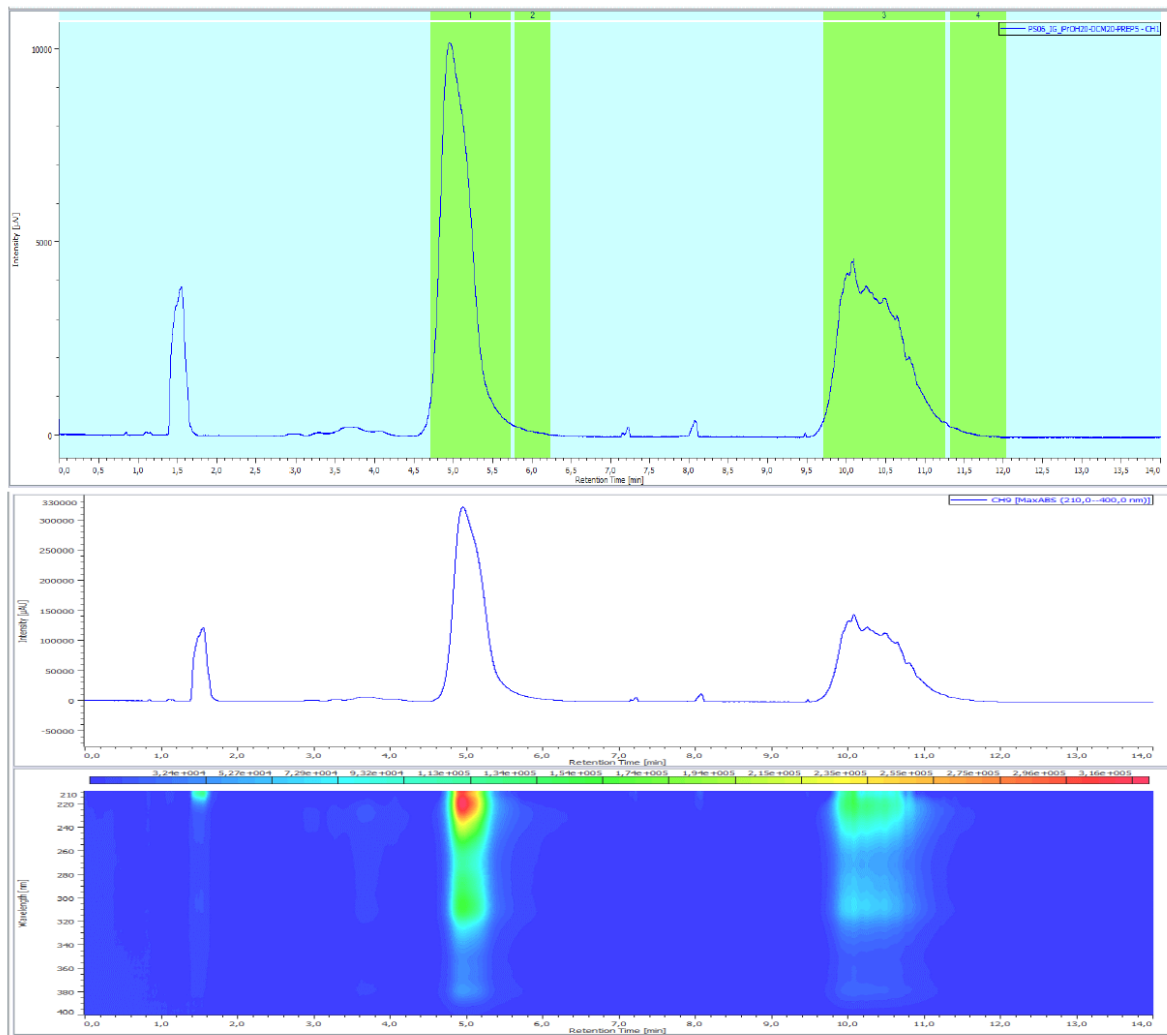
Figure S18. Chiral HPLC of **Hel-*o*-CHO**.

Conditions Analytiques :	
Colonne :	CHIRALPAK IG 250 x 4,6 mm, 5µm
Débit :	4 mL/min
Détection :	200-400 nM MaxAbs
température pression BPR	40°C - 120bars
Solvant :	A : CO ₂
	B : i-PrOH/DCM 20/20
Gradient :	Isocratique
%A : 60	%B : 40

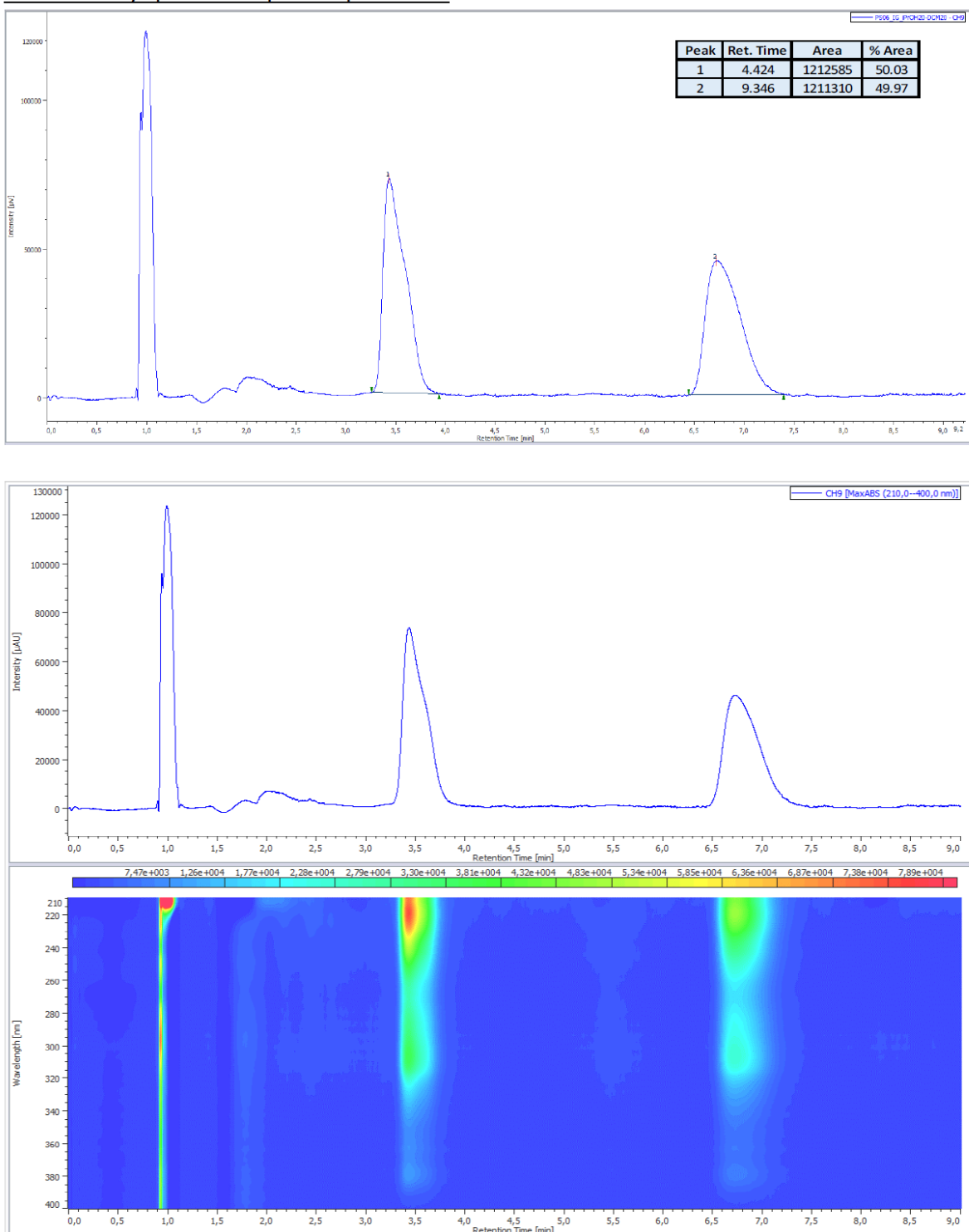
Date : 17/05/2021
Opérateur : LEBREQUIER Sabrina
Demandeur : PIETERS Grégory
Encadrant : PIETERS Grégory

Conditions Prep :	
Colonne :	CHIRALPAK IG 250 x 21 mm, 5µm
Débit :	80 mL/min
Détection :	200-400 nM MaxAbs
température pression BPR	40°C - 100 bars
Solvant :	A : CO ₂
	B : i-PrOH/DCM 20/20
Gradient :	Isocratique
%A : 60	%B : 40

Profil de purification :

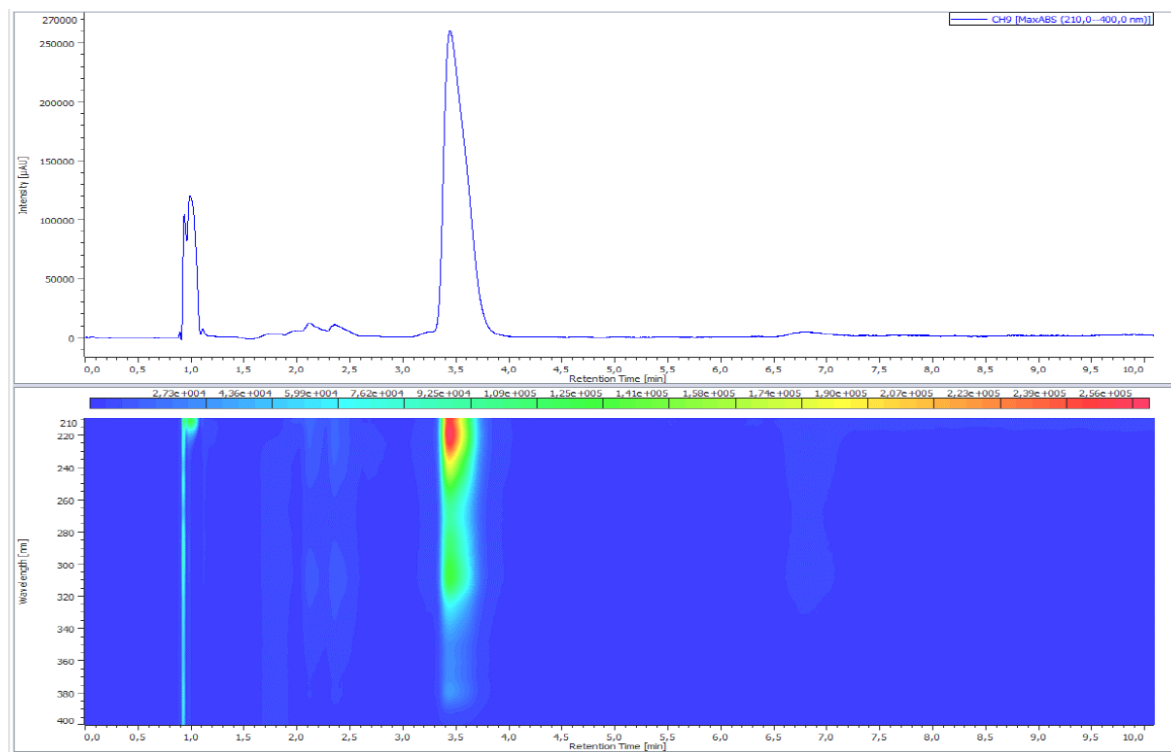
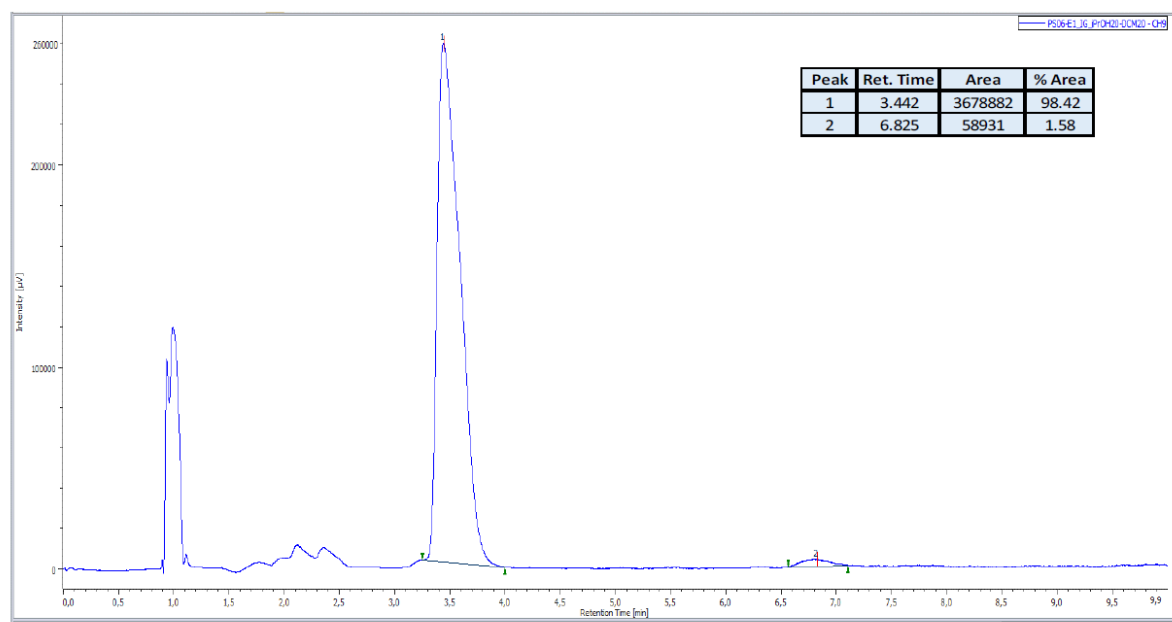


Conditions analytiques : Racémique avant purification :



Vérification des énantiomères

E1



E2

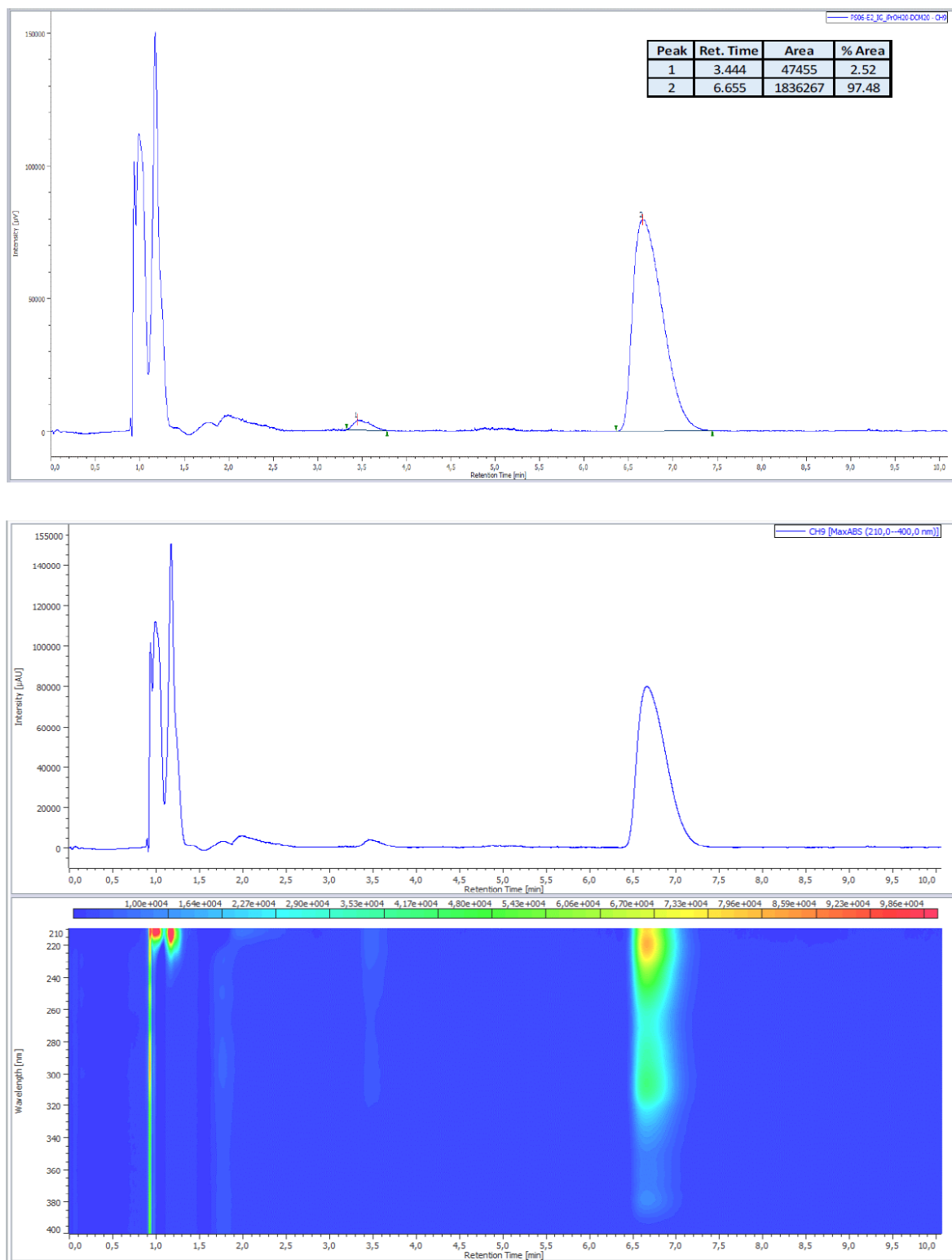


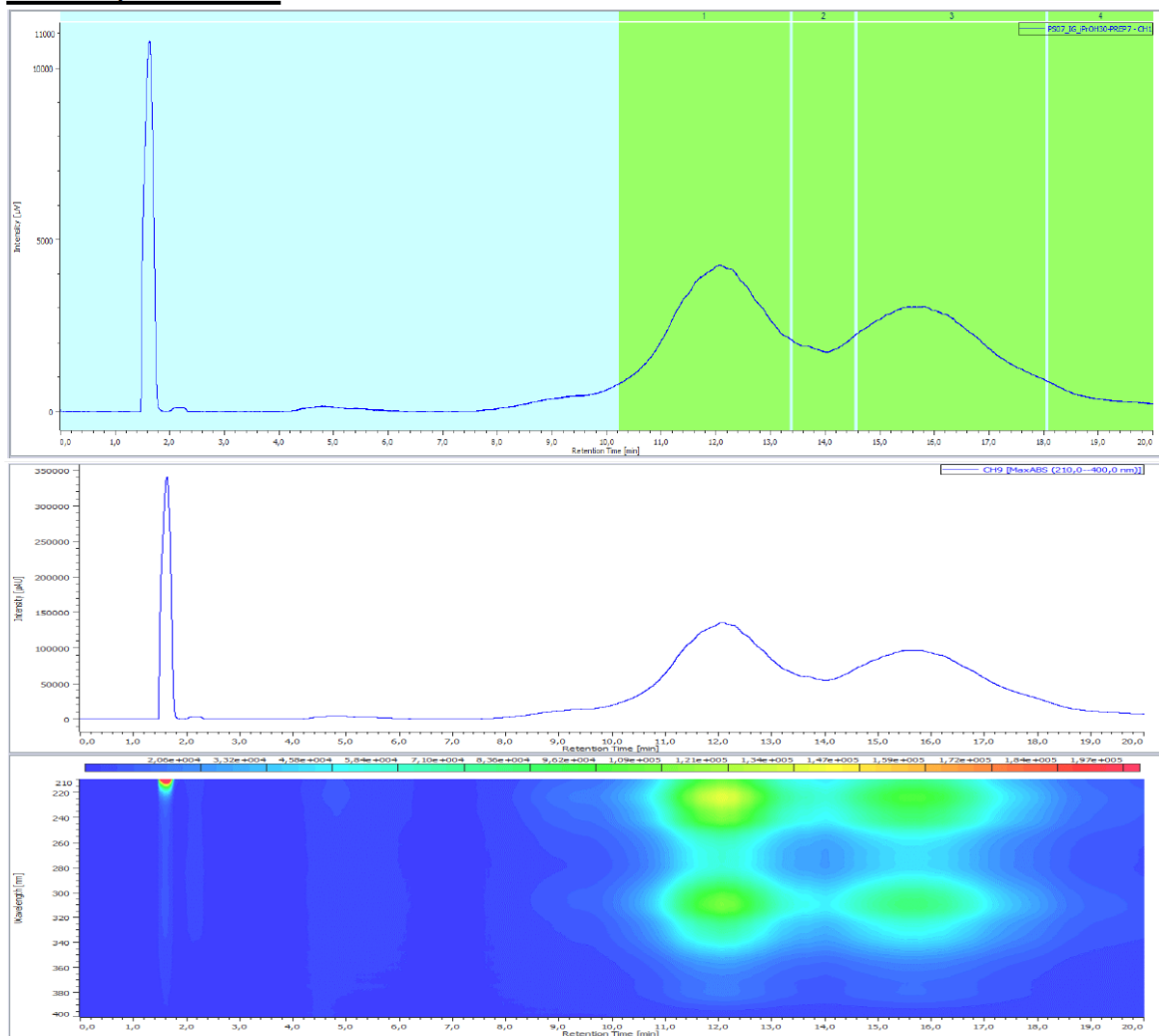
Figure S19. Chiral HPLC of Ax-*o*-CN.

Conditions Analytiques :	
Colonne :	CHIRALPAK IG 250 x 4,6 mm, 5µm
Débit :	4 mL/min
Détection :	200-400 nM MaxAbs
température pression BPR	40°C - 120bars
Solvant :	A : CO ₂
	B : i-PrOH
Gradient :	Isocratique %A : 60 %B : 40

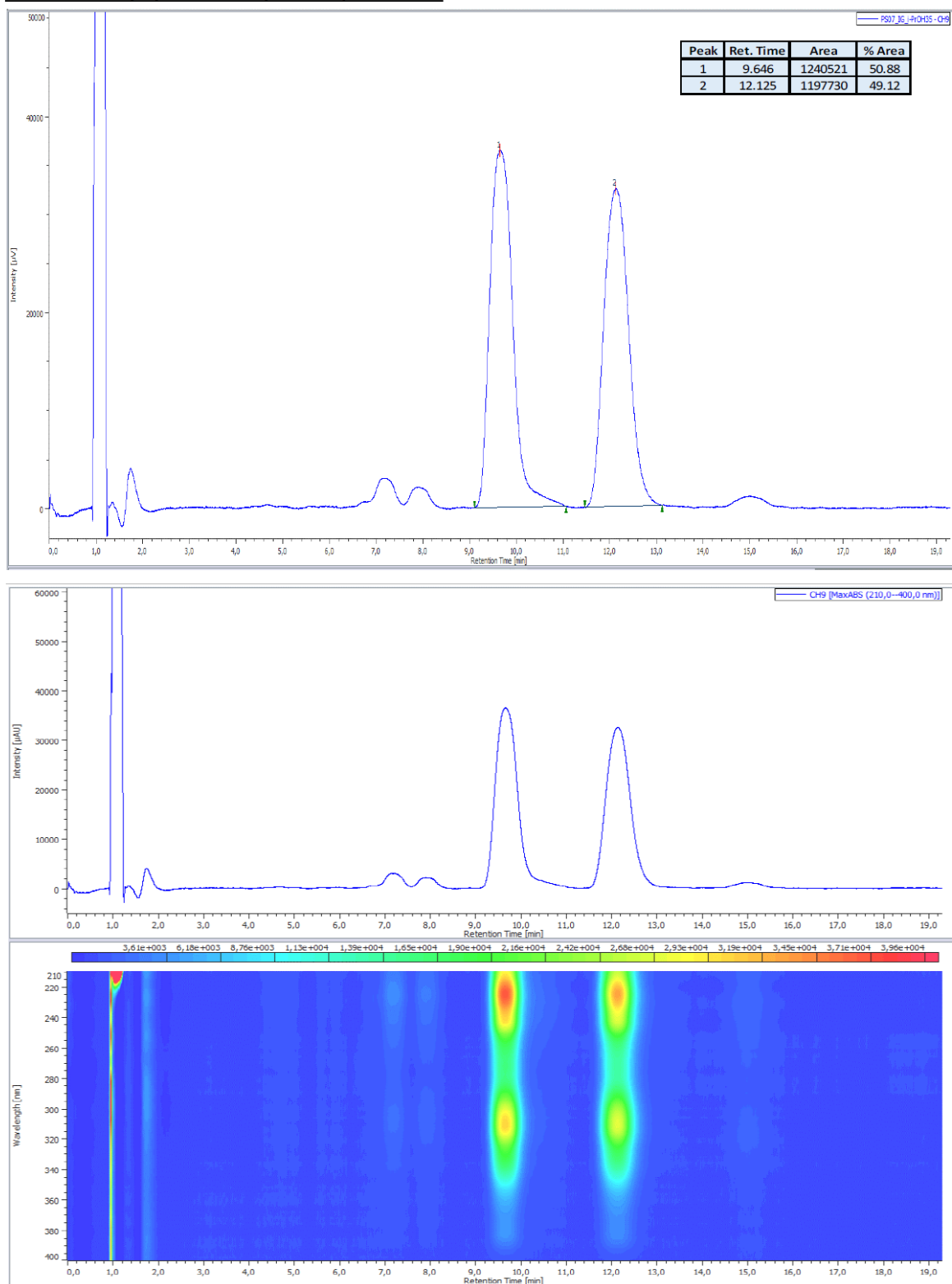
Date : 17/05/2021
Opérateur : LEBREQUIER Sabrina
Demandeur : PIETERS Grégory
Encadrant : PIETERS Grégory

Conditions Prep :	
Colonne :	CHIRALPAK IG 250 x 21 mm, 5µm
Débit :	80 mL/min
Détection :	200-400 nM MaxAbs
température pression BPR	40°C - 100 bars
Solvant :	A : CO ₂
	B : i-PrOH
Gradient :	Isocratique %A : 70 %B : 30

Profil de purification :

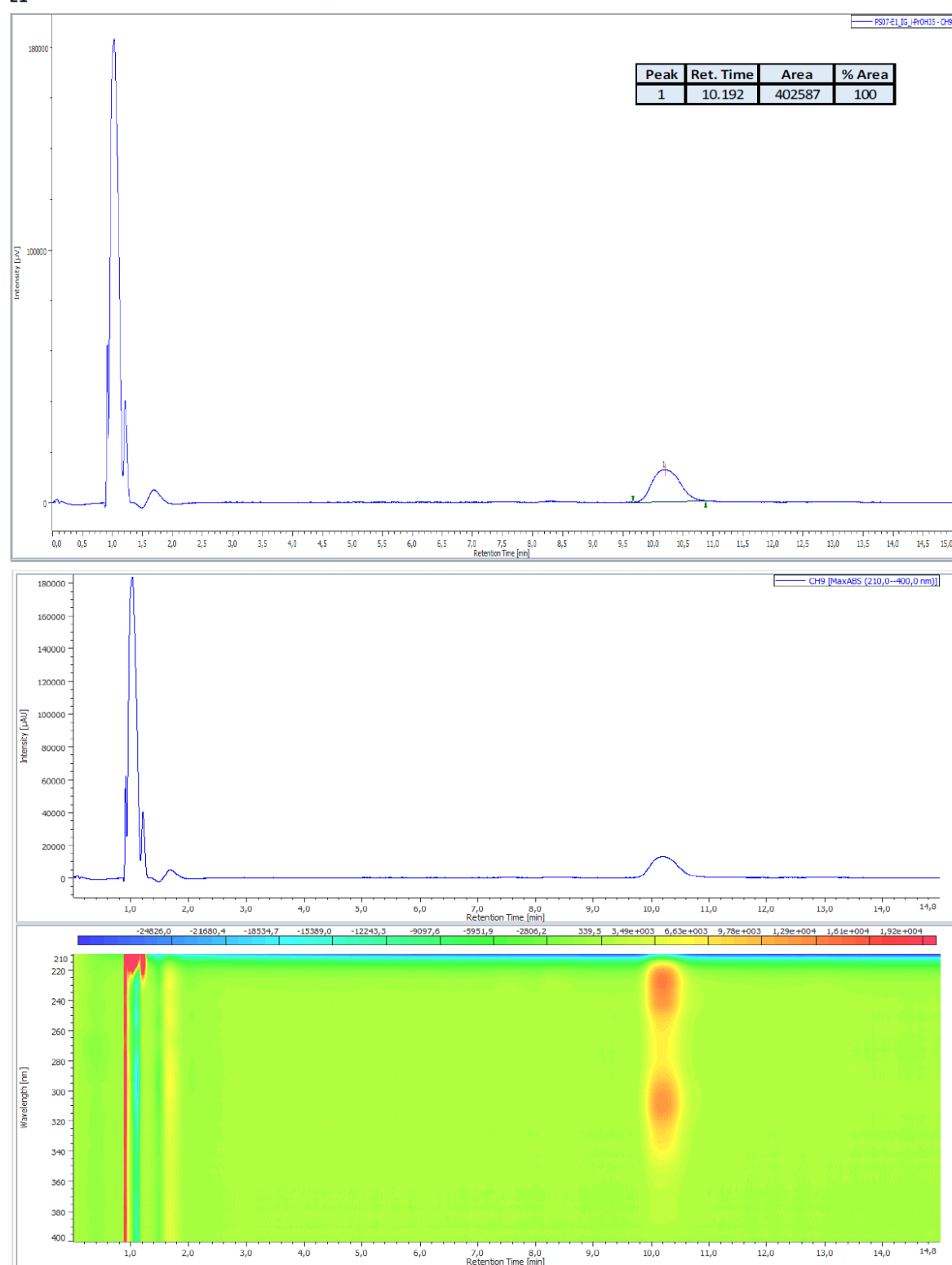


Conditions analytiques : Racémique avant purification :



Vérification des énantiomères

E1



E2

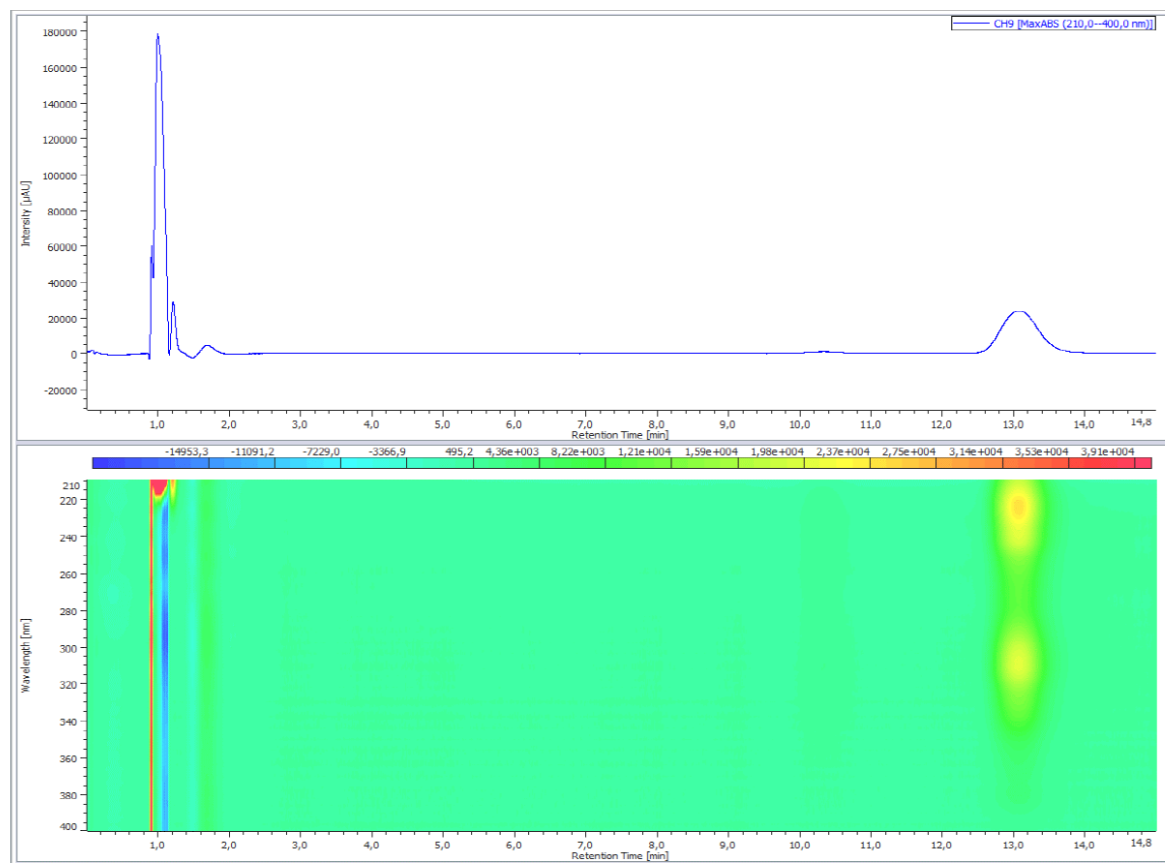
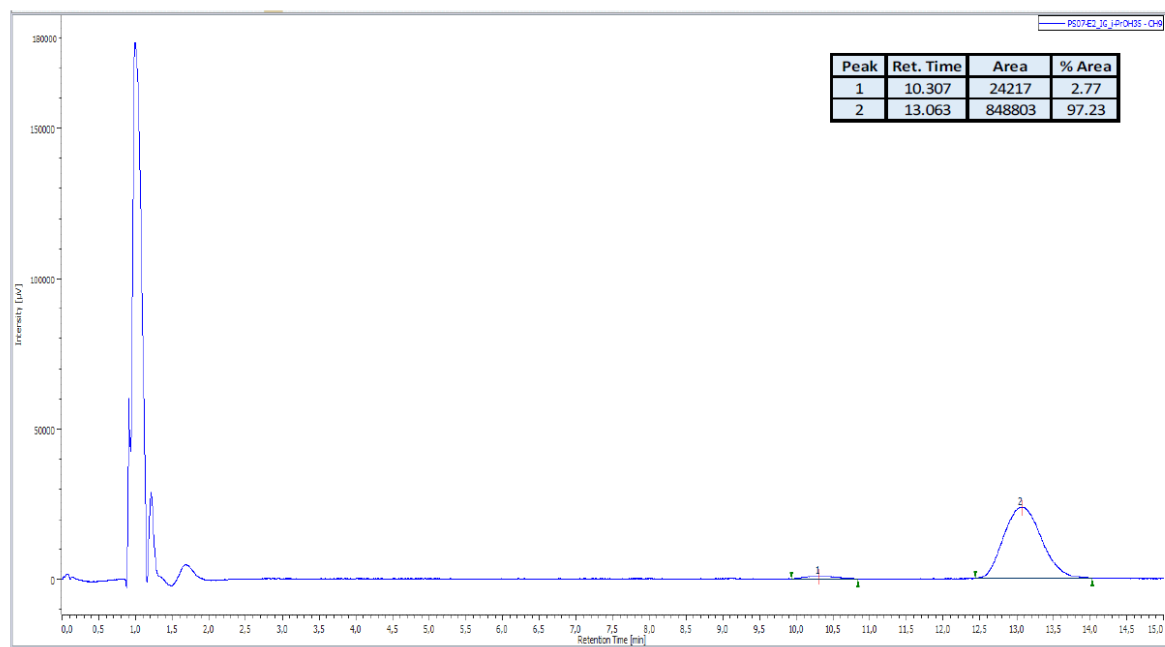


Figure S20. Chiral HPLC of **Hel-*p*-CN**.

F. NMR spectra

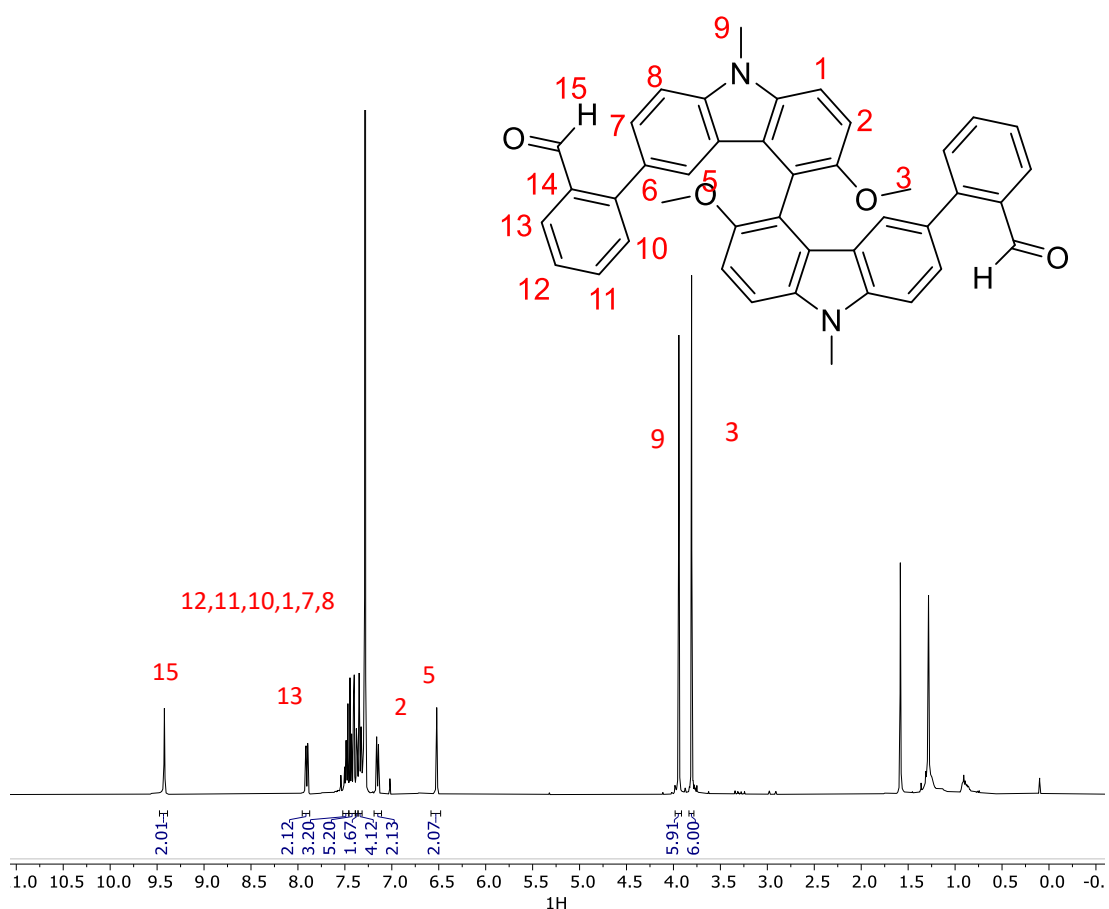


Figure S21. ¹H NMR spectrum of Ax-o-CHO in CDCl₃ at 298 K (400 MHz).

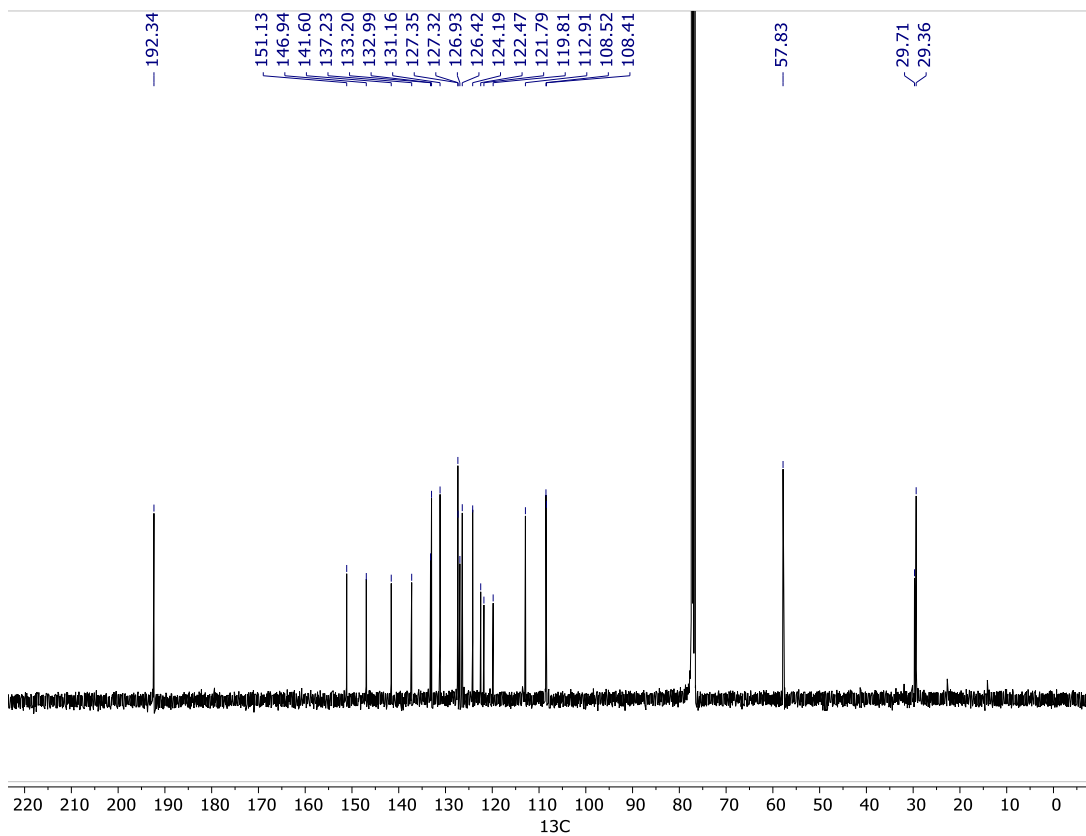


Figure S22. ^{13}C NMR spectrum of **Ax-o-CHO** in CDCl_3 at 298 K (101 MHz).

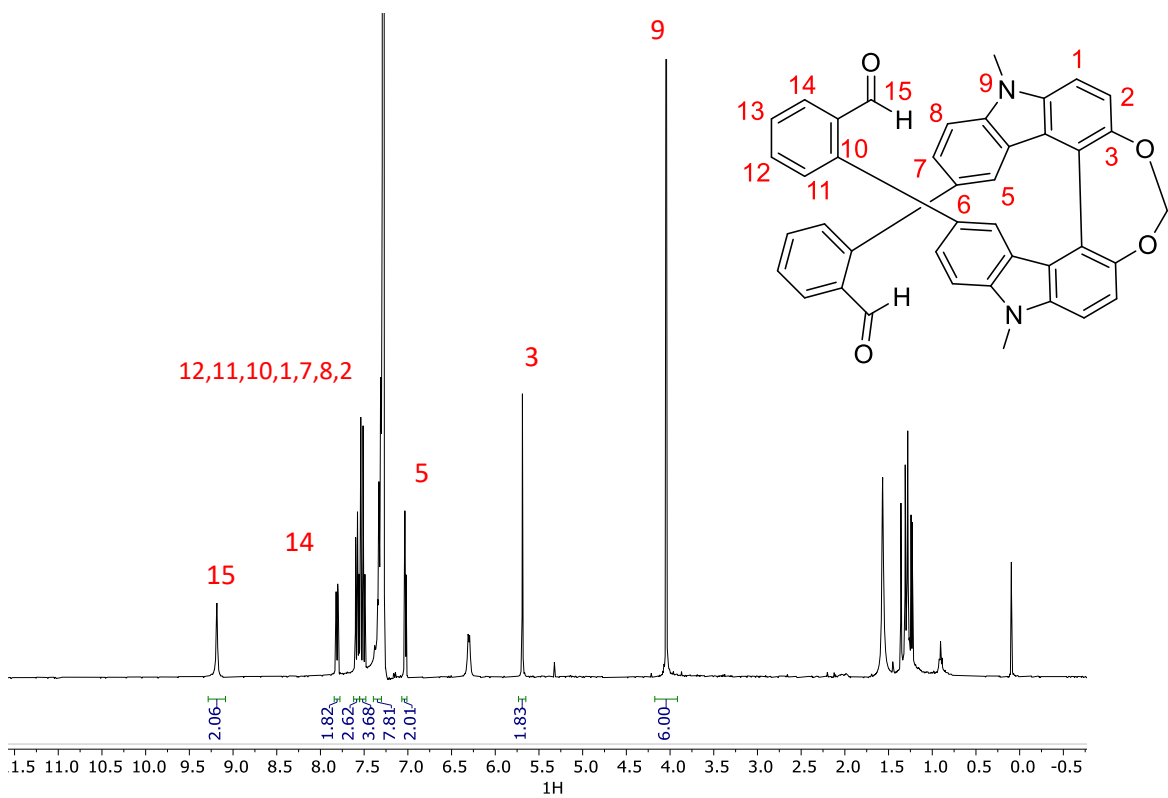


Figure S23. ^1H NMR spectrum of **Hel-o-CHO** in CDCl_3 at 298 K (400 MHz).

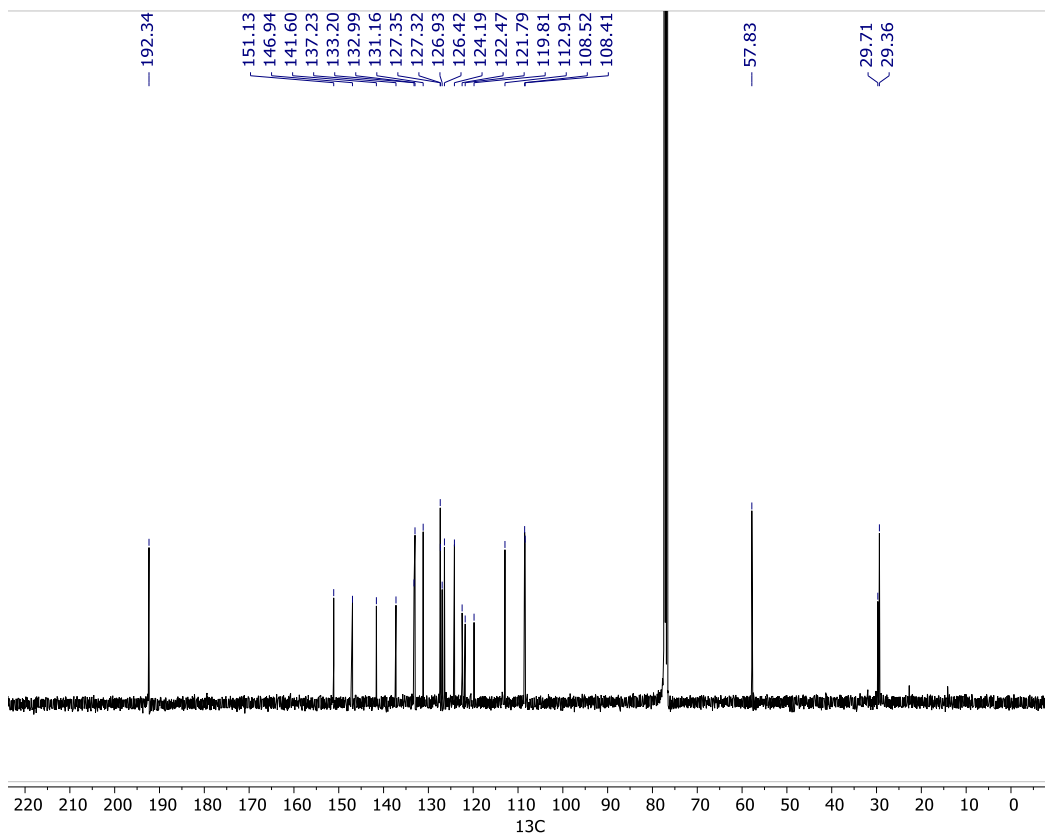


Figure S24. ^{13}C NMR spectrum of **Hel-o-CHO** in CDCl_3 at 298 K (101 MHz).

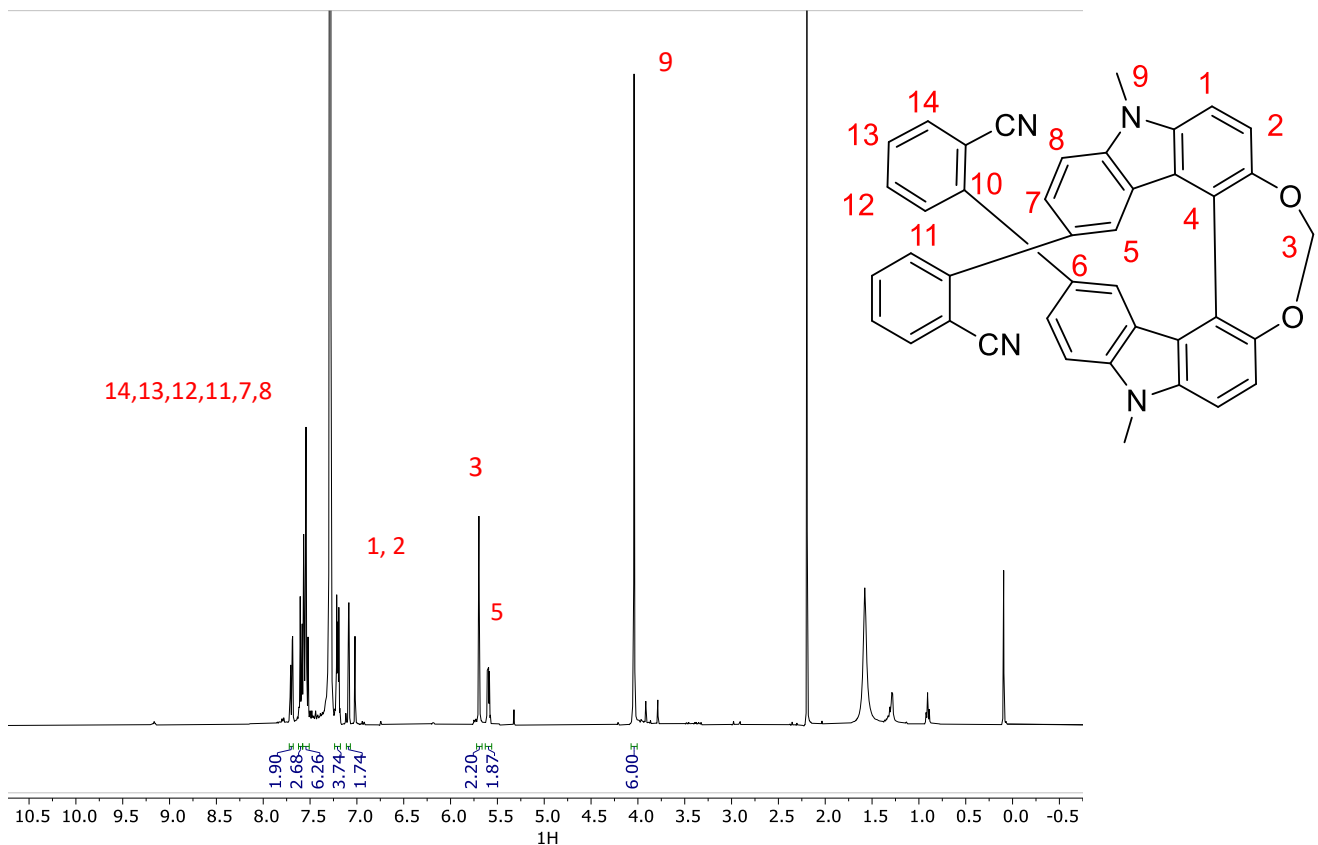


Figure S25. ^1H NMR spectrum of **Hel-o-CN** in CDCl_3 at 298 K (400 MHz).

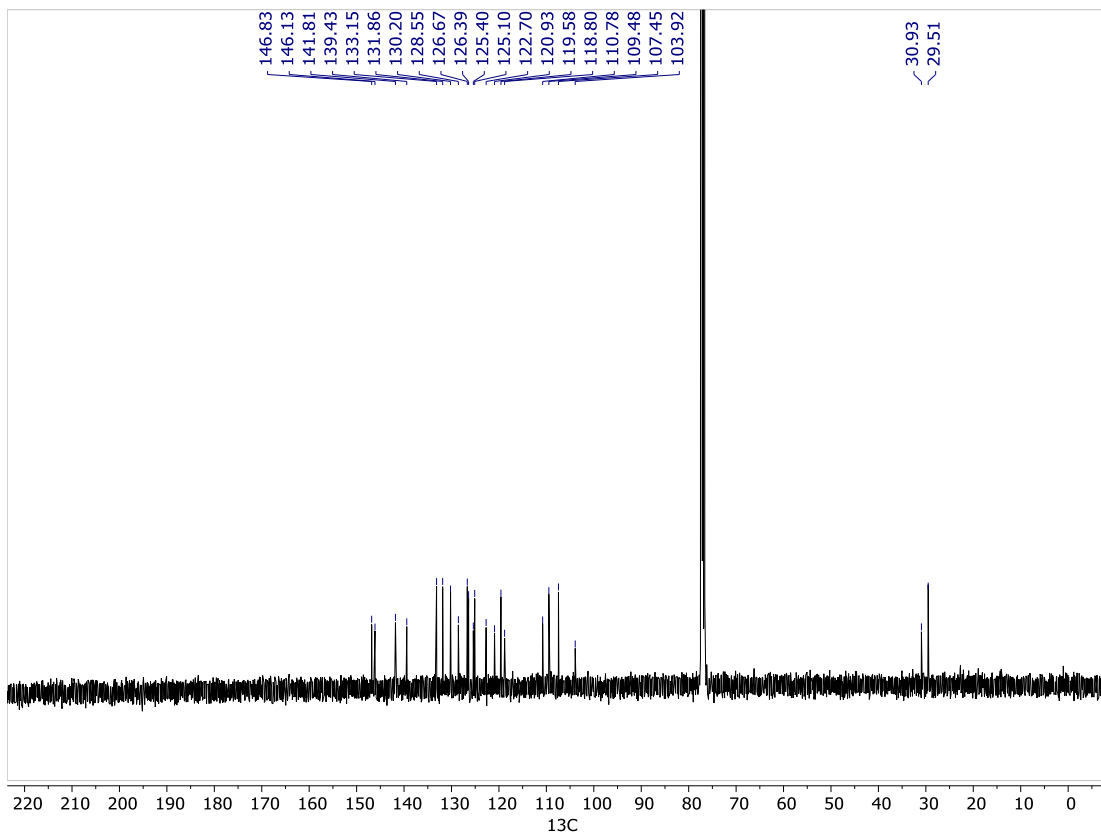


Figure S26. ¹³C NMR spectrum of **Hel-o-CN** in CDCl₃ at 298 K (101 MHz).

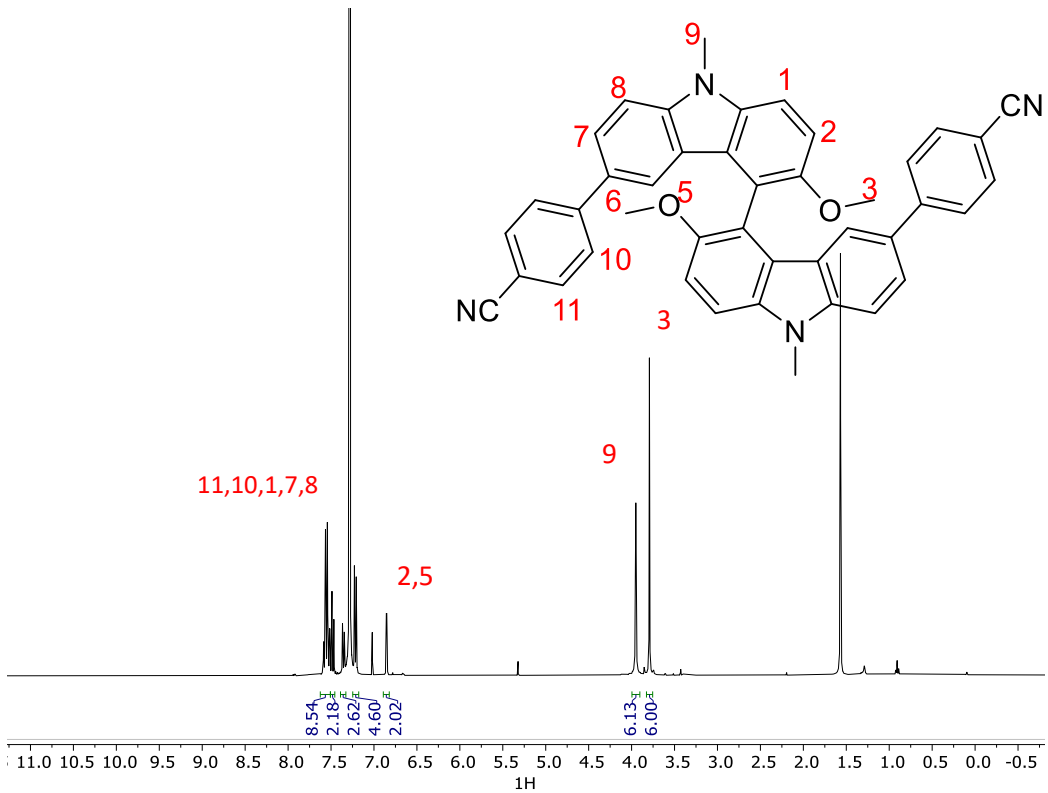


Figure S27. ¹H NMR spectrum of **Ax-p-CN** in CDCl₃ at 298 K (400 MHz).

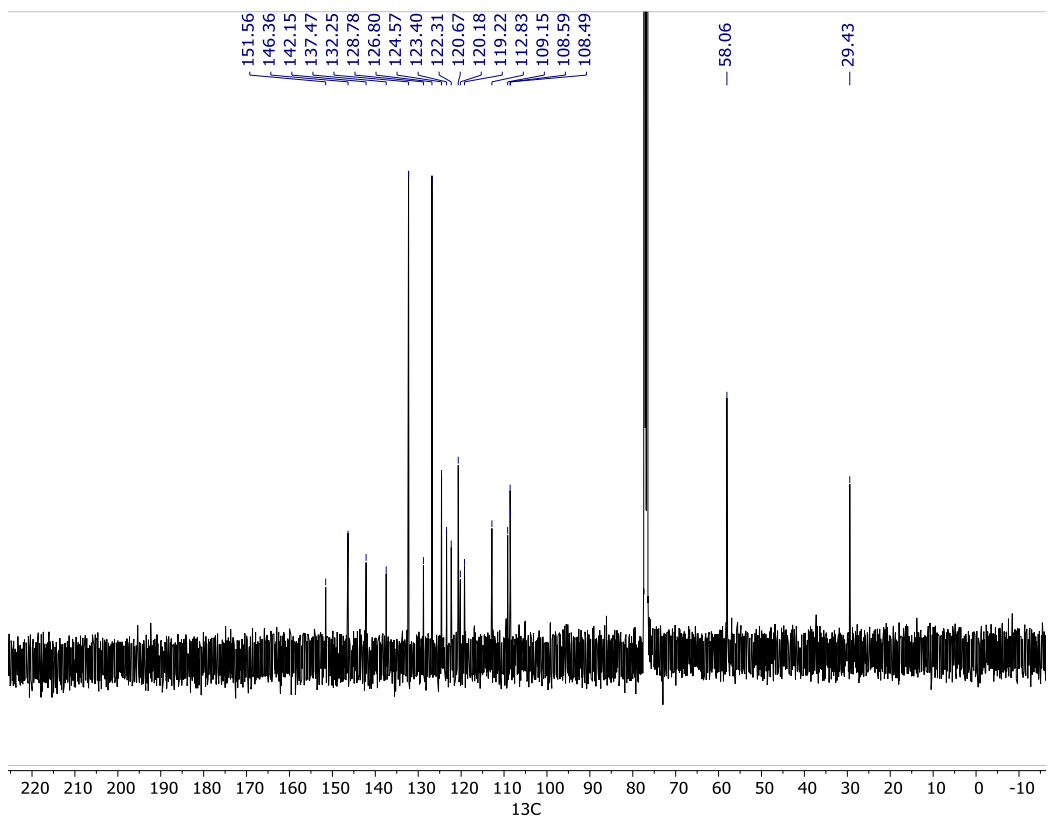


Figure S28. ^{13}C NMR spectrum of Ax-*p*-CN in CDCl_3 at 298 K (101 MHz).

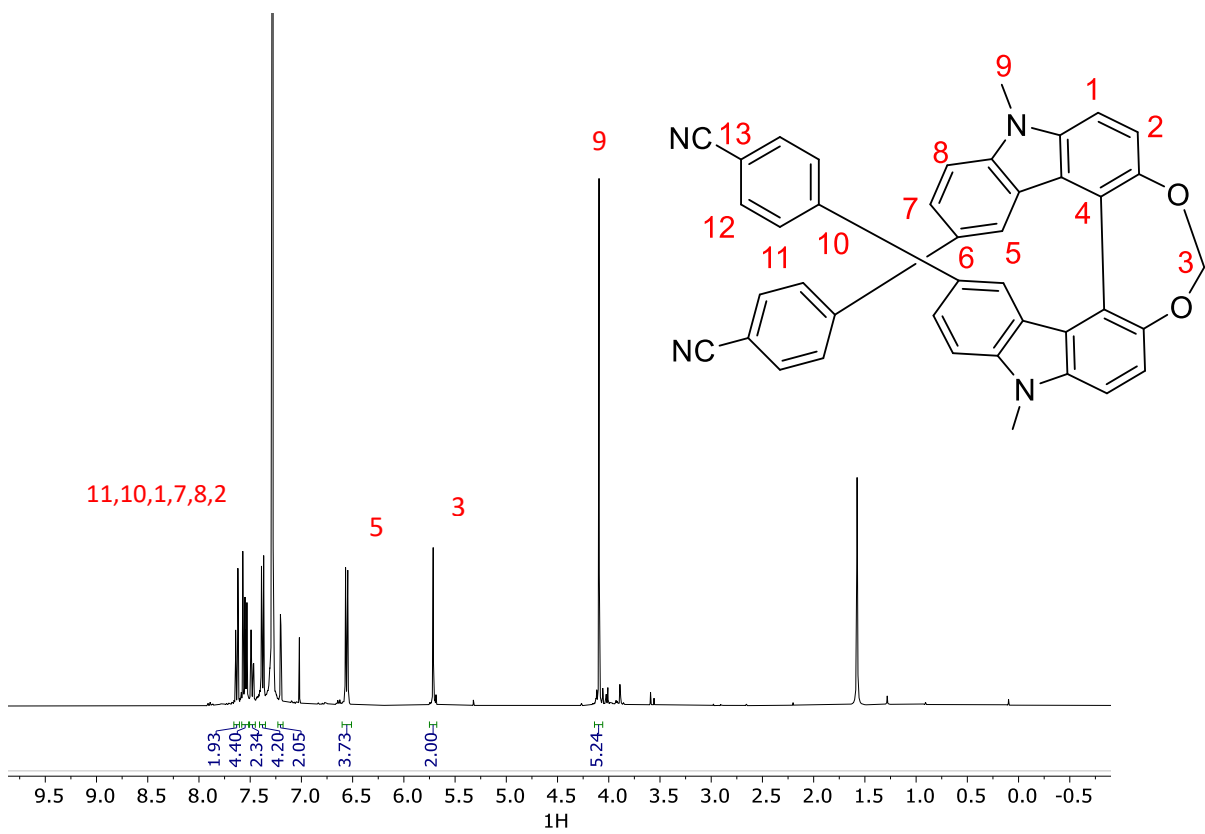


Figure S29. ^1H NMR spectrum of Hel-*p*-CN in CDCl_3 at 298 K (400 MHz).

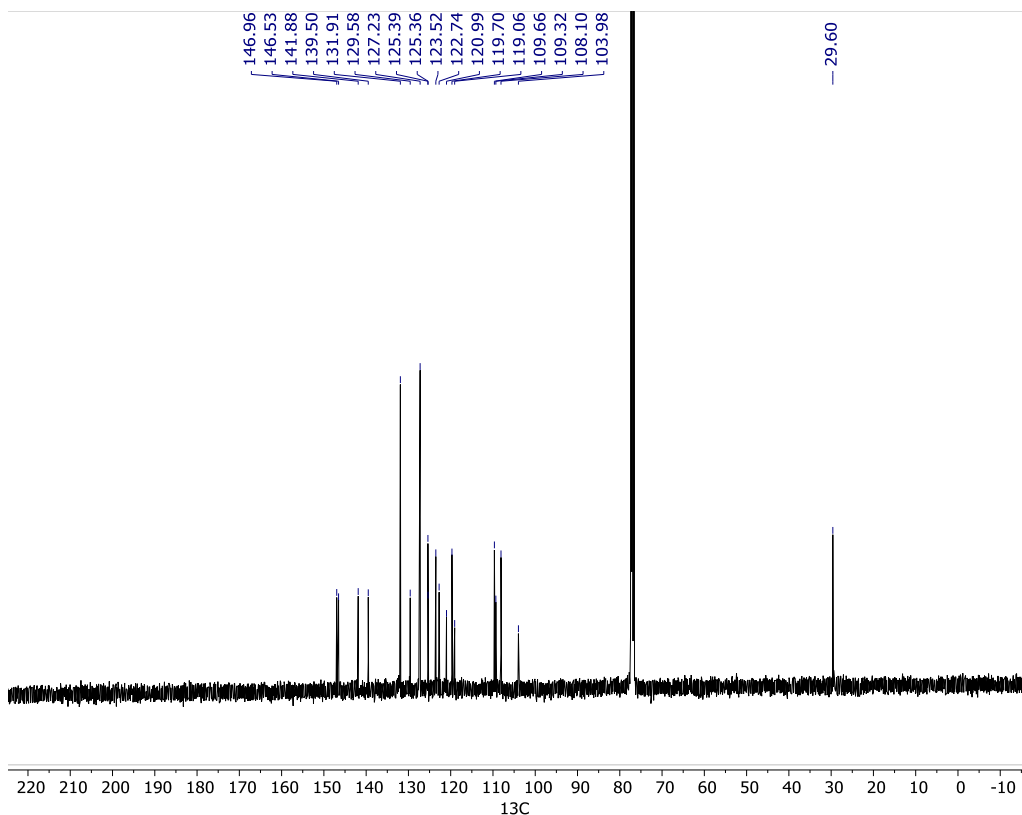


Figure S30. ^{13}C NMR spectrum of **HeI-*p*-CN** in CDCl_3 at 298 K (101 MHz).

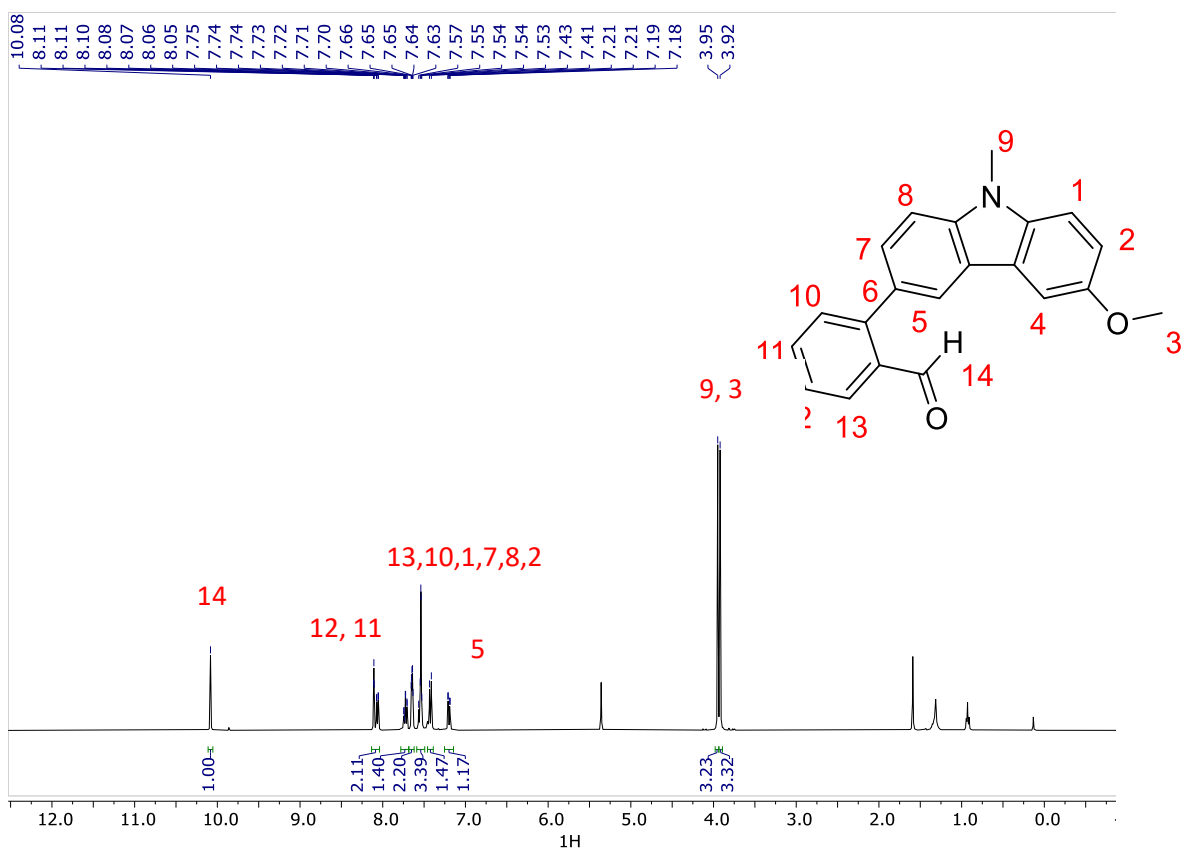


Figure S31. ^1H NMR spectrum of **CBz-CHO** in CD_2Cl_2 at 298 K (400 MHz).

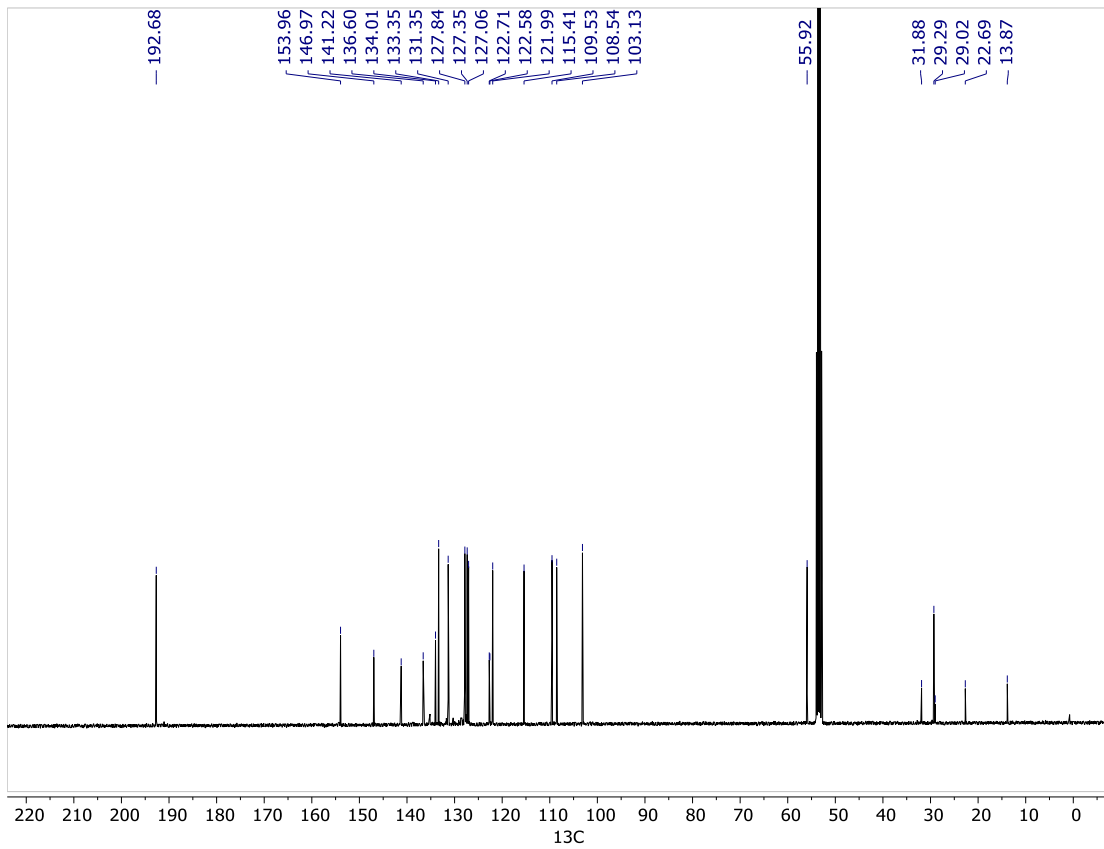


Figure S32. ¹H NMR spectrum of **CBz-CHO** in CD_2Cl_2 at 298 K (101 MHz).

G. Theoretical calculations

All computations were performed by using Kohn-Sham Density functional theory (DFT) as implemented in the Gaussian (G16) package,² along the PBE0 functional³ and the def2-SV(P) basis.⁴ Solvent effects were included by means of the polarizable continuum model (PCM)⁵ for toluene and dimethylformamide (DMF) to match the experimental conditions. Dispersion corrections from Grimme ‘D3’ were considered in the calculations.⁶

The 200 lowest-energy vertical spin-allowed electronic excitations were calculated for the absorption and electronic circular dichroism (ECD) spectra. In order to simulate the spectral envelopes, the transitions were subsequently Gaussian-broadened with $\sigma = 0.20$ eV. For overviews of the theoretical approach to model natural optical activity by quantum chemical calculations, esp. via TD-DFT, see, for example, References [7,8].⁷

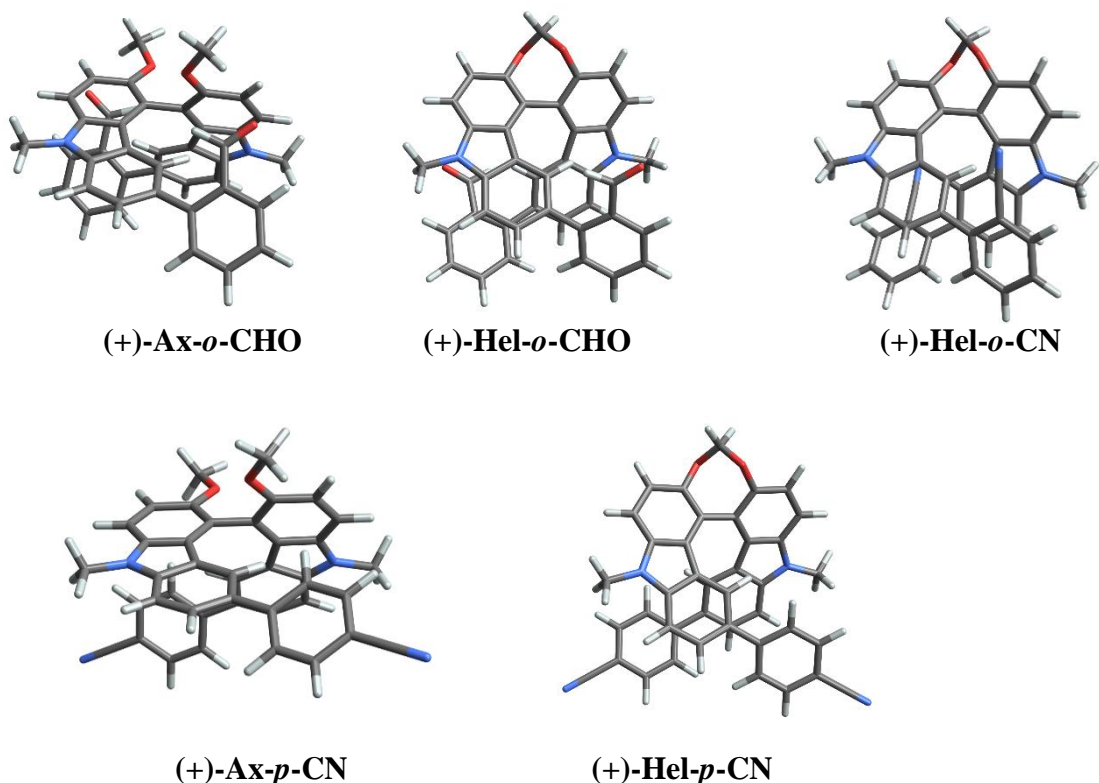


Figure S33. Optimized molecular structures of (+)-Hel-*o*-CHO, (+)-Hel-*o*-CN, (+)-Ax-*o*-CHO, (+)-Ax-*p*-CN and (+)-Hel-*p*-CN.

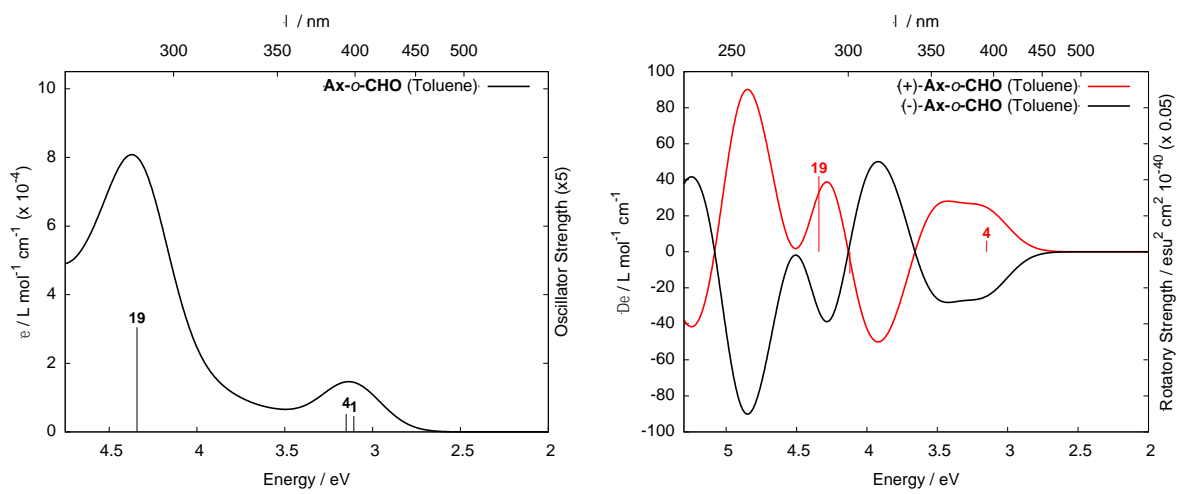


Figure S34. (Left) Calculated absorption and (right) ECD spectra of (\pm) -Ax-o-CHO. Selected transitions and, oscillator and rotatory strengths are indicated as ‘stick spectra’. Predominant transitions for $(+)$ -Ax-o-CHO are numbered according to Table S3.

Table S3. Selected excitations and occupied (occ)-unoccupied (unocc) MO pair contributions (greater than 10%) for $(+)$ -Ax-o-CHO with toluene. H and L indicate the HOMO and LUMO, respectively.

Excitation	E [eV]	λ [nm]	f	R [10^{-40} cgs]	occ. no.	unocc no.	%
#1	3.107	399	0.092	30.04	165(H)	166(L)	45
#4	3.150	394	0.105	122.46	164	167	47
#15	4.121	301	0.045	-242.43	165	170	34
#16	4.134	300	0.169	138.83	165	171	24
					164	170	17
#19	4.341	286	0.610	843.43	163	168	23
#20	4.361	284	0.140	-161.49	161	166	10
					163	168	10
#21	4.362	284	0.111	-273.45	161	167	11
#22	4.384	283	0.115	-286.56	162	168	22
					161	167	12
#25	4.591	270	0.059	-287.31	163	169	42
#26	4.628	268	0.366	337.27	162	169	41

#30	4.934	251	0.175	250.40	165	172	10
-----	-------	-----	-------	--------	-----	-----	----

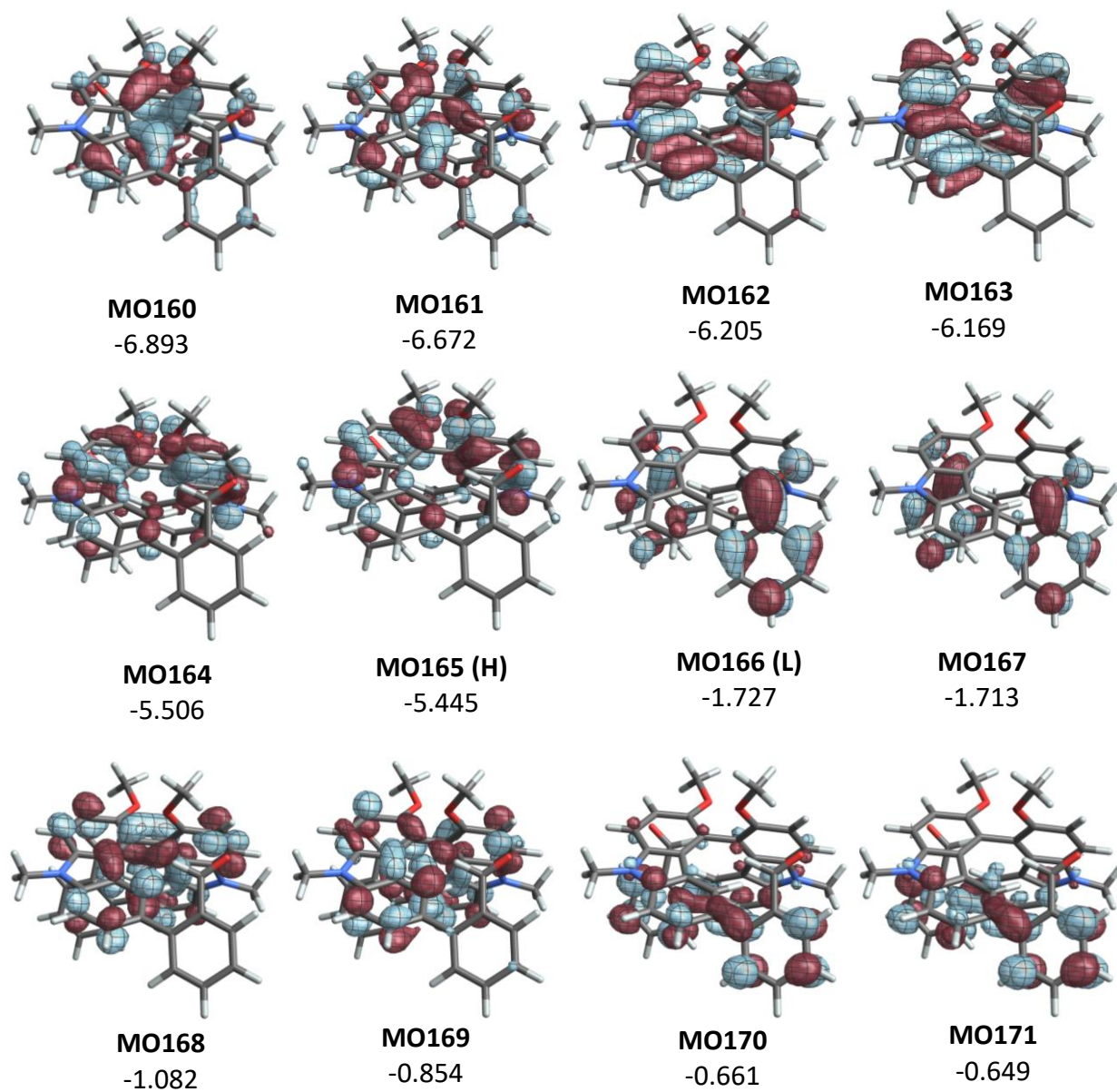


Figure S35. Isosurfaces (± 0.035 au) of Molecular Orbitals (MOs) for (+)-Ax-o-CHO (toluene). Values listed in parentheses are the corresponding orbital energies in eV.

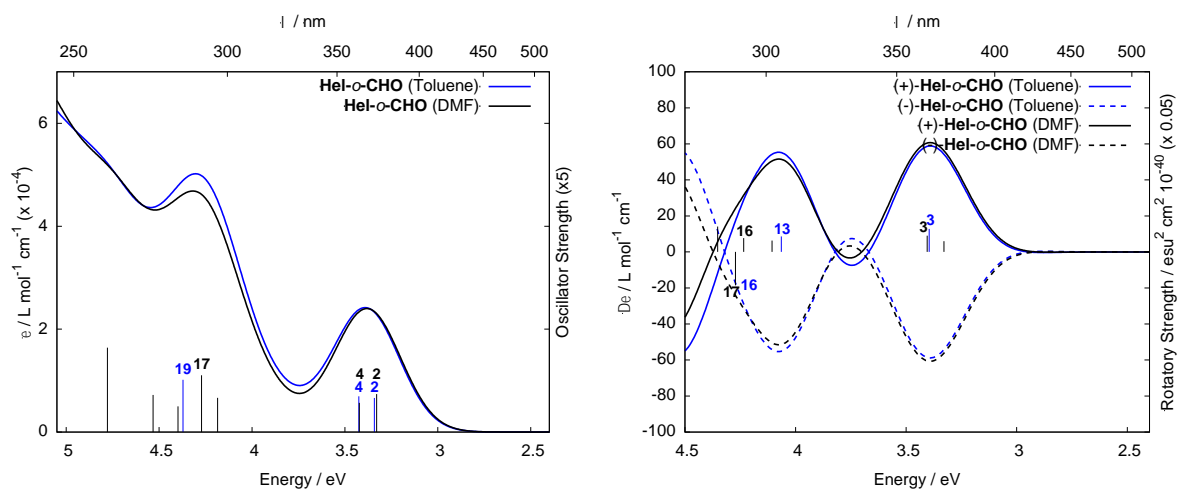


Figure S36. Calculated UV/Vis (left) and ECD (right) spectra of **(±)-Hel-o-CHO**. Selected transitions and, oscillator and rotatory strengths are indicated as ‘stick spectra’. Predominant transitions for **(+)-Hel-o-CHO** are numbered according to Table S4.

Table S4. Selected excitations and occupied (occ)-unoccupied (unocc) MO pair contributions (greater than 10%) for **(+)-Hel-o-CHO** with toluene. H and L indicate the HOMO and LUMO, respectively.

Excitation	E [eV]	λ [nm]	f	R [10^{-40} cgs]	occ. no.	unocc no.	%
#2	3.341	371	0.132	2.69	160(H)	162	40
#3	3.396	365	0.073	255.78	159	161(L)	38
#4	3.425	362	0.139	-57.71	160	163	35
#13	4.065	305	0.058	171.98	158	163	26
#16	4.205	295	0.159	-264.00	160	164	22
					160	165	16
#17	4.261	291	0.143	175.17	159	164	20
#18	4.316	287	0.101	102.58	159	165	36
#19	4.371	284	0.203	-60.92	160	166	40
#26	4.759	261	0.222	169.06	158	164	32
#27	4.780	259	0.138	-4.95	157	164	22

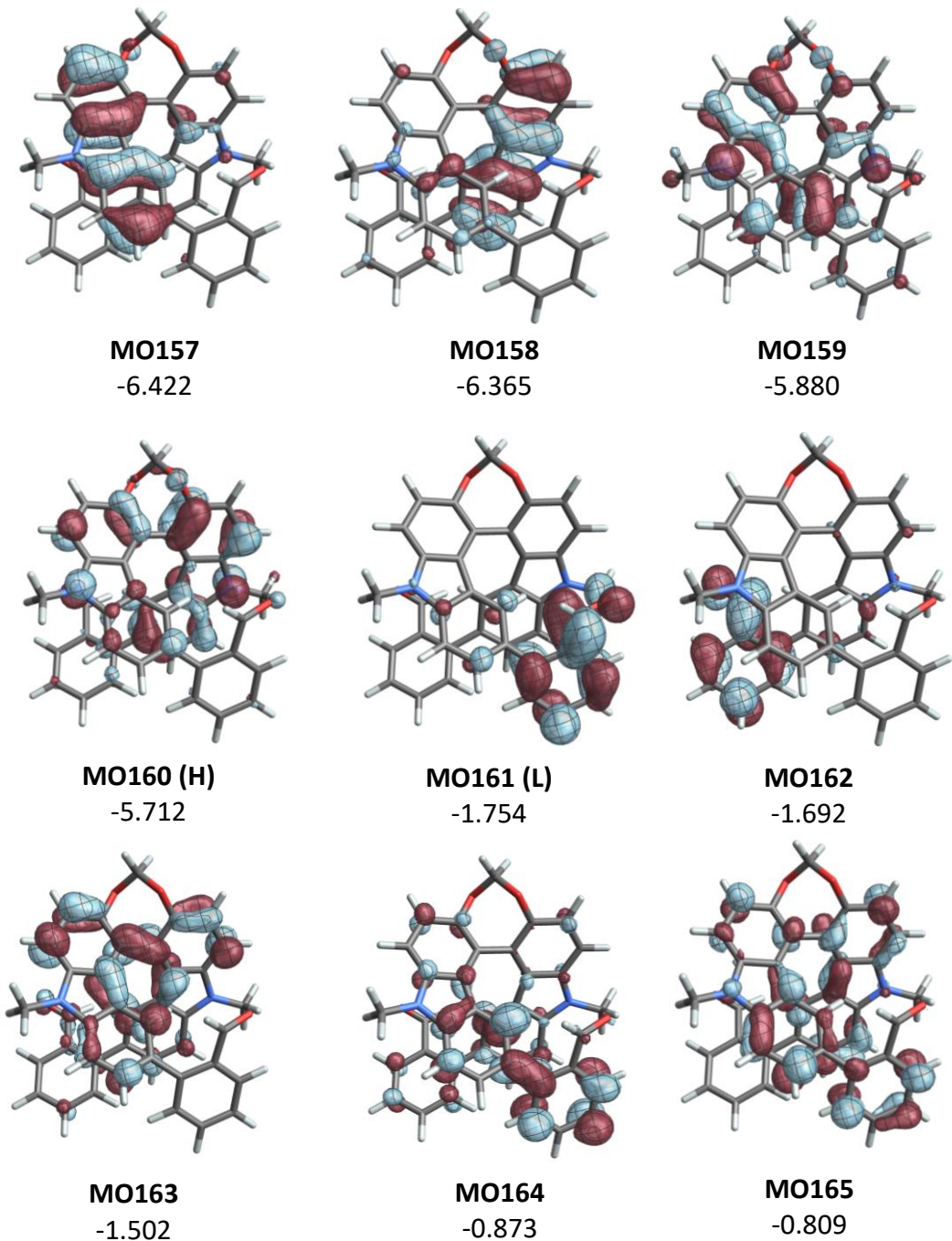


Figure S37. Isosurfaces (± 0.035 au) of Molecular Orbitals (MOs) for (+)-**Hel-*o*-CHO (toluene)**. Values listed in parentheses are the corresponding orbitals energies in eV.

Table S5. Selected excitations and occupied (occ)-unoccupied (unocc) MO pair contributions (greater than 10%) for (+)-**Hel-o-CHO** with DFM. H and L indicate the HOMO and LUMO, respectively.

Excitation	E [eV]	λ [nm]	f	R [10^{-40} cgs]	occ. no.	unocc no.	%
#2	3.329	372	0.148	119.22	160	162	26
					160(H)	161(L)	17
#3	3.405	364	0.045	180.67	160	163	29
#4	3.423	262	0.114	-34.31	159	162	40
#15	4.185	296	0.133	-60.07	160	164	13
#16	4.235	293	0.067	153.45	159	164	31
#17	4.271	290	0.221	-370.98	160	165	36
#18	4.352	285	0.100	282.69	159	165	40
#19	4.400	282	0.100	52.79	160	166	40
#22	4.532	274	0.144	-251.38	159	166	38
#27	4.778	259	0.328	360.77	158	164	42

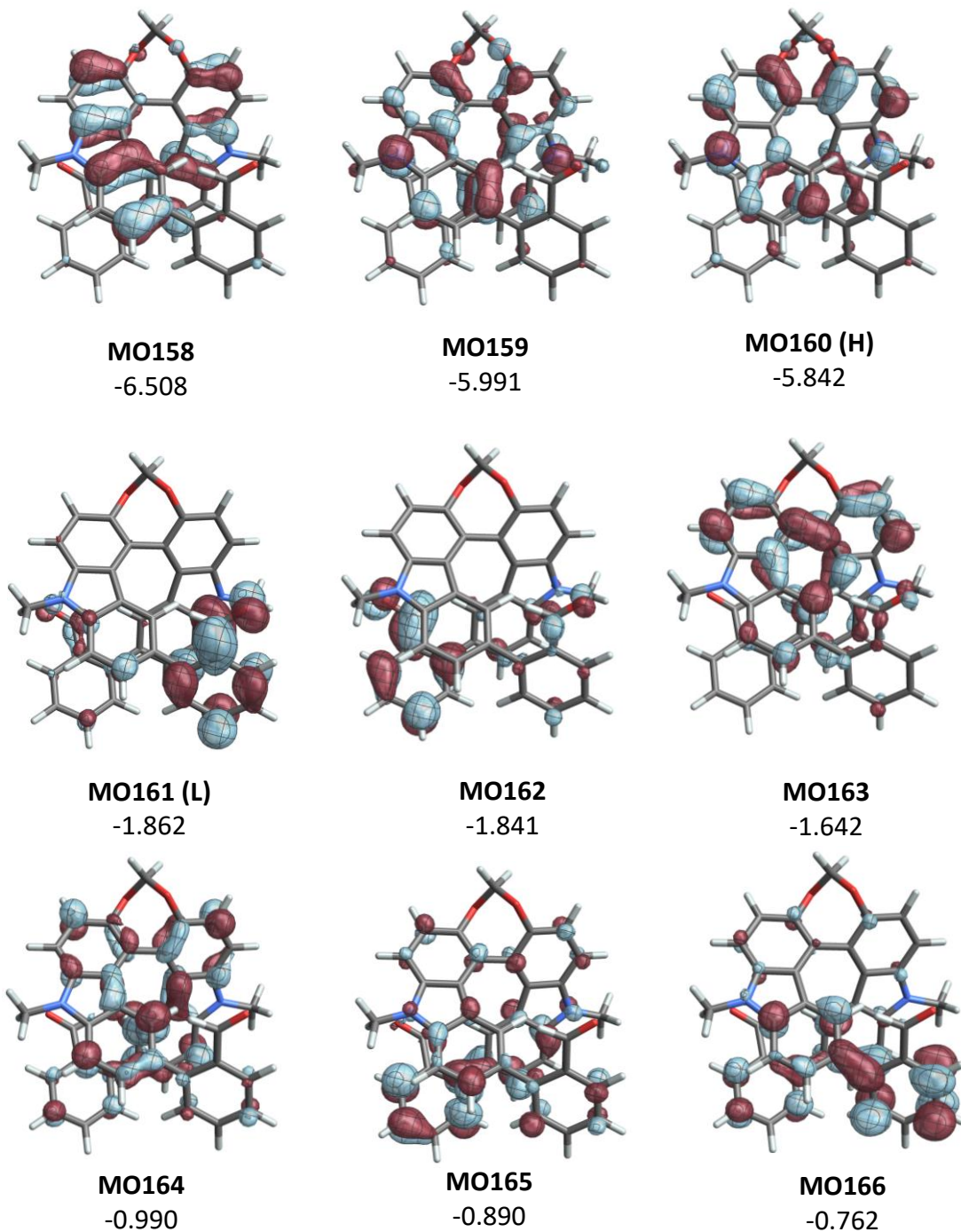


Figure S38. Isosurfaces (± 0.035 au) of Molecular Orbitals (MOs) for (+)-**Hel-*o*-CHO (DMF)**. Values listed in parentheses are the corresponding orbital energies in eV.

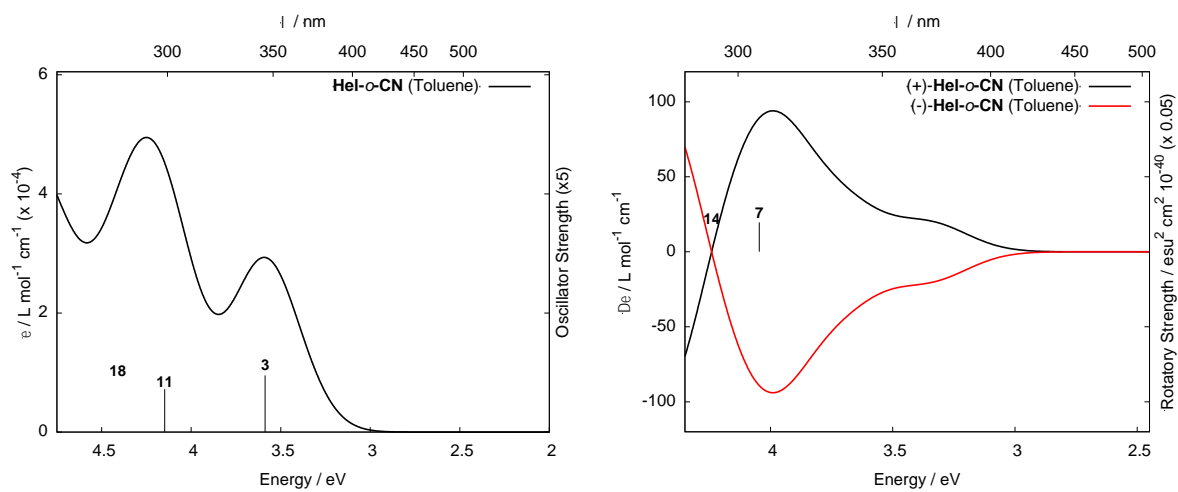


Figure S39. Calculated UV/Vis (left) and ECD (right) spectra of (\pm) -**Hel-o-CN**. Selected transitions and, oscillator and rotatory strengths are indicated as ‘stick spectra’. Predominant transitions for $(+)$ -**Hel-o-CN** are numbered according to Table S6.

Table S6. Selected excitations and occupied (occ)-unoccupied (unocc) MO pair contributions (greater than 10%) for $(+)$ -**Hel-o-CN** with toluene. H and L indicate the HOMO and LUMO, respectively.

Excitation	E [eV]	λ [nm]	f	R [10^{-40} cgs]	occ. no.	unocc no.	%
#1	3.414	363	0.077	108.34	158(H)	160	46
#2	3.529	351	0.049	-126.88	158	159(L)	47
#3	3.587	346	0.191	63.20	158	161	48
#5	3.663	338	0.109	193.05	157	159	48
#7	4.046	306	0.080	391.05	155	160	34
#10	4.144	299	0.089	-151.96	156	159	22
#11	4.148	299	0.144	-262.99	158	162	18
#14	4.236	293	0.109	308.73	157	162	20
					158	163	17
#17	4.344	285	0.142	-30.66	157	164	34
#18	4.410	281	0.181	-308.64	157	163	42

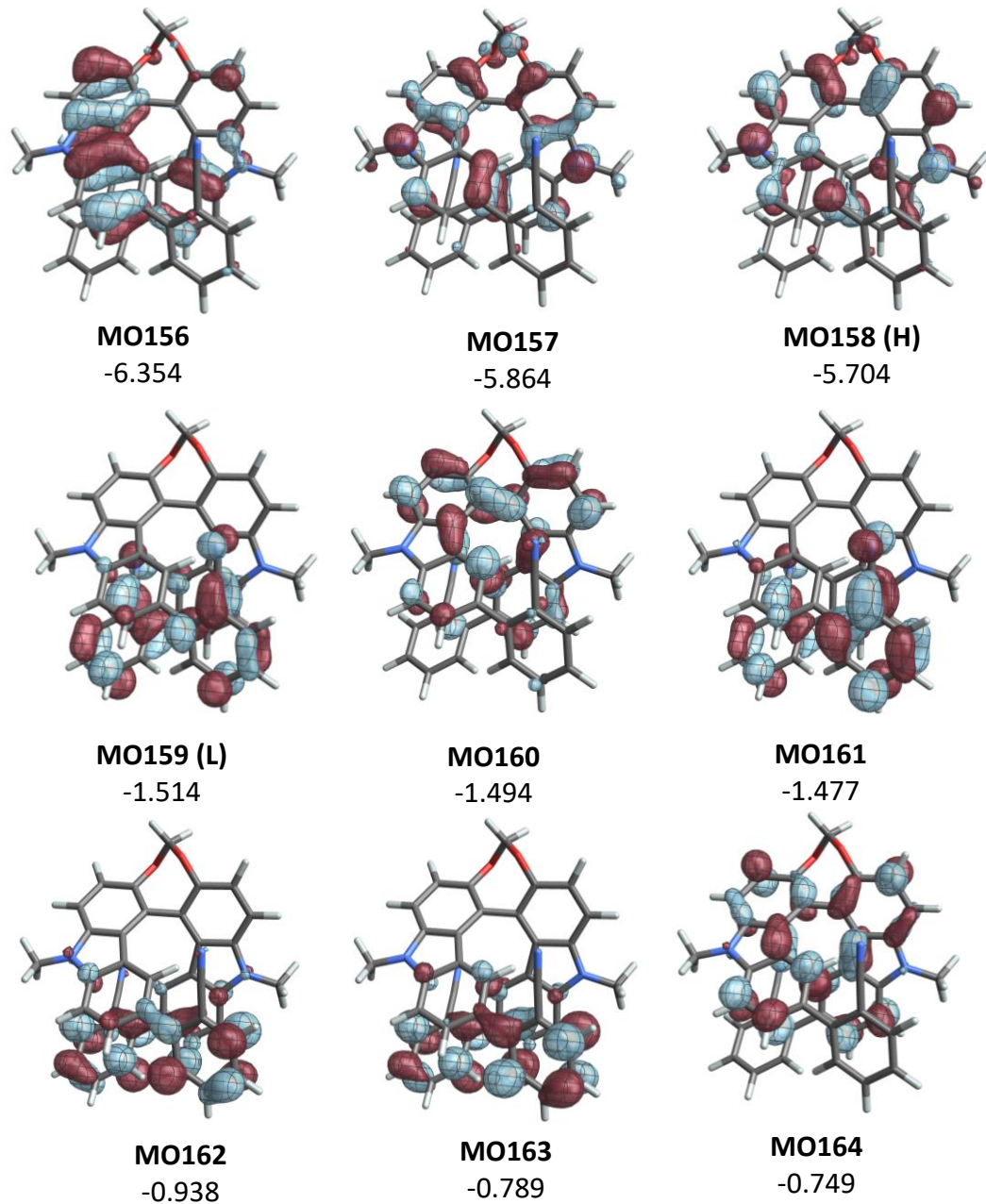


Figure S40. Isosurfaces (± 0.035 au) of Molecular Orbitals (MOs) for (+)-**Hel-*o*-CN (toluene)**. Values listed in parentheses are the corresponding orbital energies in eV.

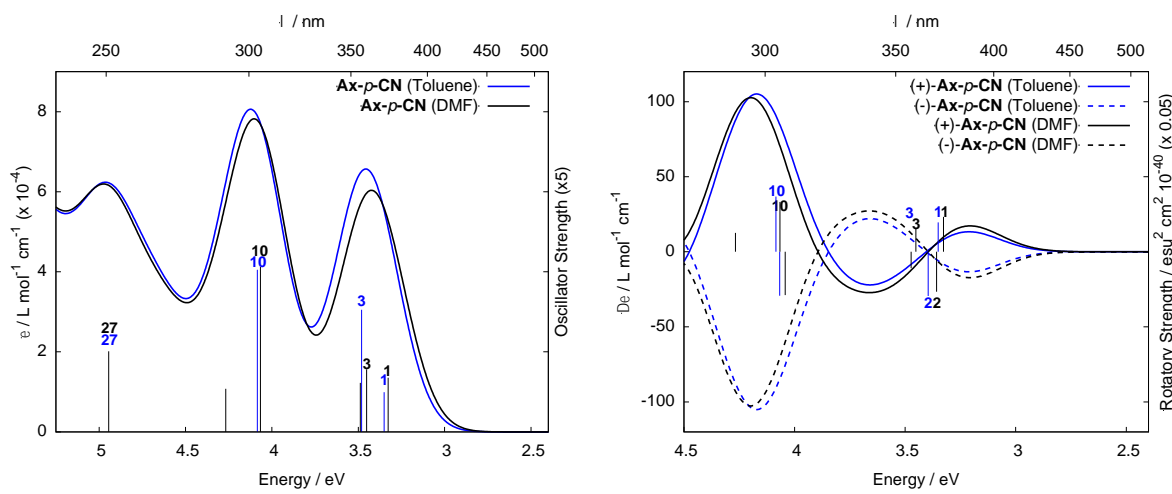


Figure S41. Calculated UV/Vis (left) and ECD (right) spectra of (\pm) -Ax-p-CN. Selected transitions and, oscillator and rotatory strengths are indicated as ‘stick spectra’. Predominant transitions for $(+)$ -Ax-p-CN are numbered according to Table S7.

Table S7. Selected excitations and occupied (occ)-unoccupied (unocc) MO pair contributions (greater than 10%) for $(+)$ -Ax-p-CN with toluene. H and L indicate the HOMO and LUMO, respectively.

Excitation	E [eV]	λ [nm]	f	R [10^{-40} cgs]	occ. no.	unocc no.	%
#1	3.350	370	0.200	392.81	163(H)	165	27
					163	166	19
#2	3.396	365	0.096	-588.51	163	164(L)	48
#3	3.481	356	0.610	413.28	163	166	26
#9	4.067	305	0.102	-585.58	161	164	26
#10	4.084	304	0.810	737.25	161	165	24
#13	4.247	292	0.211	199.03	161	166	34
#21	4.640	267	0.066	-264.83	161	167	41
#27	4.940	251	0.418	427.80	163	170	39

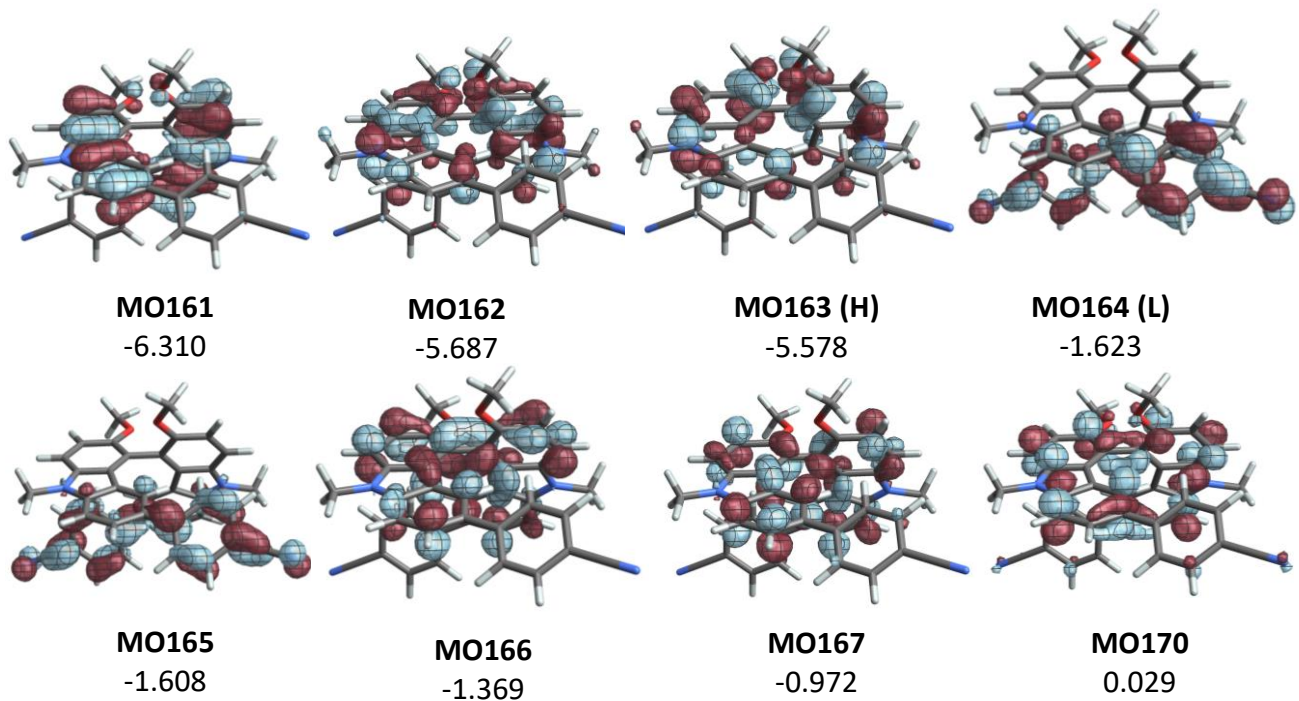


Figure S42. Isosurfaces (± 0.035 au) of Molecular Orbitals (MOs) for (+)-Ax-p-CN (Toluene). Values listed in parentheses are the corresponding orbitals energies in eV.

Table S8. Selected excitations and occupied (occ)-unoccupied (unocc) MO pair contributions (greater than 15%) for (+)-Ax-p-CN with DFM. H and L indicate the HOMO and LUMO, respectively.

Excitation	E [eV]	λ [nm]	f	R [10^{-40} cgs]	occ. no.	unocc no.	%
#1	3.327	373	0.271	466.59	163(H)	165	35
#2	3.358	369	0.086	-532.28	163	164(L)	48
#3	3.451	359	0.313	305.76	162	164	47
#4	3.473	357	0.040	-218.15	162	165	47
#5	3.488	355	0.245	86.26	163	166	34
#9	4.042	307	0.093	-575.91	161	164	27
#10	4.066	305	0.824	664.72	161	165	27
#13	4.267	291	0.216	252.49	161	166	39
#21	4.633	268	0.065	-263.98	161	167	39
#27	4.944	251	0.403	426.93	163	170	38

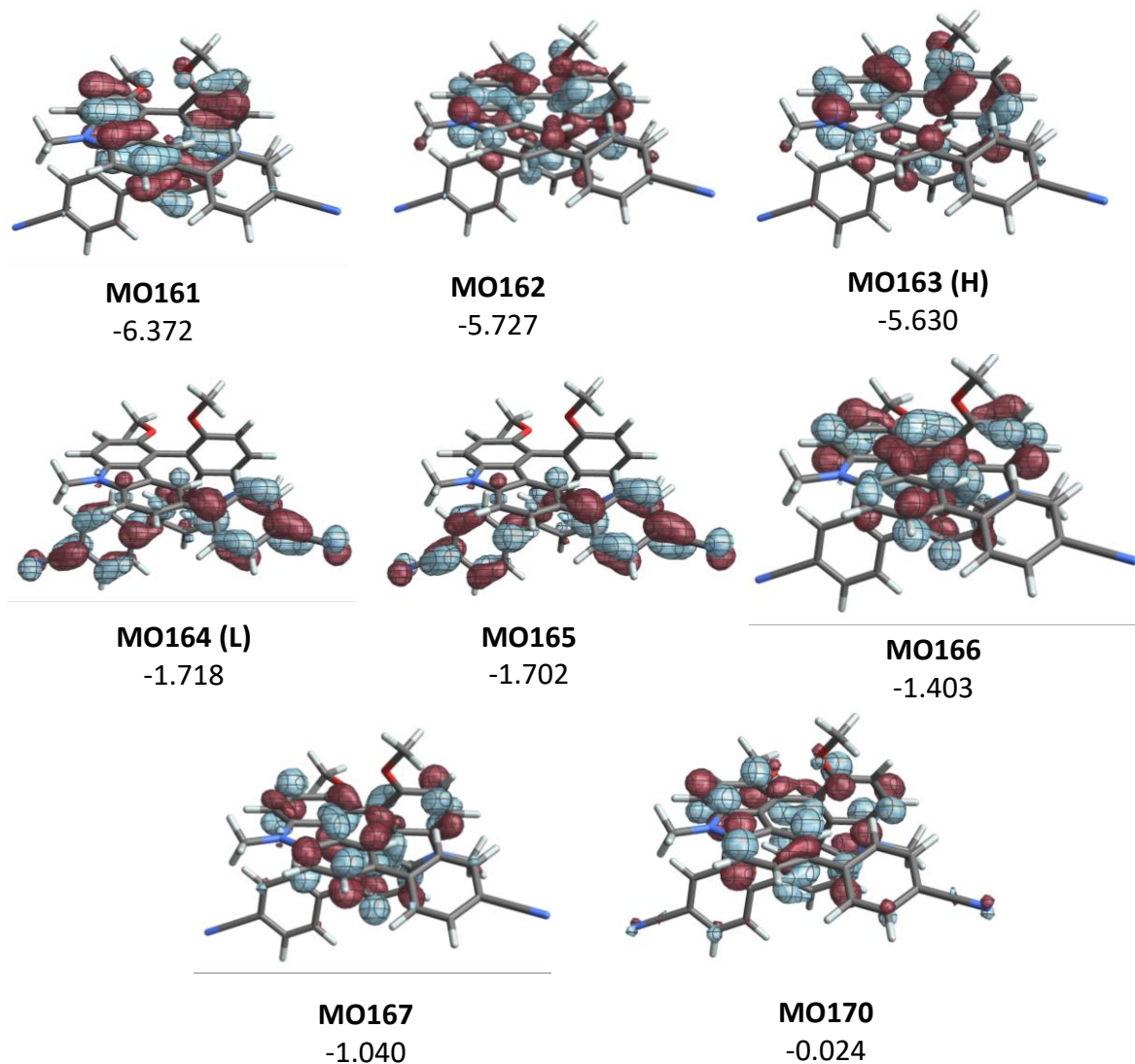


Figure S43. Isosurfaces (± 0.035 au) of Molecular Orbitals (MOs) for (+)-Ax-*p*-CN (DMF). Values listed in parentheses are the corresponding orbitals energies in eV.

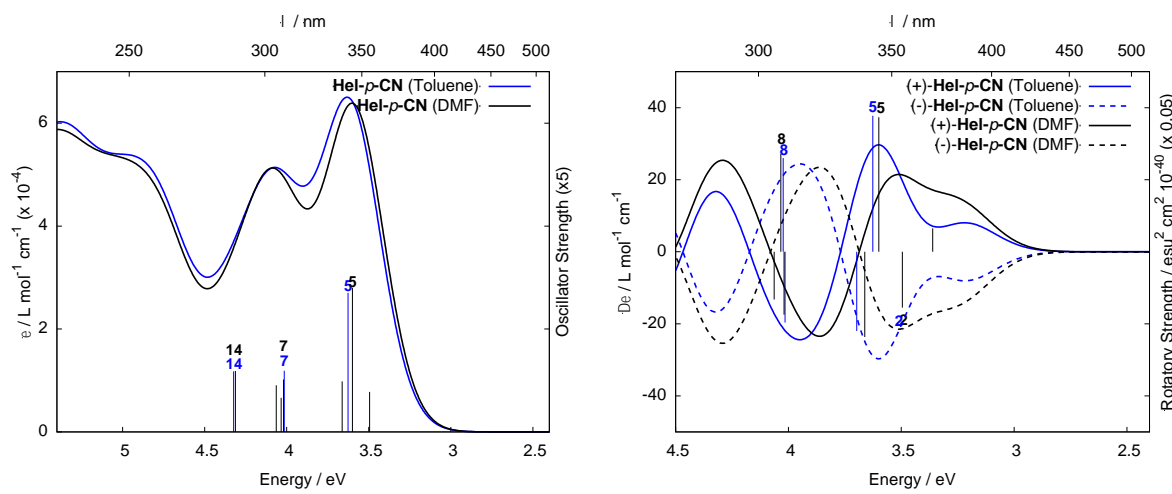


Figure S44. Calculated UV/Vis (left) and ECD (right) spectra of (\pm) -**Hel-p-CN**. Selected transitions and, oscillator and rotatory strengths are indicated as ‘stick spectra’. Predominant transitions for $(+)$ -**Hel-p-CN** are numbered according to Table S8.

Table S8. Selected excitations and occupied (occ)-unoccupied (unocc) MO pair contributions (greater than 10%) for $(+)$ -**Hel-p-CN** with toluene. H and L indicate the HOMO and LUMO, respectively.

Excitation	E [eV]	λ [nm]	f	R [10^{-40} cgs]	occ. no.	unocc no.	%
#1	3.366	368	0.044	102.37	158(H)	160	48
#2	3.518	352	0.160	-331.09	158	159(L)	49
#5	3.627	342	0.540	755.04	157	159	37
#6	3.697	335	0.179	-439.87	157	161	40
#7	4.015	309	0.238	-392.92	156	160	39
#8	4.023	308	0.119	520.71	155	160	45
#9	4.072	304	0.150	-215.00	158	162	24
#10	4.113	301	0.110	15.69	156	159	35
#14	4.324	287	0.235	43.96	157	162	22
					155	161	22

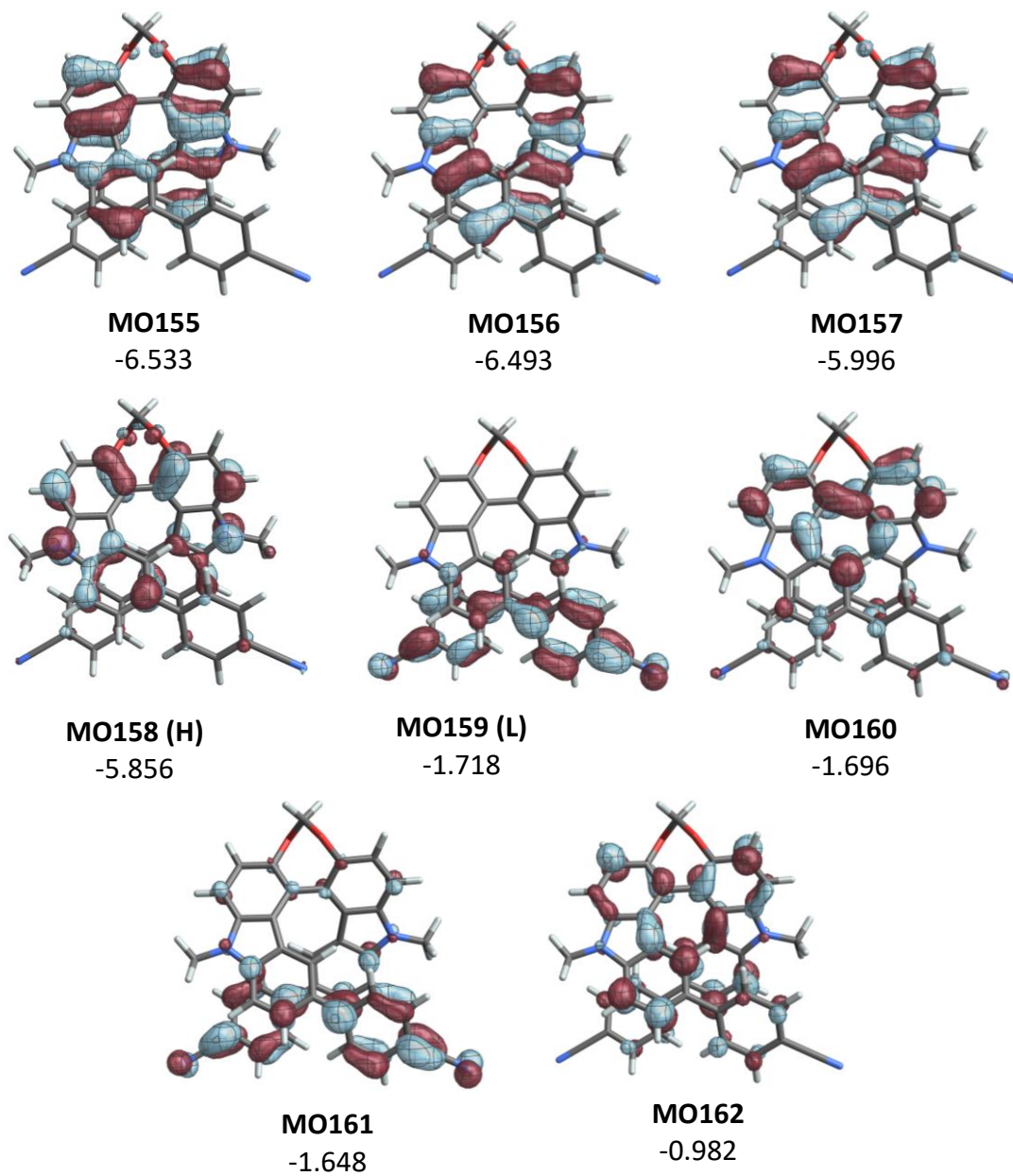


Figure S45. Isosurfaces (± 0.035 au) of Molecular Orbitals (MOs) for (+)-**Hel-p-CN (toluene)**. Values listed in parentheses are the corresponding orbitals energies in eV.

Table S9. Selected excitations and occupied (occ)-unoccupied (unocc) MO pair contributions (greater than 10%) for (+)-**Hel-p-CN** with toluene. H and L indicate the HOMO and LUMO, respectively.

Excitation	E [eV]	λ [nm]	f	R [10^{-40} cgs]	occ. no.	unocc no.	%
#1	3.366	368	0.044	102.37	158(H)	160	48
#2	3.518	352	0.160	-331.09	158	159(L)	49
#5	3.627	342	0.540	755.04	157	159	37
#6	3.697	335	0.179	-439.87	157	161	40
#7	4.015	309	0.238	-392.92	156	160	39
#8	4.023	308	0.119	520.71	155	160	45
#9	4.072	304	0.150	-215.00	158	162	24
#10	4.113	301	0.110	15.69	156	159	35
#14	4.324	287	0.235	43.96	157	162	22
					155	161	22

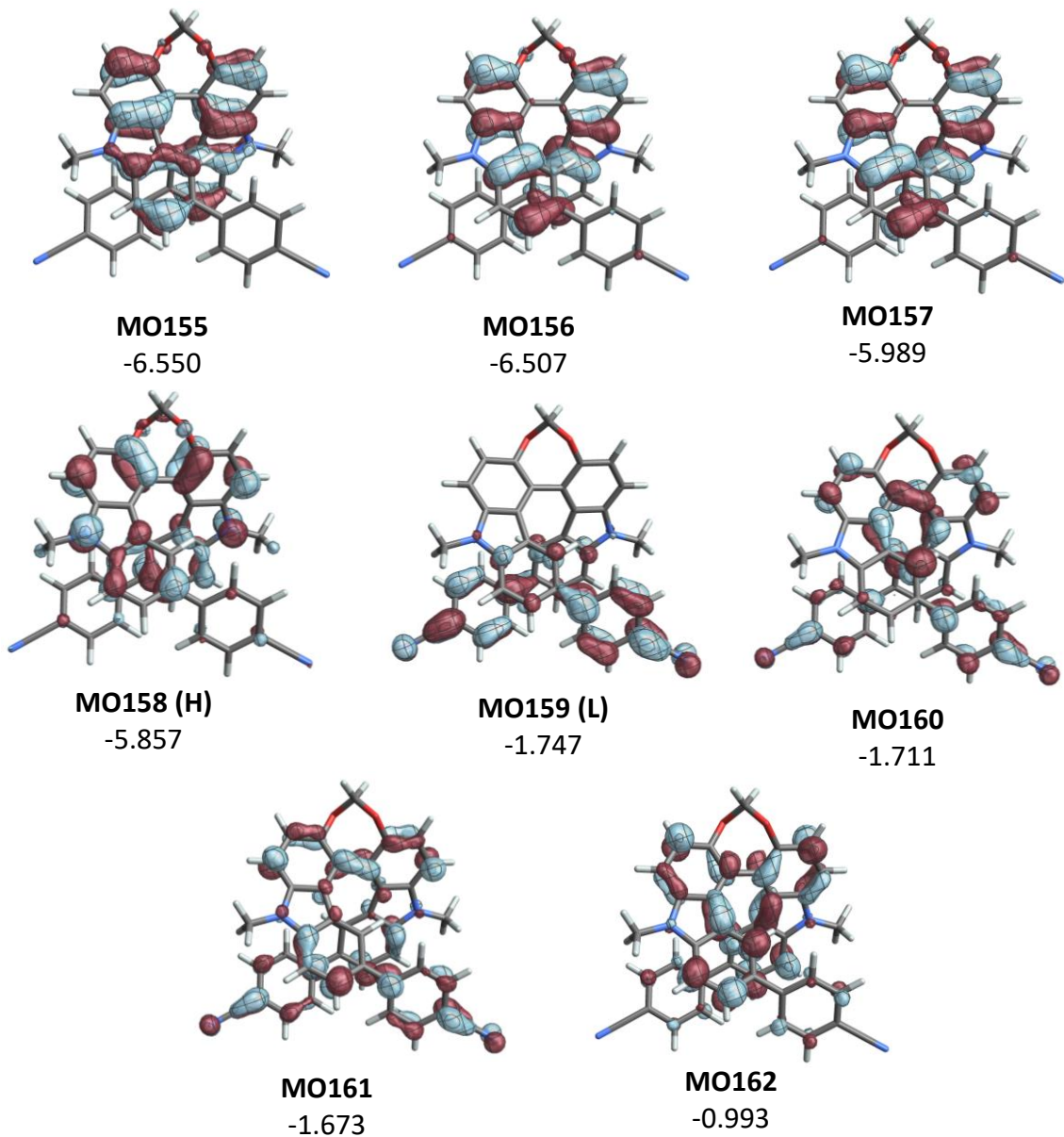


Figure S46. Isosurfaces (± 0.035 au) of Molecular Orbitals (MOs) for (+)-Hel-p-CN (DMF). Values listed in parentheses are the corresponding orbitals energies in eV.

H. References

- 1 S. Kasemthaveechok, L. Abella, M. Jean, M. Cordier, T. Roisnel, N. Vanthuyne, T. Guizouarn, O. Cador, J. Autschbach, J. Crassous and L. Favereau, *J. Am. Chem. Soc.*, 2020, **142**, 20409-20418.
- 2 G. W. T. M. J. Frisch, H. B. Schlegel, G. E. Scuseria, , J. R. C. M. A. Robb, G. Scalmani, V. Barone, , H. N. G. A. Petersson, X. Li, M. Caricato, A. V. Marenich, , B. G. J. J. Bloino, R. Gomperts, B. Mennucci, H. P. Hratchian, , A. F. I. J. V. Ortiz, J. L. Sonnenberg, D. Williams-Young, , F. L. F. Ding, F. Egidi, J. Goings, B. Peng, A. Petrone, , D. R. T. Henderson, V. G. Zakrzewski, J. Gao, N. Rega, , W. L. G. Zheng, M. Hada, M. Ehara, K. Toyota, R. Fukuda, , M. I. J. Hasegawa, T. Nakajima, Y. Honda, O. Kitao, H. Nakai, , K. T. T. Vreven, J. A. Montgomery, Jr., J. E. Peralta, , M. J. B. F. Ogliaro, J. J. Heyd, E. N. Brothers, K. N. Kudin, , T. A. K. V. N. Staroverov, R. Kobayashi, J. Normand, , A. P. R. K. Raghavachari, J. C. Burant, S. S. Iyengar, , M. C. J. Tomasi, J. M. Millam, M. Klene, C. Adamo, R. Cammi, , R. L. M. J. W. Ochterski, K. Morokuma, O. Farkas, and D. J. F. J. B. Foresman, *Journal*, 2016. URL: www.gaussian.com.
- 3 C. Adamo and V. Barone, *J. Chem. Phys.*, 1999, **110**, 6158-6170.
- 4 aF. Weigend and R. Ahlrichs, *Phys. Chem. Chem. Phys.*, 2005, **7**, 3297-3305; bF. Weigend, *Phys. Chem. Chem. Phys.*, 2006, **8**, 1057-1065.
- 5 G. Scalmani and M. J. Frisch, *J. Chem. Phys.*, 2010, **132**, 114110.
- 6 S. Grimme, J. Antony, S. Ehrlich and H. Krieg, *J. Chem. Phys.*, 2010, **132**, 154104.
- 7 aJ. Autschbach, L. Nitsch-Velasquez and M. Rudolph, *Top. Curr. Chem.*, 2011, **298**, 1-98; bM. Srebro-Hooper and J. Autschbach, *Annu. Rev. Phys. Chem.*, 2017, **68**, 399-420.